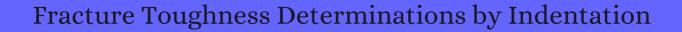
CITATION REPORT List of articles citing



DOI: 10.1111/j.1151-2916.1976.tb10991.x Journal of the American Ceramic Society, 1976, 59, 371-372.

Source: https://exaly.com/paper-pdf/12770673/citation-report.pdf

Version: 2024-04-17

This report has been generated based on the citations recorded by exaly.com for the above article. For the latest version of this publication list, visit the link given above.

The third column is the impact factor (IF) of the journal, and the fourth column is the number of citations of the article.

#	Paper	IF	Citations
1746	Strength Degradation of Glass Resulting from Impact with Spheres. <i>Journal of the American Ceramic Society</i> , 1977 , 60, 451-458	3.8	96
1745	An Indentation Technique for Measuring Stresses in Tempered Glass Surfaces. <i>Journal of the American Ceramic Society</i> , 1977 , 60, 86-87	3.8	205
1744	A model for crack initiation in elastic/plastic indentation fields. 1977 , 12, 2195-2199		396
1743	Dynamic solid particle damage in brittle materials: an appraisal. 1977 , 12, 97-116		129
1742	Effect of stress-induced phase transformation on the properties of polycrystalline zirconia containing metastable tetragonal phase. 1978 , 13, 1464-1470		377
1741	Analysis of Localized Impact Damage in Biaxially Stressed Glass Plates. <i>Journal of the American Ceramic Society</i> , 1978 , 61, 161-163	3.8	3
1740	On impact damage in the elastic response regime. 1978 , 49, 3304-3310		7
1739	Application of fracture mechanics to ceramic materials A state-of-the-art review. 1979 , 12, 479-498		25
1738	Micromechanics of crack nucleation during indentations. 1979 , 14, 2975-2980		150
1737	<1210>-zone fracture anisotropy of sapphire. 1979 , 52, K45-K48		8
1736	Microstructure dependence of the brittle fracture of alumina. 1979 , 55, 537-544		3
1735	Microstructural Development in MgO-Partially Stabilized Zirconia (Mg-PSZ). <i>Journal of the American Ceramic Society</i> , 1979 , 62, 298-305	3.8	304
1734	Crack Nucleation About Pointed Indentations in Glasses. <i>Journal of the American Ceramic Society</i> , 1979 , 62, 318-319	3.8	7
1733	Development of Surface Stresses During the Oxidation of Several Si3N4/CeO2 Materials. <i>Journal of the American Ceramic Society</i> , 1979 , 62, 629-630	3.8	11
1732	Hardness, Toughness, and Brittleness: An Indentation Analysis. <i>Journal of the American Ceramic Society</i> , 1979 , 62, 347-350	3.8	561
1731	Fracture Toughness of Si3N4 as a Function of the Initial Phase Content. <i>Journal of the American Ceramic Society</i> , 1979 , 62, 428-430	3.8	204
1730	Fracture of single crystal MgAl2O4. 1980, 15, 67-72		63

1729	Mechanical Properties of Silicon Nitride. 1980 , 11, 361-367		4
1728	Vickers hardness and microfracture of single and polycrystalline Al2O3. 1980 , 15, 1467-1474		9
1727	Abrasive wear of brittle solids. 1980 , 60, 123-140		186
1726	Fracture toughness of piezoelectric ceramics. 1980 , 12, 1492-1497		2
1725	High temperature structural ceramic materials manufactured by the CNTD process. 1980 , 6, 3-10		6
1724	Fracture of Polycrystalline MgAl2O4. <i>Journal of the American Ceramic Society</i> , 1980 , 63, 619-623	3.8	43
1723	Compressive Surface Stresses Developed in Ceramics by an Oxidation-Induced Phase Change. Journal of the American Ceramic Society, 1980 , 63, 38-40	3.8	75
1722	PHASE RETENTION AND FRACTURE TOUGHNESS OF MATERIALS CONTAINING TETRAGONAL ZrO2. 1980 , 45-56		
1721	Use of Vickers indentation method for evaluation of fracture toughness of phase-separated glasses. 1980 , 38-39, 391-396		21
1720	Fracture toughness of human enamel. 1981 , 60, 820-7		113
1719	Neutron irradiation effects on SiO2 and SiO2-based glass ceramics. 1981, 103, 767-771		13
1718	Erosion of MgO by solid particle impingement at normal incidence. 1981 , 16, 1579-1591		2
1717	Indentation plasticity and fracture of Si3N4 ceramic alloys. 1981, 16, 3437-3446		30
1716	Fabrication and characterization of SiC-AIN alloys. 1981 , 16, 3479-3488		133
1715	Strength and fracture surface energy of phase-separated glasses. 1981 , 16, 2205-2217		28
1714	Alumina structure with improved fracture properties. 1981 , 63, 183-192		11
1713	Transient Thermal Stress Behavior in ZrO2-Toughened Al2O3. <i>Journal of the American Ceramic Society</i> , 1981 , 64, 37-39	3.8	106

1711	A Critical Evaluation of Indentation Techniques for Measuring Fracture Toughness: I, Direct Crack Measurements. <i>Journal of the American Ceramic Society</i> , 1981 , 64, 533-538	3.8	4163
1710	Study of ferroe lectric ceramic fracture by indentation. 1981 , 13, 1031-1035		
1709	Structure and some properties of niobium carbide single crystals. 1981 , 20, 894-898		1
1708	Aboriginal Thermal Alteration of a Central Pennsylvania Jasper: Analytical and Behavioral Implications. 1982 , 47, 526-544		59
1707	Developments in fabrication of piezoelectric ceramics. 1982 , 41, 77-96		60
1706	Indentation microfracture in the Palmqvist crack regime: implications for fracture toughness evaluation by the indentation method. 1982 , 1, 493-495		173
1705	Evaluation ofK Ic of brittle solids by the indentation method with low crack-to-indent ratios. 1982 , 1, 13-16		1413
1704	Mechanical properties of multi-phase ceramics in the CaO-TiO2-ZrO2 system. 1982 , 1, 119-120		6
1703	Fracture toughness in the PbO-GeO2 and PbO-SiO2 binary glass systems. 1982 , 1, 314-315		1
1702	Fracture toughness and fracture surface energy of lead borate glasses. 1982 , 1, 156-158		9
1701	Transformation toughening. 1982 , 17, 240-246		276
1700	Transformation toughening. 1982 , 17, 247-254		255
1699	Transformation toughening. 1982 , 17, 255-263		104
1698	Fracture-induced photon emission of aluminium oxide and its application to fracture mechanical investigations. 1982 , 17, 1649-1655		14
1697	Critical Microstructures for Microcracking in Al2O3-ZrO2 Composites. <i>Journal of the American Ceramic Society</i> , 1982 , 65, 610-614	3.8	187
1696	A Simple Method for Determining Elastic-ModulusEo-Hardness Ratios using Knoop Indentation Measurements. <i>Journal of the American Ceramic Society</i> , 1982 , 65, c175-c176	3.8	392
1695	Temperature Dependence of KIC for High-Pressure Hot-Pressed Si3N4 Without Additives. <i>Journal of the American Ceramic Society</i> , 1982 , 65, c48-c48	3.8	9
1694	Measurement of the Crystallographically Transformed Zone Produced by Fracture in Ceramics Containing Tetragonal Zirconia. <i>Journal of the American Ceramic Society</i> , 1982 , 65, 284-288	3.8	240

1693	Room-Temperature Strength and Fracture of ZrO2-Y2O3 Single Crystals. <i>Journal of the American Ceramic Society</i> , 1982 , 65, c108-c109	3.8	44
1692	Further Reply to Comment on Elastic/Plastic Indentation Damage in Ceramics: The Median/Radial Crack System <i>Journal of the American Ceramic Society</i> , 1982 , 65, c116-c116	3.8	45
1691	Critical Load for Median Crack Initiation in Vickers Indentation of Glasses. <i>Journal of the American Ceramic Society</i> , 1982 , 65, c124-c127	3.8	39
1690	Effect of Water Content on Mechanical Properties of Na2O-SiO2 Glasses. <i>Journal of the American Ceramic Society</i> , 1982 , 65, c156-c157	3.8	17
1689	Controlled Flaws in Ceramics: A Comparison of Knoop and Vickers Indentation. <i>Journal of the American Ceramic Society</i> , 1983 , 66, 127-131	3.8	89
1688	Transformation Strengthening of PAl2O3 with Tetragonal ZrO2. <i>Journal of the American Ceramic Society</i> , 1983 , 66, C-50-C-52	3.8	16
1687	Toughening by Monoclinic Zirconia. <i>Journal of the American Ceramic Society</i> , 1983 , 66, 328-332	3.8	49
1686	Dielectric, Electromechanical, Optical, and Mechanical Properties of Lanthanum-Modified Lead Titanate Ceramics. <i>Journal of the American Ceramic Society</i> , 1983 , 66, 363-366	3.8	90
1685	Intergranular Crack-Deflection Toughening in Silicon Carbide. <i>Journal of the American Ceramic Society</i> , 1983 , 66, C-94-C-95	3.8	79
1684	Effect of Crystallites on Surface Damage and Fracture Behavior of a Glass-Ceramic. <i>Journal of the American Ceramic Society</i> , 1983 , 66, 673-682	3.8	28
1683	A Modified Indentation Toughness Technique. Journal of the American Ceramic Society, 1983, 66, c200-	c2 j 08	155
1682	Fracture Toughness Anisotropy of Sodium 🛮 Alumina. <i>Journal of the American Ceramic Society</i> , 1983 , 66, c204-c205	3.8	26
1681	Relation of Load to Radial Crack Length for Spherical Indentations in Hot-Pressed ZnS. <i>Journal of the American Ceramic Society</i> , 1983 , 66, 293-296	3.8	4
1680	Crack deflection processes II. Experiment. 1983 , 31, 577-584		385
1679	Influence of Yttria content on phase composition and mechanical properties of Y-PSZ. 1983 , 9, 8-12		29
1678	A fracture mechanics analysis of indentation-induced Palmqvist crack in ceramics. 1983 , 2, 221-223		547
1677	Fracture characteristics of titanium carbide with titanium nitride additions. 1983 , 22, 285-287		1
1676	Transfomation toughening of 🛭 alumina by incorporation of zirconia. 1983 , 18, 109-113		47

1675	Fracture of metastable tetragonal zirconia crystals. 1983 , 18, 2618-2628		106
1674	Mechanical properties and fracture behaviour of ZrO2-Y2O3 ceramics. 1983 , 18, 1958-1966		45
1673	Characterization of AIN ceramics containing long-period polytypes. 1983 , 18, 525-532		55
1672	Analysis of Brittle Failure of Cutting Tools Based on Fracture Mechanics. 1983, 32, 37-41		7
1671	Hardness testing of aluminas in air and a simulated body environment. 1983 , 61, L1-L5		8
1670	Internal stress anisotropies induced by electric field in lanthanum modified PbTiO3 ceramics. 1983 , 50, 273-278		36
1669	Microstructural studies of the temperature-dependence of deformation structures around hardness indentations in ceramics. 1983 , 130, 345-360		31
1668	Aging change in mechanical properties of (Pb, La)TiO3 ceramics. 1983 , 49, 81-86		3
1667	Mechanical properties of grain oriented piezo -ceramics with bismuth-layer and tungsten-bronze structures. 1983 , 49, 189-194		7
1666	Microstructure and properties of some electrooptic ceramics. 1983 , 49, 141-150		6
1665	Transformation Toughening of BetaEAlumina. 1983,		
1664	ANISOTROPY OF FRACTURE TOUGHNESS OF PIEZOELECTRIC CERAMICS. 1984 , 2711-2719		1
1663	Elastic/plastic indentation in ceramics: a fracture toughness determination method. 1984 , 10, 147-152		85
1662	Preparation and Mechanical Properties of Mg-Al-Si-O-N Glasses. <i>Journal of the American Ceramic Society</i> , 1984 , 67, c225-c227	3.8	50
1661	Contact Damage in Hot-Pressed and Chemically-Vapor-Deposited Zinc Sulfide. <i>Journal of the American Ceramic Society</i> , 1984 , 67, C-188-C-190	3.8	
1660	Fracture analysis of single crystal manganese zinc ferrites using indentation flaws. 1984 , 32, 1719-1729		20
1659	The fracture behaviour of Chromium- and Titanium-doped sapphire monocrystals. 1984 , 19, 1113-1120		1
1658	Hertzian indentation of sintered alumina. 1984 , 19, 254-258		18

1657	Crack-size dependence of fracture toughness in transformation-toughened ceramics. 1984 , 19, 2233-2238	25
1656	Microhardness and brittle fracture of garnet single crystals. 1984 , 19, 1159-1170	16
1655	Indentation testing of nuclear-waste glasses. 1984 , 19, 2533-2545	24
1654	Properties of Yttria Stabilized Tetragonal Zirconia Polycrystals. 1985 , 60, 483	O
1653	Toughening of hot pressed beta-alumina using zirconia additions prepared from zirconate, tartrate and carbonate precursor materials. 1985 , 140, 183-194	3
1652	Microindentation analysis of di-ammonium hydrogen citrate single crystals. 1985 , 20, 3150-3156	18
1651	Comments on T rack-size dependence of fracture toughness in transformation-toughened ceramics 1985 , 20, 4239-4241	5
1650	Reply to Comments on Crack-size dependence of fracture toughness in transformation-toughened ceramics 1985 , 20, 4241-4244	4
1649	Transformation toughening and grain size control in P-Al2O3/ZrO2 composites. 1985, 20, 2639-2646	35
1648	Mechanical properties of ZrO2-toughened Al2O3 ceramics from CVD powders. 1985 , 4, 413-416	44
1647	ZrO2-toughened MgO and critical factors in toughening ceramic materials by incorporating zirconia. 1985 , 4, 63-66	11
1646	Thermal shock resistance of Mg-PSZ. 1985 , 20, 3421-3427	22
1645	Hot-pressing of Si3N4 in high nitrogen pressure. 1985 , 4, 1473-1475	
1644	The elastic/plastic indentation of ceramics. 1985 , 4, 1539-1541	83
1643	Indentation fracture of titanium diboride. 1985 , 4, 694-696	6
1642	The measurement ofK IC in single crystal SiC using the indentation method. 1985 , 4, 783-786	24
1641	Palmqvist cracking in WC-Co composites. 1985 , 4, 207-210	15
1640	Effect of Crystallites on Subcritical Crack Growth and Strain-Rate Sensitivity of Strength of Cordierite Glass-Ceramics. <i>Journal of the American Ceramic Society</i> , 1985 , 68, 112-119	13

1639	Strength Recovery in Degraded Yttria-Doped Tetragonal Zirconia Polycrystals. <i>Journal of the American Ceramic Society</i> , 1985 , 68, C-213-C-213	3.8	17
1638	Indenter Flaw Geometry and Fracture Toughness Estimates for a Glass-Ceramic. <i>Journal of the American Ceramic Society</i> , 1985 , 68, C-282-C-284	3.8	3
1637	Mechanical Properties of Hot-Pressed TiB2-ZrO2 Composites. <i>Journal of the American Ceramic Society</i> , 1985 , 68, C-34-C-36	3.8	10
1636	Fabrication of Si3N4 Ceramics with Metal Nitride Additives by Isostatic Hot-Pressing. <i>Journal of the American Ceramic Society</i> , 1985 , 68, C-38-C-40	3.8	17
1635	Anisotropy of Fracture Toughness of Piezoelectric Ceramics. <i>Journal of the American Ceramic Society</i> , 1985 , 68, 259-265	3.8	139
1634	Effect of Densification Conditions on the Stabilization of the Tetragonal Phase in ZrO2 Polycrystals. Journal of the American Ceramic Society, 1985 , 68, C-242-C-243	3.8	5
1633	Mechanical properties of (Pb,Ca)TiO3 family ceramics with zero planar coupling factor. 1985 , 11, 75-79		21
1632	Engineering property requirements for high performance ceramics. 1985 , 71, 3-21		52
1631	Physical properties and cutting performance of silicon nitride ceramic. 1985 , 102, 195-210		78
1630	Temperature relationship of the crack resistance of monocrystalline gallium arsenide. 1985 , 17, 904-90	7	
1629	Crack resistance of a constructional ceramic. 1985 , 17, 445-451		1
1628	The effect of elevated-temperature neutron irradiation on fracture toughness of ceramics. 1985 , 133-134, 701-704		40
1627	Improvement of Productivity and Reduction Disintegration of Iron Ore Sinter by Increasing Size of Limestone Particles. 1985 , 71, 1880-1887		14
1626	Silicon Nitride Swirl Lower-Chamber for High Power Turbocharged Diesel Engines. 1985,		13
1625	Wurtzitic boron nitride∃ review. 1985 , 1, 139-153		24
1624	The alumina fibre/tetragonal zirconia polycrystal composite system. 1986 , 17, 137-140		7
1623	Cutting Tool Materials: Mechanical Properties Wear-Resistance Relationships. 1986, 29, 347-352		24
	The study of influence of various structural factors on mechanic properties of PLZT ceramics. 1986 ,		

1621	Fracture toughness determination of dental amalgams through microindentation. 1986 , 20, 135-42	6
1620	A sclerometric study of unidirectionally solidified Cr-Mo white cast irons. 1986 , 111, 203-215	13
1619	Effects of self-radiation damage in Cm-doped Gd2Ti2O7 and CaZrTi2O7. 1986 , 138, 196-209	206
1618	Unusual thermal expansion behaviour of PbO-rich PbO-B2O3 glasses. 1986 , 21, 1289-1292	2
1617	Mechanical property changes in sapphire by nickel ion implantation and their dependence on implantation temperature. 1986 , 21, 1321-1328	97
1616	Zirconia-toughened sodium beta?-alumina solid electrolyte. 1986 , 21, 4221-4226	2
1615	Effect of test method and crack size on the fracture toughness of a chain-silicate glass-ceramic. 1986 , 21, 2365-2372	24
1614	Effects of attrition milling and post-sintering heat treatment on fabrication, microstructure and properties of transformation toughened ZrO2. 1986 , 21, 768-774	26
1613	Grain size dependences of vickers microhardness and fracture toughness in Al2O3 and Y2O3 ceramics. 1986 , 12, 33-37	56
1612	Toughening of Dental Porcelain by Tetragonal ZrO2 Additions. <i>Journal of the American Ceramic Society</i> , 1986 , 69, C-75-C-77	13
1611	Strength-Toughness Relations in Sintered and Isostatically Hot-Pressed ZrO2-Toughened Al2O3. <i>Journal of the American Ceramic Society</i> , 1986 , 69, 169-172	69
1610	Influence of Surface Stress on indentation Cracking. <i>Journal of the American Ceramic Society</i> , 1986 , 69, 223-225	16
1609	Fracture toughness of commercial dental porcelains. 1986 , 2, 58-62	105
1608	Toughening behavior in ceramics associated with the transformation of tetragonal ZrO2. 1986 , 34, 1885-189	1 69
1607	Shape profiles of cracks formed under a Vickers pyramid indenter. 1986 , 5, 247-248	13
1606	On estimating fracture toughness of cemented carbides from Palmqvist crack sizes. 1986 , 5, 365-368	24
1605	Chapter 3 Surfaces in Contact. 1987 , 48-79	
1604	Structural ceramics based on Si3N4ZrO2(+ Y2O3) compositions. 1987 , 2, 66-76	38

1603	Appropriate use of the strength parameter in solid-state slab laser design. 1987 , 62, 1595-1604	19
1602	Ceramic Optical Package: Material Requirements and Guidelines for Material Selection. 1987 , 108, 439	
1601	Laboratory scale erosion testing of a wear resistant glass@eramic. 1987, 3, 807-813	8
1600	Improvement of Mechanical Properties of Metaphosphate Glass by Addition of Chromium Oxide. 1987 , 16, 1711-1714	1
1599	Machinability and Microstructure of (Ni0.8Mg0.2)O Ceramics. 1987, 95, 937-941	
1598	Fracture Mechanics Analysis of the Brittle Failure of Cutting Tools (3rd Report). 1987 , 53, 473-479	1
1597	The effect of composition on crack propagation in lead silicate glasses. 1987 , 95-96, 1039-1046	3
1596	Ceramic cutting toolsA review. 1987 , 3, 113-127	10
1595	Strength and crack resistance of ceramics. Communication 4. Ceramics based on boron carbide. 1987 , 19, 1359-1363	
1594	Influence of surface treatments on the dynamic fatigue of soda-lime glass with indentation flaws. 1987 , 85, L25-L29	4
1593	Fracture toughness and acoustic emission in silicon nitride. 1987 , 6, 1459-1462	3
1592	Mechanical properties of barium hexaferrite sintered in the presence of a low-melting glass. 1987 , 6, 1098-1100	6
1591	Fracture toughness and fracture surface energy of sintered uranium dioxide fuel pellets. 1987 , 6, 260-262	27
1590	Palmqvist indentation toughness in WC-Co composites. 1987 , 6, 897-900	85
1589	Impact attrition of sodium chloride crystals. 1987 , 42, 843-853	48
1588	Subcritical crack growth of glass. 1987 , 28, 77-84	13
1587	Fracture toughness of pressureless sintered silicon carbide: A comparison of Klc measurement methods. 1987 , 13, 159-165	26
1586	Relevant properties of ceramics for immobilization of high level waste. An example: A glass-ceramic through a sol-gel route. 1987 , 17, 475-484	1

1585	Si3N4-Al2O3-ZrO3 hot pressed composites. 1987 , 18, 205-229		2
1584	Evaluation of Fracture Toughness Determination Methods as Applied to Ceria-Stabilized Tetragonal Zirconia Polycrystal. <i>Journal of the American Ceramic Society</i> , 1987 , 70, C-366-C-368	3.8	36
1583	Effect of Joint Thickness and Residual Stresses on the Properties of Ceramic Adhesive Joints: II, Experimental Results. <i>Journal of the American Ceramic Society</i> , 1987 , 70, 110-118	3.8	30
1582	Reaction Sintering of Submicrometer Silicon Powder. <i>Journal of the American Ceramic Society</i> , 1987 , 70, C-52-C-55	3.8	19
1581	Growth and Coalescence of Indentation Cracks in Glass. <i>Journal of the American Ceramic Society</i> , 1987 , 70, C-301-C-302	3.8	9
1580	Effect of Grain-Boundary Oxidation on Fracture Toughness of SiC. <i>Journal of the American Ceramic Society</i> , 1987 , 70, 548-552	3.8	20
1579	Apparent fracture toughness of dental porcelain with a metal substructure. 1988 , 4, 187-90		7
1578	Subcritical crack growth and crack coalescence in glass. 1988 , 29, 189-196		2
1577	Application of indentation technique in determining fracture toughness of ceramics. 1988 , 31, 309-313		4
1576	Evaluation of static and dynamic fracture toughness in ceramics. 1988 , 31, 873-885		22
1575	Properties of the partially stabilized zirconium dioxide crystals. 1988, 29, 333-335		
1574	Elevated temperature properties of WC-Co cemented carbides. 1988 , 105-106, 363-367		13
1573	Microindentation characterization of silicide coatings on niobium and titanium. 1988, 7, 952-954		8
1572	Preparation of a composite powder of the system SiC-AIN. 1988 , 7, 1151-1153		6
1571	Characterization of some mechanical properties of polycrystalline yttrium iron garnet (YIG) by non-destructive methods. 1988 , 7, 1217-1220		14
1570	Structure and cracking resistance of TiC-steel hard alloys. 1988 , 27, 488-492		
1569	Toughening mechanisms in duplex alumina-zirconia ceramics. 1988, 23, 804-808		36
1568	Effect of particulate additions on the contact damage resistance of hot-pressed Si3N4. 1988 , 23, 946-9.	57	19

1567	The mechanical and electrical properties of ZrO2-NaP-Al2O3 composites. 1988, 23, 958-967		24
1566	Indentation fracture in the In1 $\mbox{1}\mbox{1}\mbox{0}$ Ga x As y P1 $\mbox{1}\mbox{0}$ /InP system and its effect on microhardness anisotropy characteristics. 1988 , 23, 272-280		10
1565	Fracture of hot-pressed alumina and SiC-whisker-reinforced alumina composite. 1988 , 23, 3782-3791		9
1564	Strength variations of reaction-sintered SiC heterogeneously containing fine-grained 卧iC. 1988 , 23, 3248-3253		15
1563	Radiation enhanced dislocation glide effect on indentation-induced fracture of GaAs single crystals. 1988 , 109, 383-393		10
1562	Indentation Deformation and Fracture of Sapphire. <i>Journal of the American Ceramic Society</i> , 1988 , 71, 29-35	3.8	70
1561	Factors Affecting the Porosity and Bending Strength of Ti(CN)-TiB2 Materials. <i>Journal of the American Ceramic Society</i> , 1988 , 71, C-202-C-204	3.8	12
1560	Mechanical and Microstructural Characterization of Mullite and Mullite-SiC-Whisker and ZrO2-Toughened-MulliteBiC-Whisker Composites. <i>Journal of the American Ceramic Society</i> , 1988 , 71, 503-512	3.8	63
1559	Method of Fabricating Ceria-Stabilized Tetragonal Zirconia Polycrystals. <i>Journal of the American Ceramic Society</i> , 1988 , 71, C-410-C-411	3.8	14
1558	Influence of Surface Structure on the Fracture Toughness of Tempered Glass. <i>Journal of the American Ceramic Society</i> , 1988 , 71, C434-C435	3.8	1
1557	Deformation and rupture of crystals with covalent interatomic bonds. 1988 , 16, 225-277		23
1556	The effect of temperature and Yttria content on the properties of hot isostatically pressed Si3N4. 1988 , 105-106, 169-174		4
1555	Indentation fracture toughness and dynamic young's modulus of ceramic biomaterials. 1988 , 105-106, 207-213		2
1554	Fracture toughness measurement by microindentation and three-point bend methods. 1988 , 105-106, 369-375		7
1553	Fracture of GaAs Wafers. 1988 , 27, 2238-2246		25
1552	Microwave Joining of Ceramics. 1988 , 124, 255		4
1551	Microstructure and Mechanical Properties of CaO/MgO-Doped Si3N4Sintered by Hot Isostatic Pressing. 1988 , 3, 403-405		2
1550	Subcritical Crack Growth of Glass Under Combined Modes I and II Loading. 1988 , 110, 219-223		5

1549	Brittleness of high Tc Bi0.7Pb0.3SrCaCu1.8Ox crystal and glass. 1989 , 66, 2069-2073		9
1548	Fracture toughness of (Ce) stabilized ZrO2/Al2O3 composites. 1989 , 15, 363-368		6
1547	Calcium phosphate glasses and glass-ceramics for medical applications. 1989 , 5, 47-53		16
1546	Mechanical properties and short-term in-vivo evaluation of yttrium-oxide-partially-stabilized zirconia. 1989 , 23, 45-61		410
1545	Reinforcement of silicon nitride ceramics by Esi3N4 Whiskers. 1989 , 5, 321-326		26
1544	Large electromechanical anisotropic modified lead titanate ceramics. 1989 , 24, 447-452		33
1543	Y(E)-doped tetragonal zirconia polycrystalline solid electrolyte. 1989 , 24, 708-716		8
1542	Effect of porosity on cracking resistance of hot-compacted boron carbide. 1989 , 28, 781-784		1
1541	Determination of the fracture toughness of structurally heterogeneous silicide layers. 1989 , 28, 294-298		Ο
1540	Thermal processing and properties of highly homogeneous alumina-zirconia composite ceramics. 1989 , 24, 3984-3990		6
1539	Effect of stress state and microstructural parameters on impact damage of alumina-based ceramics. 1989 , 24, 2516-2532		43
1538	Crack growth of C(T) specimens and indentation cracks in glass. 1989 , 39, R23-R28		10
1537	Preparation, Sintering, and Properties of Translucent Er2O3-Doped Tetragonal Zirconia. <i>Journal of the American Ceramic Society</i> , 1989 , 72, 2088-2093	8	40
1536	Indentation Fracture Toughness of Sintered Silicon Carbide in the Palmqvist Crack Regime. <i>Journal of the American Ceramic Society</i> , 1989 , 72, 904-911	8	168
1535	Effect of Nonstoichiometry on Fracture Toughness and Hardness of Yttrium Oxide Ceramics. <i>Journal of the American Ceramic Society</i> , 1989 , 72, 1562-1563	8	41
1534	Characterization of superplastic Yttria-stabilized tetragonal Zirconia by a hot indentation technique. 1989 , 23, 1261-1264		15
1533	Ceramics and Temper: A Response to Feathers. 1989 , 54, 589-593		6
1532	Investigation of the infrared properties of ZnS:diamond composites. 1989 , 14, 1260-2		3

1531	Vickers indentation fracture toughness test Part 1 Review of literature and formulation of standardised indentation toughness equations. 1989 , 5, 865-872		489
1530	Vickers indentation fracture toughness test Part 2 Application and critical evaluation of standardised indentation toughness equations. 1989 , 5, 961-976		218
1529	Characterization of Mechanical Strengths for Simulated High-Level Waste Forms. 1989 , 176, 433		1
1528	Subcritical Crack Growth Characteristics on Compact Type Specimens and Indentation Cracks in Glass. 1989 , 111, 399-403		2
1527	Effect of Green Microstructure and Processing Variables on the Microwave Sintering of Alumina. 1990 , 189, 283		5
1526	Decomposition Reactions and Toughening in NiAl-Cu Alloys. 1990 , 194, 405		2
1525	Direct Observation and Analysis of Indentation Cracking in Glasses and Ceramics. <i>Journal of the American Ceramic Society</i> , 1990 , 73, 787-817	3.8	825
1524	Pressureless Sintering of SiC-Whisker-Reinforced Al2O3 Composites: II, Effects of Sintering Additives and Green Body Infiltration. <i>Journal of the American Ceramic Society</i> , 1990 , 73, 1894-1900	3.8	16
1523	Combustion Synthesis of Silicon Nitride-Silicon Carbide Composites. <i>Journal of the American Ceramic Society</i> , 1990 , 73, 3514-3517	3.8	24
1522	Fracture Toughness of Ceramic Precracked Bend Bars. <i>Journal of the American Ceramic Society</i> , 1990 , 73, 2519-2522	3.8	27
1521	Studies on fracture toughness of dental ceramics. 1990 , 17, 551-63		47
1520	Investigation of a ceramic in indentation of a Vickers diamond pyramid. 1990 , 22, 1306-1313		4
1519	Effects of neutron irradiation and subsequent annealing on strength and toughness of SiC ceramics. 1990 , 170, 95-100		28
1518	Determination of KISCC by indentation in ceramics. 1990 , 25, 5077-5080		3
1517	Slip casting of Al2O3 and Al2O3/ZrO2 composites. 1990 , 25, 4331-4340		8
1516	Fracture toughness and hardness of zinc sulphide as a function of grain size. 1990 , 25, 1347-1352		43
1515	Injection moulding of ceria-stabilized tetragonal zirconia polycrystals (Ce-TZP). 1990 , 9, 209-210		3
1514	Mechanical properties of single-crystal lanthanum hexaboride with local loading. 1990 , 29, 967-972		2

1513	Some properties of hot-compacted aluminum oxide with additions of tungsten carbide. 1990 , 29, 932-934	1
1512	Evaluation by indentation of fracture toughness of ceramic materials. 1990 , 25, 207-214	136
1511	Characterization of engineering ceramics by indentation methods. 1990 , 25, 3731-3738	22
1510	Observations of crack patterns in NaSbF4 and NaSb2F7 single crystals. 1990 , 25, 1451-1454	3
1509	Effects of scattering centers and absorbing coatings on the structure of shaped sapphire. 1990 , 104, 154-156	2
1508	Mechanical behaviour of zirconia and zirconia-toughened alumina in a simulated body environment. 1990 , 11, 505-8	57
1507	Solid solution strengthening of ZnS. 1990 ,	4
1506	Studies on Zirconia Dispersed Alumina Ceramics. 1990 , 49, 21-25	6
1505	Survey of Eutectic Systems as Potential Intermetallic Matrix Composites for High Temperature Application. 1990 , 194, 155	11
1504	Abrasion and Erosion of WC-Co with Controlled Microstructures. 1990 , 33, 611-617	77
1503	Microhardness, surface toughness and average coordination number in chalcogenide glasses. 1990 , 125, 250-257	53
1502	Study of SiC-whisker-reinforced ZrO2 ceramics using the sol-gel method. 1991 , 175, 205-208	1
1501	Microstructural Aspects of Si3N4-TiC Composites Affecting Abrasion and Erosion Resistance. 1991 , 34, 553-558	15
1500	Fracture toughness measurements of some dental core ceramics: a methodologic study. 1991 , 99, 527-32	
		1
	Fracture toughness measurements of some dental core ceramics: a methodologic study. 1991 , 99, 527-32	1
1499	Fracture toughness measurements of some dental core ceramics: a methodologic study. 1991 , 99, 527-32 Fracture Behavior of CVD Diamond. 1991 , 239, 561 Fracture toughness evaluation for advanced materials using chevron-notched compact specimens.	1 29

Fracture Toughness of Chemically Vapor-Deposited Diamon Society, 1991 , 74, 3148-3150	d. Journal of the American Ceramic 3.8 42	2
1494 Direct Measurement of Crack Tip Stresses. <i>Journal of the Am</i>	nerican Ceramic Society, 1991 , 74, 2897-2901 ₃ .8 27	7
Comment on Indentation Fracture Toughness of Sintered Sil Regime I Journal of the American Ceramic Society, 1991 , 74, 8	• 28 6	
1492 Rapid Hot-Pressing of Ultrafine PSZ Powders. <i>Journal of the</i>	American Ceramic Society, 1991 , 74, 1547-15 58 10)
1491 Structural analysis of a TiAl3 + ZrO2 particulate composite. 1	1991 , 148, 115-122	
Strengthening and toughening of cordierite by the addition and particles. 1991 , 26, 6800-6808	of silicon carbide whiskers, platelets 29)
1489 Effect of CeO2 on reaction-sintered mullite-ZrO2 ceramics.	1991 , 26, 4631-4636)
Transformation behaviour of yttria tetragonal zirconia polyc 1991 , 10, 1374-1376	crystals in a metal-cutting environment.	
1487 Some properties of aluminum nitride compacts prepared by	shock-wave loading. 1991 , 30, 833-837	
1486 Structure and properties of hot-pressed material based on s	ilicon nitride. 1991 , 30, 840-844	
Strengthening and toughening of cordierite by the addition and particles. 1991 , 26, 6800-6808	of silicon carbide whiskers, platelets	
Physical and mechanical properties of Si3N4 sintered from s powders. 1991 , 26, 263-273	hock-activated and unshocked	
1483 Microindentation studies on BaFCl single crystals. 1991 , 26,	899-903 25	5
Microstructure and mechanical properties of hot pressed Alaultrafine powders. 1991 , 7, 490-494	२०३ $f B$ rO2 ceramics prepared from $_{15}$;
1481 Mechanical properties of H. P. or H. I. P. SiC-whisker reinforc	ed Si3N4-matrix composites. 1991 , 7, 310-312	
$_{1480}$ New method for the evaluation of brittleness in ceramics. 19	991 , 58, 2084-2086 12	2
1479 The role of ferroelasticity in toughening of brittle materials.	1991 , 35, 27-46 29)
1478 Slow crack growth of CVD diamond. 1992, 7, 781-783	3	

1477 X-RAY RESIDUAL STRESS MEASUREMENT OF PLASMA SPRAYED ALUMINA FILM. **1992**, 8-9, 965-974

1476	Mechanical characterization of modified Pb TiO3 ceramics and boron glasses for piezoelectric composites preparation. 1992 , 127, 167-172		
1475	Mechanical Properties of SiC Whisker-Reinforced Glass Ceramic Composites (Part 2). 1992 , 100, 541-546	;	2
1474	Mechanica and Physical Properties of Microwave Sintered Si3N4. 1992 , 269, 301		
1473	Effect of Processing on the High Temperature Mechanical Properties of MoSi2. 1992 , 288, 829		3
1472	Comparison of fracture toughness testing methods applied to Si3N4 + Si3N4-whisker system. 1992 , 26, 337-342		5
1471	The mechanical properties of ceramic composites produced by melt oxidation. 1992 , 40, 177-184		22
1470	Reliability of Ceramics Fracture Toughness Measurements by Indentation. 1992 , 109-118		3
1469	Influence of green state processing on the properties of diamond/zinc sulphide composites. 1992 , 27, 3021-3025		1
1468	Chemiomechanical effects on crack propagation: Polycrystalline 🖽 12O3. 1992 , 27, 2377-2382		5
1467	The cryochemical method for producing powders from the Al2O3-ZrO2-MgO system. 1992 , 31, 504-506		
1466	Sol G el Processed Y-PSZ Ceramics with 5 wt% Al2O3. <i>Journal of the American Ceramic Society</i> , 1992 , 75, 1032-1034	3.8	4
1465	Homogeneous Fabrication of Al2O3IrO2BiC Whisker Composite by Surface-Induced Coating. Journal of the American Ceramic Society, 1992 , 75, 3369-3376	3.8	38
1464	SiC-Whisker-Reinforced Glass-Ceramic Composites: Interfaces and Properties. <i>Journal of the American Ceramic Society</i> , 1992 , 75, 1205-1216	3.8	27
1463	Development and performance of zirconia-toughened alumina ceramic tools. 1992 , 156, 365-383		41
1462	Effect of Y2BaCuO5 on fracture toughness of YBCO prepared by a MPMG process. 1992 , 203, 103-110		68
1461	The effects of notch width on the SENB toughness for oxide ceramics. 1992 , 10, 21-31		33
1460	Structure/property relationships in sintered and thermally sprayed WC-Co. 1992 , 1, 307-315		98

1459	Behavior of polycrystalline zirconium dioxide and single crystals during indentation. 1992 , 33, 453-461	1
1458	Hot isostatic pressing of Bilicon carbide ceramics. 1993 , 19, 347-351	28
1457	Scale of microstructure effects on the impact resistance of Al2O3. 1993 , 162-164, 1073-1080	8
1456	Relationships of tetragonal precipitate statistics with bulk properties in magnesia-partially stabilized zirconia. 1993 , 11, 471-480	4
1455	Reversible 🛮 sialon transformation in heat-treated sialon ceramics. 1993, 12, 421-429	119
1454	The ratio of hardness to yield point of porous iron. 1993 , 32, 274-276	2
1453	Influence of texture on the strength and supporting capacity of boride coatings. 1993 , 32, 314-320	1
1452	Wear resistance of silicon carbide and nitride based ceramic materials. 1993 , 32, 381-385	3
1451	Adhesion testing of glass-ceramic thick films on metal substrates. 1993 , 28, 2989-2998	19
1450	Densification of zirconia-containing sialon composites by Sm2O3. 1993 , 28, 3097-3102	2
1449	Strength and toughness of barium titanate ceramics. 1993 , 28, 4988-4993	9
1448	Sintering anisotropy in slip-cast SiC-whisker/Si3N4-powder compacts. 1993 , 28, 5548-5553	7
1447	The effect of surface-limited microcracks on the effective Young's modulus of ceramics. 1993 , 28, 1910-1918	8
1446	A simple preparation method to determine fracture toughness using the single edge notched beam technique for porcelain ceramics. 1993 , 12, 417-419	1
1445	The fracture toughness of doped bismuth oxide electrolytes. 1993 , 12, 719-720	
1444	Transient Plastic Phase Processing of Titanium B oron C arbon Composites. <i>Journal of the American Ceramic Society</i> , 1993 , 76, 1445-1451	94
1443	Microstructural Characterization of Structural Ceramics Using Image Processing and Analysis. <i>Journal of the American Ceramic Society</i> , 1993 , 76, 1551-1557	3
1442	Error Propagation Biases in the Calculation of Indentation Fracture Toughness for Ceramics. <i>Journal of the American Ceramic Society</i> , 1993 , 76, 2665-2668	6

1441	Mechanical Properties of Hot Isostatically Pressed Zirconia-Toughened Alumina Ceramics Prepared from Coprecipitated Powders. <i>Journal of the American Ceramic Society</i> , 1993 , 76, 2677-2680	17
1440	Properties of Silicon NitrideMolybdenum Disilicide Particulate Ceramic Composites. <i>Journal of the American Ceramic Society</i> , 1993 , 76, 2879-2883	43
1439	Wear of Some Advanced Ceramics under a Sharp Indenter in Unidirectional Sliding. <i>Journal of the American Ceramic Society</i> , 1993 , 76, 2376-2378	9
1438	Comparison of Bulk Properties of Mg-PSZ with TemperatureII ime Contour Diagrams. <i>Journal of the American Ceramic Society</i> , 1993 , 76, 1993-1997	2
1437	Formation and sintering of corundum-rutile composite powders prepared from alkoxides. 1993 , 28, 305-312	2
1436	Mechanical fatigue of a feldspathic dental procelain. 1993 , 9, 260-4	29
1435	Structural aspects of increasing the efficiency of coatings made of high-strength materials. 1993 , 25, 662-667	2
1434	Fracture toughness of thermal spray ceramic coatings determined by the indentation technique. 1993 , 2, 35-38	59
1433	A study on the influence of workpiece properties in ultrasonic machining. 1993 , 33, 495-505	87
1432	Fracture Toughness- and Hardness-Dependent Polishing Wear of Silicon Nitride Ceramics. 1993 , 36, 652-660	11
1431	Uniaxial Compaction Modelled using the Properties of Single Crystals. 1993 , 19, 2197-2240	10
1430	Flexural strength and fracture toughness of Dicor glass-ceramic after embedment modification. 1993 , 72, 572-6	25
1429	Micro-Indentation Fracture Behavior of Al2O3-24 vol%ZrO2(Y2O3) Composites Studied by Transmission Electron Microscopy. 1993 , 34, 682-688	18
1428	Effect of whisker orientation on toughening behaviour and cutting performance of SiCwAl2O3 composite. 1993 , 9, 21-25	3
1427	Microstructure, chemical aspects, and mechanical properties of TiB2/Si3N4 and TiN/Si3N4 composites. 1994 , 9, 2349-2354	38
1426	Crack propagation and deformation behavior of Al2O3-24 vol. % ZrO2 composite studied by transmission electron microscopy. 1994 , 9, 1199-1207	18
1425	Surface toughening of liquid phase sintered silicon carbide by surface nitridation. 1994 , 13, 159-166	7
1424	Microstructure and fracture behavior of hot-pressed composites. 1994 , 20, 49-55	7

1423 Estimation of endurance of structural ceramics by dynamic fatigue testing. **1994**, 35, 154-158

1422	Analysis of Vickers indentation. 1994 , 31, 2679-2708	306
1421	Effect of randomization on ductility of brittle Fe-Si-B glass. 1994 , 29, 5589-5592	6
1420	Kinetic microhardness measurements of sialon-based ceramics. 1994 , 29, 6551-6560	11
1419	Interfacial fracture toughness measurement using indentation. 1994 , 29, 4022-4026	13
1418	Microstructural features of sintered Si3N4/SiC-whiskers composites: mechanical integrity of whiskers. 1994 , 29, 250-254	7
1417	Mechanical characterization of calcium-modified lead titanate ceramics by indentation methods. 1994 , 29, 3248-3254	16
1416	Hot isostatic pressing of tetragonal ZrO2 solid-solution powders prepared from acetylacetonates in the system ZrO2-Y2O3-Al2O3. 1994 , 29, 3719-3723	5
1415	Fracture toughness of CaO-P2O5-B2O3 glasses and glass-ceramics determined by indentation. 1994 , 29, 824-829	9
1414	Driving force for cracking by indentation in ceramics containing transformable particles. 1994 , 13, 1153-1156	
1413	Trapped cracks at indentations. 1994 , 29, 2133-2142	24
1412	Investigation of microstructure and crack behaviors in hot-pressed TiB2?Si3N4 composites. 1994 , 174, 157-164	10
1411	Microstructure and mechanical behaviour of self-reinforced Si3N4 and Si3N4-SiC whisker composites. 1994 , 13, 299-312	15
1410	The brittle/ductile transition in cubic stabilised zirconia. 1994 , 14, 447-453	14
1409	Liquid-phase hot-pressing and WC-particle reinforcement of SiC-Si composites. 1994 , 14, 549-555	6
1408	Combustion synthesis and properties of zirconia?alumina powders. 1994 , 20, 57-66	25
1407	Microstructure and fracture behavior of an Al2O3?ZrO2?SiCw ceramic composite. 1994 , 20, 91-97	5
1406	A new parameter for assessment of ceramic wear. 1994 , 179, 69-73	21

1405	The effect of nanoscale microstructures on the mechanical behavior of silicon-carbon - titanium-carbon composites. 1994 , 29, 895-902	5
1404	Metastable zirconia phases prepared from zirconium alkoxide and yttrium acetylacetonate Part 2: Hot isostatic pressing of tetragonal zirconia solid solution powders. 1994 , 29, 277-285	1
1403	Fracture toughness and evaluation of coating strength with an initial residual stress field. 1994 , 26, 40-48	6
1402	Erosion Wear Properties of Tetragonal ZrO2(Y2O3)-Toughened Al2O3 Composites. <i>Journal of the American Ceramic Society</i> , 1994 , 77, 666-672	13
1401	Indentation Studies on Y2O2-Stabilized ZrO2: I, Development of Indentation-Induced Cracks. <i>Journal of the American Ceramic Society</i> , 1994 , 77, 1185-1193	74
1400	Indentation Studies on Y2O3-Stabilized ZrO2: II, Toughness Determination from Stable Growth of Indentation-Induced Cracks. <i>Journal of the American Ceramic Society</i> , 1994 , 77, 1194-1201	51
1399	Formation and Sintering of Yttria-Doped Tetragonal Zirconia with 50 mol% Alumina Prepared by the Hydrazine Method. <i>Journal of the American Ceramic Society</i> , 1994 , 77, 1694-1696	16
1398	MECHANICAL PROPERTIES OF STONE ARTEFACT MATERIALS AND THE EFFECT OF HEAT TREATMENT*. 1994 , 36, 177-208	99
1397	Mechanical properties of natural diamonds at 1200 °C. 1994 , 3, 198-204	8
1396	Synthesis and microstructural evolution of Al?Ni?Fe?Gd metallic glass by mechanical alloying. 1994 , 42, 2275-2283	38
1395	Stoichiometry and Alloying Effects on the Phase Stability and Mechanical Properties of TiCr2-Base Laves Phase Alloys. 1994 , 364, 1401	23
1394	Fracture Toughness of Diamond Measured by Vickers Indenter Reloading Technique. 1995 , 383, 255	
1393	A simplified approach for ceramic fracture toughness evaluation by indentation. 1995 , 51, 209-215	6
1392	An analysis of the residual stress intensity factor of vickers indentation cracks. 1995 , 52, 773-776	16
1391	Investigation of silicon nitride composites toughened with prenitrided TiB2. 1995 , 21, 77-83	14
1390	Processing and properties of pressureless-sintered Si3N4?SiC composites. 1995 , 54, 348-354	10
1389	Mechanical behaviour of partially stabilized zirconia crystals with terbia and ceria additives. 1995 , 15, 1177-1184	4
1388	Effect of microstructure on erosive wear behavior of SiC ceramics. 1995 , 180, 35-41	26

1387	Zirconia crystals with yttrium and cerium oxides. 1995 , 36, 199-207		4
1386	Comparison of the effectiveness of rare-earth sintering additives on the high-temperature stability of Bialon ceramics. 1995 , 30, 5901-5909		31
1385	Mechanical properties of ⊞i3N4 whisker reinforced ♣SiAlON ceramics. 1995 , 30, 6023-6027		15
1384	Subcritical Growth of Indentation Median Cracks in Soda-Lime-Silica Glass. <i>Journal of the American Ceramic Society</i> , 1995 , 78, 650-656	3.8	24
1383	Influence of Processing Conditions on the Microstructure and Mechanical Properties of Sintered Yttrium Oxides. <i>Journal of the American Ceramic Society</i> , 1995 , 78, 716-722	3.8	18
1382	Measurement of Indentation Residual Stresses in Materials Susceptible to Slow Crack Growth. Journal of the American Ceramic Society, 1995 , 78, 173-177	3.8	5
1381	Grain Size Dependence of Hardness in Dense Submicrometer Alumina. <i>Journal of the American Ceramic Society</i> , 1995 , 78, 1118-1120	3.8	176
1380	Nonlinear Hertzian Indentation Fracture Mechanics. <i>Journal of the American Ceramic Society</i> , 1995 , 78, 2321-2327	3.8	8
1379	Nonlinear Compliance Testing Applied to Indentation Cracking in Ceramics. <i>Journal of the American Ceramic Society</i> , 1995 , 78, 2328-2334	3.8	5
1378	Direct Synthesis and Sintering of Silicon Nitridenitanium Nitride Composite. <i>Journal of the American Ceramic Society</i> , 1995 , 78, 495-496	3.8	17
1377	Alumina of high reliability by centrifugal casting. 1995 , 15, 811-821		59
1376	Determining the fracture toughness of brittle materials by Hertzian indentation. 1995 , 15, 201-207		75
1375	The mechanical properties of thin alumina films deposited by metal-organic chemical vapour deposition. 1995 , 254, 153-163		21
1374	Effect of grain boundary dopants and mean grain size on tribomechanical behavior of highly purified ⊞lumina in the mild wear regime. 1995 , 181-183, 165-177		1
1373	Factors influencing the crystallization and the densification of ultrafine Si/N/C powders. 1995 , 41, 46-5-	4	9
1372	Mechanical properties of hot isostatically pressed zirconia (2 mol% yttria)-reinforced molybdenum disilicide composite. 1995 , 30, 851-857		10
1371	Microstructure and mechanical properties of hot isostatically pressed zirconia (2 mol% yttria)-reinforced tungsten disilicide composites. 1995 , 30, 953-958		3
1370	Zirconia-mullite ceramics made from composite particles coated with amorphous phase: Part II. Effects of boria additions to the amorphous phase. 1995 , 10, 2592-2598		8

1369	Zirconia-mullite ceramics made from composite particles coated with amorphous phase: I. Effect of zirconia addition. 1995 , 10, 63-70	12
1368	An experimental fracture mechanics study of a strong interface: The silicon/glass anodic bond. 1995 , 10, 387-400	19
1367	Microstructural Uniformity and Homogeneity in Alumina Sintered by Microwave (Hybrid) Heating at 2.45 GHz. 1995 , 54, 156-161	1
1366	Microstructural characterization of a microwave-sintered silicon nitride based ceramic. 1995 , 10, 1387-1396	14
1365	Influence of indentation crack configuration on strength and fatigue behaviour of soda-lime silicate glass. 1995 , 43, 965-972	31
1364	The hot hardness testing for superplasticity in nanocrystalline Yttria Stabilized Tetragonal Zirconia. 1995 , 33, 761-766	10
1363	Evaluation of nanoscale mechanically-milled NiAl using a Miniaturized Disk-Bend Test. 1995 , 5, 337-347	9
1362	Relative fracture toughness and hardness of new dental ceramics. 1995 , 74, 145-50	128
1361	Applications in Ceramic Structures. 1995 , 707-735	1
1360	1 The mechanical properties of powders. 1995 , 1-IV	17
1359	Full-density nanocrystalline FeII9AlIICr intermetallic consolidated from mechanically milled powders. 1996 , 11, 72-80	56
1358	Surface microroughness of optical glasses under deterministic microgrinding. 1996 , 35, 4448-62	53
1357	Effect of Microstructure on the Properties of MoSi2 and its Composites. 1996 , 460, 593	
1356	Mechanical Behaviors of Si3N4-SiC/Si3N4-Si3N4 Layered Composites. 1996 , 104, 699-704	4
1355	Microstructure and Mechanical Properties of TiB2-W Cermets Prepared by HIP. 1996 , 37, 1078-1083	6
1354	Electrical and mechanical properties of composites and their laminated materials. 1996 , 31, 405-411	1
1353	Electrical and mechanical properties of composites and their laminated materials. 1996 , 31, 397-404	1
1352	Hot isostatic pressing of TiB2-ZrO2(2 mol% Y2O3) composite powders. 1996 , 31, 787-792	29

1351	Measurement of the microhardness and Young's modulus of human enamel and dentine using an indentation technique. 1996 , 41, 539-45	210
1350	Powder preparation, mechanical and electrical properties of cubic zirconia ceramics. 1996 , 16, 71-77	7
1349	Influence of CoO and Al2O3 on the phase partitioning of ZrO2-3 mol% Y2O3. 1996 , 22, 249-256	5
1348	Indentation resistance of zirconia ceramics and crystals. 1996 , 37, 73-82	1
1347	Problem of evaluating the crack resistance in ceramics of Si3N4 and ZrO2. 1996 , 37, 21-26	1
1346	The sub-critical indentation fracture process in soda-lime-silica glass. 1996 , 55, 35-46	17
1345	Apparent interface toughness of substrate and coating couples from indentation tests. 1996 , 283, 151-157	104
1344	Wear behaviour of alumina toughened zirconia materials. 1996 , 199, 113-121	19
1343	Indentation hardness and fracture toughness in single crystal TiC0.96. 1996 , 209, 329-336	71
1342	The compression mechanism of powders. 1996 , 56, 581-588	1
1341	Si3N4 and Si3N4?SiC particulate composite ceramics. 1996 , 56, 346-353	3
1340	Influence of the oxygen pressure on the chemical state of yttrium in polycrystalline ⊞lumina. Relation with microstructure and mechanical toughness. 1996 , 16, 1099-1106	20
1339	Toughening of the Al2O3?TiC ceramics by depositing thin coatings. 1996 , 79, 192-199	8
1338	Indentation size effect of thermoset polymer: Allyl diglycol carbonate (CR-39). 1996 , 15, 1523-1525	2
1337	Duplex spinel-ZrO2 ceramics. 1996 , 31, 2457-2460	7
1336	Abrasive wear of aluminium composites∄ review. 1996 , 201, 132-144	203
1335	Fracture and fracture toughness of stoichiometric MgAl2O4 crystals at room temperature. 1996 , 31, 1353-1360	7
1334	Formation and sintering of 75 mol% alumina/25 mol% zirconia (2B.5 mol% yttria) composite powder prepared by the hydrazine method. 1996 , 31, 204-208	5

1333	Microstructure, chemical reaction and mechanical properties of TiC/Si3N4 and TiN-coated TiC/Si3N4 composites. 1996 , 31, 4899-4906		6
1332	Effect of high pressure on the structure and properties of materials based on boron carbide. 1996 , 34, 491-495		2
1331	Prediction of cyclic fatigue life in ceramics. 1996 , 15, 662-663		1
1330	Indentation fracture of small brittle particles. 1996 , 15, 688-690		4
1329	Microstructural Evolution during Transient Plastic Phase Processing of Titanium Carbide-Titanium Boride Composites. <i>Journal of the American Ceramic Society</i> , 1996 , 79, 1945-1952	3.8	79
1328	Mechanical Properties of Polycrystalline Translucent Cubic Boron Nitride as Characterized by the Vickers Indentation Method. <i>Journal of the American Ceramic Society</i> , 1996 , 79, 547-549	3.8	59
1327	Crack Stability and Its Effect on Fracture Toughness of Hot-Pressed Silicon Nitride Beam Specimens. <i>Journal of the American Ceramic Society</i> , 1996 , 79, 2300-2308	3.8	28
1326	Toughness determination of zirconia toughened alumina ceramics from growth of indentation-induced cracks. 1996 , 11, 3057-3063		16
1325	Scanning electron-acoustic imaging of residual stress distributions in aluminum metal and ZrSiO4 multiphase ceramics. 1997 , 70, 589-591		18
1324	Investigation of Si3N4IIiN/Si3N4IIi3N4 trilayer composites with residual surface compression. 1997 , 12, 2357-2365		8
1323	Superplastic forming of an Ephase rich silicon nitride. 1997 , 12, 480-492		39
1322	Fabrication of multilaminated Si3N4Bi3N4/TiN composites and its anisotropic fracture behavior. 1997 , 12, 2337-2344		13
1321	Influence of porosity on the mechanical properties of cold isostatically pressed and sintered YBa2Cu3O7⊠ superconductors. 1997 , 75, 505-523		18
1320	Glass-ceramics: deterministic microgrinding, lapping, and polishing. 1997,		4
1319	BIOCOMPATIBLE PHOSPHATE GLASSES COATINGS ON TA6V: ELABORATION IN RELATION WITH MECHANICAL PROPERTIES. 1997 , 7, 17-22		
1318	Mechanical Properties of Gallium Nitride and Related Materials. 1997 , 468, 201		8
1317	Use of Indentation Technique to Measure Elastic Modulus of Plasma-Sprayed Zirconia Thermal Barrier Coating. 191-200		17
1316	Effect of Carbide Grain Size on the Sliding and Abrasive Wear Behavior of Thermally Sprayed WC-Co Coatings. 1997 , 40, 470-478		138

1315	Loose abrasive lapping hardness of optical glasses and its interpretation. 1997 , 36, 1501-16	36
1314	Crystallization of oxynitride glasses in the system Mg?Ca?Al?Si?O?N prepared with the aid of a polymeric precursor. 1997 , 217, 55-65	3
1313	Oxynitride glasses in the system Mg?Ca?Al?Si?O?N prepared with the aid of a polymeric precursor: preparation and properties. 1997 , 217, 66-71	6
1312	Influence of SiC particle size and drying method on mechanical properties and microstructure of nanocomposite. 1997 , 32, 251-257	23
1311	A new approach for toughening of ceramics. 1997 , 33, 237-240	54
1310	FRACTURE CHARACTERISTICS OF BOROSILICATE GLASSES REINFORCED BY METALLIC PARTICLES. 1997 , 20, 1235-1253	34
1309	Influence of thermal cycling on the mechanical properties of VGF melt-textured YBCO. 1997 , 279, 173-180	78
1308	Hardness variation in a cathodic hydrogen-charged austenitic stainless steel. 1997 , 37, 1499-1504	18
1307	A new method of fracture toughness determination in brittle ceramics by open-crack shape analysis. 1997 , 32, 1473-1477	6
1306	Electrical and mechanical properties of ZrO2(2Y)/TiN composites and laminates made from these materials. 1997 , 32, 583-587	7
1305	Piezoelectric and mechanical properties of Pb(Zr0.52Ti0.48)O3Pb(Y2/3W1/3)O3 (PZTPYW) ceramics. 1997 , 32, 779-782	14
1304	Prediction of static fatigue life of ceramics. 1997 , 16, 1352-1353	2
1303	Synthesis and properties of spodumene-modified mullite ceramics formed by sol-gel processing. 1997 , 16, 982-984	11
1302	Composite piezoelectric ceramicsin the PZT-SrBi2Ta2O9 system. 1997 , 8, 147-150	4
1301	Indentation brittleness of ceramics: a fresh approach. 1997 , 32, 4331-4346	332
1300	Delamination study using four-point bending of bilayers. 1997 , 32, 3851-3856	32
1299	The effect of heat-treatment on the performance of submicron SiCp-reinforced ⊞ialon composites: III. Mechanical properties. 1997 , 17, 593-598	3
1298	High-Toughness B4C-AlB12 Composites Prepared by Al Infiltration. 1997 , 17, 879-884	19

1297	SiC nanoparticle-reinforced Al2O3 matrix composites: Role of intra- and intergranular particles. 1997 , 17, 921-928	51
1296	Processing, microstructure and toughness of Al2O3 platelet-reinforced hydroxyapatite. 1997 , 17, 1361-1369	59
1295	Sintering and mechanical properties of sol-gel derived alumina-zirconia composites. 1997 , 67, 67-70	10
1294	Influences of powder preparation routes on the sintering behaviour of doped ZrO2-3 mol%Y2O3. 1997 , 23, 171-177	4
1293	A study on wear and erosion of sialon-Si3N4 whisker ceramic composites. 1997 , 203-204, 284-290	19
1292	Processing of Ultrafine Oxide-Metal Powders in the System nAl2O3[mNiO-Ni. 1998 , 33, 349-355	
1291	Effect of Copper Oxide Content on Intrinsic Properties of MgCuZn Ferrite. 1998 , 33, 915-925	34
1290	Comparison of three fracture toughness testing techniques using a dental glass and a dental ceramic. 1998 , 14, 246-55	89
1289	Microstructure and mechanical behavior of reaction hot-pressed titanium silicide and titanium silicide and tomposites. 1998 , 29, 1629-1641	73
1288	The coated surface hardness: a kinematic model. 1998 , 335, 153-159	9
1288	The coated surface hardness: a kinematic model. 1998 , 335, 153-159 Evaluation of Young's modulus of polymers from Knoop microindentation tests. 1998 , 39, 2387-2390	9
1287		
1287 1286	Evaluation of Young's modulus of polymers from Knoop microindentation tests. 1998 , 39, 2387-2390	28
1287 1286 1285	Evaluation of Young's modulus of polymers from Knoop microindentation tests. 1998 , 39, 2387-2390 Processing-microstructure-property relations in mullite-cordierite composites. 1998 , 18, 837-848	28
1287 1286 1285	Evaluation of Young's modulus of polymers from Knoop microindentation tests. 1998 , 39, 2387-2390 Processing-microstructure-property relations in mullite-cordierite composites. 1998 , 18, 837-848 Mechanical properties of toughened Al2O3@rO2@iN ceramics. 1998 , 18, 381-388	28 33 11
1287 1286 1285 1284	Evaluation of Young's modulus of polymers from Knoop microindentation tests. 1998, 39, 2387-2390 Processing-microstructure-property relations in mullite-cordierite composites. 1998, 18, 837-848 Mechanical properties of toughened Al2O3\(\textit{Z}\)rO2\(\textit{I}\)in ceramics. 1998, 18, 381-388 Toughening of PZT piezoelectric ceramics by in-situ complex structures. 1998, 18, 1059-1062 Strength/crack-size relationship for Knoop-indented bending specimens and its application to	28 33 11
1287 1286 1285 1284 1283	Evaluation of Young's modulus of polymers from Knoop microindentation tests. 1998, 39, 2387-2390 Processing-microstructure-property relations in mullite-cordierite composites. 1998, 18, 837-848 Mechanical properties of toughened Al2O3\(\textit{Q}\)rO2\(\textit{Ti}\)r Ceramics. 1998, 18, 381-388 Toughening of PZT piezoelectric ceramics by in-situ complex structures. 1998, 18, 1059-1062 Strength/crack-size relationship for Knoop-indented bending specimens and its application to silicon nitride ceramics. 1998, 18, 891-899	28 33 11 15 4

1279	Microstructural design and mechanical properties of a ternary partially stabilised zirconia alloy. 1998 , 24, 45-51	2
1278	Indentation microcracking and toughness of newly discovered ternary intermetallic phases in the Ni?Si?Mg system. 1998 , 6, 379-393	22
1277	Auto ignition synthesis and consolidation of Al2O3@rO2 nano/nano composite powders. 1998 , 13, 156-165	100
1276	Mechanical Properties of Hot-Pressed TZP Ceramics Doped with Y2O3 and Nb2O5. 1998 , 39, 262-267	1
1275	Ultrasonic Treatment of Nanostructured Powders for the Production of Zirconia Ceramics. 1998 , 520, 197	2
1274	Mechanical Properties of Zr-Al-Cu-Ni Alloy Glass at Different Quenching Condition. 1998 , 554, 149	1
1273	Models for hardness and adhesion of coatings. 1999 , 15, 447-453	22
1272	Microstructure in silicon nitride containing Ephase seeding: Part I. 1999 , 14, 2966-2973	25
1271	Sintering of cubic boron nitride without additives at 7.7 GPa and above 2000 °C. 1999 , 14, 162-169	65
1270	Sliding behaviors of a unidirectionally oriented Si3N4W/Si3N4 composite. 1999, 224, 202-210	12
1269	Effects of whisker distribution and sintering temperature on friction and wear of Si3N4-whisker-reinforced Si3N4-composites. 1999 , 225-229, 1327-1337	24
1268	Glass-reinforced hydroxyapatite composites: fracture toughness and hardness dependence on microstructural characteristics. 1999 , 20, 2085-90	108
1267	Determining indentation toughness by incorporating true hardness into fracture mechanics equations. 1999 , 19, 1585-1592	25
1266	Mechanical and electrical properties of PZT ceramics (Zr:Ti=0.40:0.60) related to Nd3+ Addition. 1999 , 60, 128-132	30
1265	LimeAluminaBilica processing incorporating minerals. 1999 , 19, 1599-1604	5
1264	Measurements of residual stresses in thin films deposited on silicon wafers by indentation fracture. 1999 , 47, 3869-3878	63
1263	Microstructure-Property Relations of Hot-Pressed Silicon Carbide-Aluminum Nitride Compositions at Room and Elevated Temperatures. <i>Journal of the American Ceramic Society</i> , 1999 , 82, 2481-2489	25
1262	Mechanical- and Physical-Property Changes of Neutron-Irradiated Chemical-Vapor-Deposited Silicon Carbide. <i>Journal of the American Ceramic Society</i> , 1999 , 82, 2490-2496	46

1261	Indentation of materials as a new method of micromechanical testing. 1999 , 38, 396-402	2
1260	Residual Stresses in Galvanizing. 1999 , 14, 413-426	2
1259	In vitro dentine hardness following gamma-irradiation and freezing. 1999 , 27, 503-7	15
1258	A review of metallic, ceramic and surface-treated metals used for bearing surfaces in human joint replacements. 1999 , 213, 107-35	122
1257	Elastic properties of translucent polycrystalline cubic boron nitride as characterized by the dynamic resonance method. 1999 , 8, 1522-1526	52
1256	CHARACTERISATION OF HYDROXYAPATITE-TRI CALCIUM PHOSPHATE BIOCERAMICS ISSUED FROM CA-DEFICIENT HYDROXYAPATITE POWDERS: INFLUENCE OF Ca/P RATIO. 1999 , 10, 214-219	5
1255	Crystallographic Orientation in Bulk Polycrystalline Silicon Carbide Produced by a Chemical Vapor Deposition (CVD) Process. 1999 , 606, 281	
1254	Comparative study on indentation fracture toughness evaluations of sodalimelilica glass. 1999 , 98, 165-171	21
1253	Effect of WC Content on Sintering, Microstructure and Properties of Ti(CN) Based Ceramics with 0-2mol% WC 1999 , 107, 1133-1136	
1252	Microstructural Characterization of GPSed-RBSN and GPSed-Si3N4 Ceramics. 2000 , 41, 312-316	18
1251	Wire Electrical Discharge Machining and Mechanical Properties of Gas Pressure Sintered MoSi2/Si3N4 Composites 2000 , 108, 469-472	3
1250	Relationship between microstructure and mechanical properties of fired Ecuadorean clay. 2000 , 99, 117-122	1
1249	Compositional effects on the fracture behaviour of alkalililicate glasses. 2000 , 23, 685-690	6
1248	Alumina ceramics toughened by a piezoelectric secondary phase. 2000 , 20, 1687-1690	52
1247	Sintering behaviour of aluminaliobium carbide composites. 2000 , 20, 1765-1769	34
1246	Effect of BaTiO3 addition on structures and mechanical properties of 3Y-TZP ceramics. 2000 , 20, 1153-1158	30
1245	Effects of composition on crystallization behaviour and mechanical properties of bioactive glass-ceramics in the MgOtaOBiO2P2O5 system. 2000 , 26, 415-420	29
1244	Effect of annealing and Fe2O3 addition on the high temperature tribological behavior of the plasma sprayed yttria-stabilized zirconia coating. 2000 , 133-134, 403-410	12

1243	Sintering behaviour of aluminalungsten carbide composites. 2000 , 284, 84-87		27
1242	Anisotropic Grain Growth and Microstructural Evolution of Dense Mullite above 1550°C. <i>Journal of the American Ceramic Society</i> , 2000 , 83, 204-10	3.8	51
1241	Effect of thermal treatments on adhesive properties of a NiCr thermal sprayed coating. 2000 , 377-378, 681-686		19
1240	Highly-Workable Alumina-Base Ceramics. 2000 , 41, 289-294		1
1239	Structural aspects of strength and methods to increase the serviceability of carbide coatings. 2000 , 39, 85-91		3
1238	Mechanical properties. 2000 , 569-624		1
1237	Micro-electrode discharge machining of TiN/Si3 N4 composites. 2000 , 99, 149-152		39
1236	Effect of SiO2 and Y2O3 additives on the anisotropic grain growth of dense mullite. 2000 , 15, 718-726		11
1235	Orientation-dependent properties of silicon nitride with aligned reinforcing grains. 2000 , 15, 130-135		20
1234	Reinforcing Al2O3 with WIII mixed carbide. 2000 , 46, 209-211		15
1233	Effect of ⊞i3N4 initial powder size on the microstructural evolution and phase transformation during sintering of Si3N4 ceramics. 2000 , 20, 1787-1794		15
1232	Abrasives. 2000,		1
1231	Mechanical properties of cubic BC2N, a new superhard phase. 2001 , 10, 2228-2231		137
1230	Fracture toughness of bone china and hard porcelain. 2001 , 100, 256-259		17
1229	Effect of rare earth (Er, Gd, Eu, Nd and La) and bismuth additives on the mechanical and piezoelectric properties of lead zirconate titanate ceramics. 2001 , 86, 134-143		82
1228	Indentation crack profiles in silicon nitride. 2001 , 21, 211-218		60
1227	3Y-TZP ceramics toughened by Sr2Nb2O7 secondary phase. 2001 , 21, 477-481		30
1226	SiCN nanocomposite: creep behaviour. 2001 , 21, 959-968		9

1225	Constrained sintering of glass, glassderamic and ceramic coatings on metal substrates. 2001 , 31, 673-681	15
1224	Specific morphological features of LaB3O6 single crystals: a new promising material for thin-layer radiation detectors. 2001 , 233, 473-476	27
1223	Synthesis and properties of cubic zirconia lumina composite by mechanical alloying. 2001, 299, 185-194	43
1222	Study of the secondary phase in gas pressure sintered Si3N4 (relation composition loughness). 2001 , 19, 419-424	4
1221	Production and indentation analysis of WC/FeMn as an alternative to cobalt-bonded hardmetals. 2001 , 47, 315-322	66
1220	Influence of annealing treatments on microstructure and toughness of liquid-phase-sintered silicon carbide. 2001 , 16, 806-816	5
1219	Surface features and residual strains in AlON grinding. 2001 , 4451, 165	1
1218	Thermal spray coating of aluminum nitride utilizing the detonation spray technique. 2002 , 17, 2514-2523	21
1217	Effect of Si2N2O content on the microstructure, properties, and erosion of silicon nitrideBi2N2O in situ composites. 2002 , 17, 2275-2280	9
1216	The mechanics of coatings. 2002 , 303-350	1
1215	Microstructures and Fracture Characteristic of Si3N4-O’SiAlON Composites using Waste-Si-Sludge. 2002 , 43, 19-23	12
1214	Rheological Modeling and Fracture of Hard Oxide Ceramics Modified by Ultra-Dispersed Diamond Nanoparticles. 2002 , 20, 209-223	2
1213	Mechanical properties of FeSi (月 FeSi2 (月and Mg2Si. 2002 , 10, 743-750	50
1212	Fabrication of silicon nitride bilayer for roller bearing by plasma activated sintering. 2002 , 56, 1093-1097	3
1211	Prestressed ceramics and improvement of impact resistance. 2002 , 57, 518-524	21
1210	Variation in the indentation toughness of silicon nitride. 2002 , 57, 643-646	7
1209	Fracture toughness of dental ceramics: comparison of bending and indentation method. 2002 , 18, 12-9	118
1208	Size effect of raw Si powder on microstructures and mechanical properties of RBSN and GPSed-RBSN bodies. 2002 , 333, 306-313	54

1207	Influence of internal stresses in superplastic joining of zirconia toughened alumina. 2002 , 50, 3475-3486	26
1206	The effect of processing conditions, amount of additives and composition on the microstructures and mechanical properties of 岳iAlON ceramics. 2002 , 22, 109-119	75
1205	Microstructural designing of silicon nitride related to toughness. 2002 , 22, 271-278	51
1204	Comparison of different alumina powders for the aqueous processing and pressureless sintering of Al2O3BiC nanocomposites. 2002 , 22, 1543-1552	32
1203	Sintering behavior and mechanical properties of nano-sized Cr3C2/Al2O3 composites prepared by MOCVI process. 2002 , 22, 2883-2892	9
1202	Microstructure of hot-pressed Ti(C,N)-based cermets. 2002 , 22, 2587-2593	62
1201	Vitrification of fly ash from municipal solid waste incinerator. 2002 , 91, 83-93	199
1200	Microstructural and mechanical properties of nanocrystalline spinel and related composites. 2002 , 28, 153-158	55
1199	Effects of Sr2Nb2O7 additive on microstructure and mechanical properties of 3YIIZP/Al2O3 ceramics. 2002 , 28, 209-215	18
1198	Conversion to glass-ceramics from glasses made by MSW incinerator fly ash for recycling. 2002 , 28, 689-694	60
1198	Conversion to glass-ceramics from glasses made by MSW incinerator fly ash for recycling. 2002 , 28, 689-694 Role of residual stresses on interface toughness of thermally sprayed coatings. 2002 , 415, 143-150	60
1197	Role of residual stresses on interface toughness of thermally sprayed coatings. 2002 , 415, 143-150 Calcium phosphate apatites with variable Ca/P atomic ratio III. Mechanical properties and	44
1197 1196	Role of residual stresses on interface toughness of thermally sprayed coatings. 2002 , 415, 143-150 Calcium phosphate apatites with variable Ca/P atomic ratio III. Mechanical properties and degradation in solution of hot pressed ceramics. 2002 , 23, 1081-9 Microstructure and mechanical properties of silicon nitride with tape cast tri-layer structures. 2003 , 9, 521-526	126
1197 1196 1195	Role of residual stresses on interface toughness of thermally sprayed coatings. 2002 , 415, 143-150 Calcium phosphate apatites with variable Ca/P atomic ratio III. Mechanical properties and degradation in solution of hot pressed ceramics. 2002 , 23, 1081-9 Microstructure and mechanical properties of silicon nitride with tape cast tri-layer structures. 2003 , 9, 521-526	144 126
1197 1196 1195	Role of residual stresses on interface toughness of thermally sprayed coatings. 2002, 415, 143-150 Calcium phosphate apatites with variable Ca/P atomic ratio III. Mechanical properties and degradation in solution of hot pressed ceramics. 2002, 23, 1081-9 Microstructure and mechanical properties of silicon nitride with tape cast tri-layer structures. 2003, 9, 521-526 Hot pressing of Bialon powder prepared by SHS method. 2003, 9, 613-618	44 126 1
1197 1196 1195 1194 1193	Role of residual stresses on interface toughness of thermally sprayed coatings. 2002, 415, 143-150 Calcium phosphate apatites with variable Ca/P atomic ratio III. Mechanical properties and degradation in solution of hot pressed ceramics. 2002, 23, 1081-9 Microstructure and mechanical properties of silicon nitride with tape cast tri-layer structures. 2003, 9, 521-526 Hot pressing of Bialon powder prepared by SHS method. 2003, 9, 613-618 Microindentation studies on samarium-modified lead titanate ceramics. 2003, 80, 446-451 Mechanical properties improvement related to the isothermal holding time in Si3N4 ceramics	44 126 1 2

1189 Sinterability, microstructure and properties of glass/ceramic composites. 2003 , 29, 251-257		54
1188 Microstructures and mechanical properties of Sr2Nb2O7-toughened 3Y-TZP ceramics. 2003 , 29, 635-640		5
Microstructural characterization of gas-pressure-sintered Bilicon nitride containing 印hase seeds. 2003 , 29, 841-846		8
Indentation fracture behavior of plasma-sprayed nanostructured Al2O3f13wt.%TiO2 coatings. 2003 , 346, 237-245		107
Formation of mullite from precursor powders: sintering, microstructure and mechanical properties. 2003 , 355, 56-61		36
1184 Toughness evaluation of HVOF WCLO coatings using non-linear regression analysis. 2003, 357, 337-345		68
TiN/Al2O3 composites and graded laminates thereof consolidated by spark plasma sintering. 2003 , 23, 1061-1068		25
Fabrication of New Cemented Carbide Containing Diamond Coated with Nanometer-Sized SiC Particles. <i>Journal of the American Ceramic Society</i> , 2003 , 86, 73-76	3.8	20
Toughening of Glass by a Piezoelectric Secondary Phase. <i>Journal of the American Ceramic Society</i> , 2003 , 86, 180-182	3.8	18
Texture in Silicon Nitride Seeded with Silicon Nitride Whiskers of Different Sizes. <i>Journal of the American Ceramic Society</i> , 2003 , 86, 1008-1013	3.8	20
Fracture toughness and crystallographic characteristics of Li6GdB3O9 single crystals. 2003 , 48, 563-567		6
Indentation behaviour of porous materials: Application to the Vickers indentation cracking of ceramics. 2003 , 83, 125-136		18
Mechanical and thermal properties of hot pressed neodymium-substituted britholite Ca9Nd(PO4)5(SiO4)F2. 2003 , 57, 3526-3531		14
1176 Synthesis and characterization of 0.3 Vf TiCIIi3SiC2 and 0.3 Vf SiCIIi3SiC2 composites. 2003 , 350, 303-312		69
Numerical modelling of the fracture behaviour of a glass matrix composite reinforced with alumina platelets. 2003 , 34, 43-51		25
1174 Improvement of mechanical property by single ion exchange process in substrate glass. 2003 , 4, 12-16		
Nanomechanical characterisation of solid surfaces and thin films. 2003 , 48, 125-164		329
1172 Microstructural Characterization of a Hot Pressed Si3N4-TiN Composite Studied by TEM. 2003 , 44, 1081-	1086	1

Examining the Fracture of Multi-Layered Coatings by Rheological Modeling of Hertzian Indentation. **2003**, 39

	Characterization of the effects of applied electric fields on fracture toughness and cyclic electric field induced fatigue crack growth for piezoceramic PIC 151. 2004 , 13, N9-N16		12
1169 (On the Mechanics of Indentation Induced Lateral Cracking. 2004 , 841, R11.11.1		
	Hardness, elasticity, and fracture toughness of polycrystalline spinel germanium nitride and tin nitride. 2004 , 19, 1392-1399		25
	Formation of in situ reinforced microstructures in Bialon ceramics: Part III. Static and dynamic ripening. 2004 , 19, 2402-2409		12
1166 l	Influence of TiN particles on the wear behavior of silicon nitrideBased composites. 2004 , 19, 542-549		7
	Effect of Carbides on the Microstructure and Properties of Ti(C,N)-Based Ceramics. <i>Journal of the American Ceramic Society</i> , 2004 , 82, 3150-3154	3.8	44
	Indentation Crack Length Anisotropy in Silicon Nitride with Aligned Reinforcing Grains. <i>Journal of the American Ceramic Society</i> , 2004 , 83, 663-665	3.8	6
	Preparation of Titanium Nitride/Alumina Laminate Composites. <i>Journal of the American Ceramic Society</i> , 2004 , 85, 1133-1138	3.8	14
	Self-Reinforced	3.8	12
	Spark-Plasma-Sintering Consolidation of SiC-Whisker-Reinforced Mullite Composites. <i>Journal of the American Ceramic Society</i> , 2004 , 87, 42-46	3.8	10
	Effects of substrate temperature during implantation on the mechanical properties of ion-implanted silicon. 2004 , 217, 598-602		2
1159	Compressive creep behavior of hot-pressed Si3N4ttRE2O3Al2O3 ceramics. 2004, 39, 1279-1289		5
1158 l	Indentation of metals by a flat-ended cylindrical punch. 2004 , 381, 281-291		76
1157 l	Indentation induced testing studies on lanthanum modified lead titanate ceramics. 2004 , 110, 177-184		11
	Dielectric and mechanical characteristics of lanthanum aluminate ceramics with strontium niobate addition. 2004 , 24, 1999-2004		11
	Synthesis of mixed disilicides/SiC composites by displacement reaction between metal carbides and silicon. 2004 , 380, 62-66		9
	Microstructure, mechanical properties and oxidation behavior of a multiphase (Mo,Cr)(Si,Al)2 intermetallic alloyBiC composite processed by reaction hot pressing. 2004 , 382, 150-161		24

1153	Scaling, dimensional analysis, and indentation measurements. 2004 , 44, 91-149	773
1152	Influence of additive content on the anisotropy in hot-pressed Si3N4 ceramics using grain orientation measurements. 2004 , 30, 653-659	17
1151	Effect of raw-Si particle size on the properties of sintered reaction-bonded silicon nitride. 2004 , 30, 965-976	30
1150	Microstructures and mechanical properties of 8Y-FSZ ceramics with BaTiO3 additive. 2004 , 30, 2269-2275	11
1149	Crack opening profiles of indentation cracks in normal and anomalous glasses. 2004 , 52, 293-297	69
1148	A new method to evaluate the fracture toughness of thin films. 2004 , 52, 3507-3517	77
1147	Anisotropy in room temperature microhardness and fracture of CaWo4 scheelite. 2004 , 52, 5529-5537	30
1146	Analysis of the influence of atmospheric plasma spray (APS) parameters on adhesion properties of alumina-titania coatings. 2004 , 18, 495-505	3
1145	New developments for fracture toughness determination by Vickers indentation. 2004 , 20, 877-884	34
1144	Application of the plasticity characteristic determined by the indentation technique for evaluation of mechanical properties of coatings: I. specific features of the test method procedure. 2004 , 36, 27-41	13
1143	Comparison of fracture characteristic of silicon nitride ceramics with and without second crystalline phase. 2004 , 58, 74-79	8
1142	Influence of porosity on the hydrostatic constraint factor for evaluating toughness from Vickers indentation cracks in brittle materials. 2004 , 84, 1-6	3
1141	Plasticity and strength of metal oxide high-temperature superconductors (Review). 2004, 30, 345-376	15
1140	Hot-Pressed Glass Matrix Composites Reinforced With Lead-Zirconate-Titanate (PZT) Particles. 2005 , 9, 25-26	
1139	P2O5 AS AN EFFECTIVE NUCLEATING AGENT OF LITHIUM DISILICATE GLASS-CERAMICS. 2005 , 19, 36-41	10
1138	Processing glasspyrochlore composites for nuclear waste encapsulation. 2005 , 341, 12-18	39
1137	Sliding wear of CrAl2O3IIrO2 and MoAl2O3IIrO2 composites. 2005, 25, 837-845	8
1136	Plasma spray formed near-net-shape MoSi2Bi3N4 bulk nanocompositesEtructure property evaluation. 2005 , 404, 165-172	14

1135	Effect of tungsten carbide additions on the microstructure and properties of hot-pressed alumina. 2005 , 406, 74-77		11
1134	AlNIIiB2 composites fabricated by spark plasma sintering. 2005 , 31, 267-270		14
1133	Crack opening displacements of Vickers indentation cracks. 2005 , 72, 647-659		52
1132	Viscous Sintering and Mechanical Properties of 3Y-TZP-Reinforced LAS Glass-Ceramic Composites. Journal of the American Ceramic Society, 2005, 80, 2982-2986	3.8	13
1131	Zinc oxide single crystals: Influence of temperature and orientation of crystals on their mechanical properties. 2005 , 50, 646-653		5
1130	Indentation of Ceramics with Spheres: A Century after Hertz. <i>Journal of the American Ceramic Society</i> , 2005 , 81, 1977-1994	3.8	498
1129	Toughening of 8Y-FSZ Ceramics by Neodymium Titanate Secondary Phase. <i>Journal of the American Ceramic Society</i> , 2005 , 88, 456-458	3.8	12
1128	Improved High-Temperature Strength of Silicon Nitride Toughened with Aligned Whisker Seeds. Journal of the American Ceramic Society, 2005, 88, 383-389	3.8	9
1127	The Mechanics of Indentation Induced Lateral Cracking. <i>Journal of the American Ceramic Society</i> , 2005 , 88, 1233-1238	3.8	67
1126	Relationship Between Microstructures and Material Properties of Novel Fibrous Al2O3[m-ZrO2)/t-ZrO2 Composites. <i>Journal of the American Ceramic Society</i> , 2005 , 88, 2874-2878	3.8	24
1125	Micromechanical Hardness of Strontium Tartrate Trihydrate Crystals. <i>Journal of the American Ceramic Society</i> , 2005 , 88, 3469-3473	3.8	5
1124	Controlled failure mechanisms toughen the dentino-enamel junction zone. 2005 , 94, 330-5		57
1123	Preparation of plate Fe60 Co8Zr10Mo5W2B15 bulk amorphous alloy and its fracture toughness. 2005 , 20, 39-41		1
1122	Mullite-SiC Whisker and Mullite-ZrO2-SiC Whisker Composites. 2005 , 325-346		
1121	Microstructure and Properties of Sintered Reaction Bonded Silicon Nitride with Aligned Whisker Seeds. 2005 , 287, 271-276		
1120	Identification of slip systems in CaWO4 scheelite. 2005 , 85, 3511-3539		13
1119	Measuring Residual Stress with the Indentation Method in Struc[tural Ceramics. 2005, 297-300, 515-520		0
1118	Hardness and fracture toughness of moissanite. 2005 , 14, 1669-1672		42

1117	Fracture Mechanics of Ceramics. 2005 ,		8
1116	Effects of Mineral Composition and Microstructure on Crack Resistance of Sintered Ore. 2006 , 13, 9-12		10
1115	Synthesis of Alumina⊠irconia Nanocomposites by Solgel Process. 2006 , 21, 652-657		4
1114	Microstructure and mechanical behaviour of reaction hot pressed multiphase Moßi B and Moßi B Al intermetallic alloys. 2006 , 14, 1461-1471		59
1113	The influence of (Ti,W)C and NbC on the mechanical behavior of alumina. 2006, 9, 171-174		15
1112	Microstructure Characterization and Mechanical Properties of TiSi2–SiC–Ti3SiC2 Composites Prepared by Spark Plasma Sintering. 2006 , 47, 845-848		11
1111	Effect of LiF on Densification and Mechanical Properties of Dy-Esialon Ceramics. 2006, 24, 225-227		2
1110	Synthesis, Microstructural Characterization, and Mechanical Property Evaluation of Vacuum Plasma Sprayed Tantalum Carbide. <i>Journal of the American Ceramic Society</i> , 2006 , 89, 1419-1425	;.8	58
1109	Fabrication of Hydroxyapatite Zirconia Composites for Orthopedic Applications. <i>Journal of the American Ceramic Society</i> , 2006 , 89, 3348-3355	3.8	43
1108	The Effect of Stoichiometry on Mechanical Properties of Boron Carbide. <i>Journal of the American Ceramic Society</i> , 2006 , 67, C-13-C-14	3.8	26
1107	The morphologies of fractured surfaces and fracture toughness in some AsBeBbBIglasses. 2006 , 252, 7917-7920		5
1106	High toughness high hardness iron based PTAW weld materials. 2006 , 428, 116-123		46
1105	Effects of residual stresses on strength and toughness of particle-reinforced TiN/Si3N4 composite: Theoretical investigation and FEM simulation. 2006 , 434, 250-258		20
1104	Estimation of fracture toughness of nitride compound layers on tool steel by application of the Vickers indentation method. 2006 , 201, 182-188		40
1103	Crack resistance and atomic structure of Li2B4O7 single crystals. 2006 , 51, 292-295		2
1102	Heat treatment effects on the tribological performance of HVOF sprayed Co-Mo-Cr-Si coatings. 2006 , 15, 802-810		45
1101	Fracture resistance of ceramics: Base diagram and R-line. 2006 , 38, 261-270		21
1100	Tribological properties of HVOF as-sprayed and heat treated CoMotrBi coatings. 2006 , 25, 43-54		14

1099	Microstructure of alumina reinforced with tungsten carbide. 2006 , 41, 3299-3302	13
1098	Palmqvist fracture toughness of a new wear-resistant weld alloy. 2006 , 37, 3617-3627	9
1097	Abrasive wear behaviour of bio-active glass ceramics containing apatite. 2006 , 29, 243-249	8
1096	Hot erosion wear and carburization in petrochemical furnaces. 2006 , 57, 135-146	1
1095	Consolidation of Al2O3 Nanopowder by Magnetic Pulsed Compaction and Sintering. 2006 , 118, 615-622	1
1094	Synthesis of Al2O3-Ni3Al Cermets by Room-Temperature Ball Milling of Al, Ni and Al2O3 Mixtures. 2006 , 509, 123-128	
1093	Residual Stress Measurement and Evaluation on Ceramics with X-Ray and Indentation Method. 2006 , 321-323, 1348-1352	
1092	Microstructure and interfacial fracture at the cementum-enamel junctions in equine and bovine teeth. 2006 , 21, 2146-2155	11
1091	Novel synthesis of advanced composites of EAl2O3 reinforced with Ce TZP through co-precipitation process. 2006 , 105, 222-227	7
1090	Microstructures and Interfaces in Melt-Growth Al2O3-Ln2O3 Based Eutectic Composites. 2006 , 45, 1377-1384	1 5
1089	Effect of some thermal treatments on interface adhesion toughness of various thick thermal spray coatings. 2006 , 22, 390-398	11
1088	Ectopic expression of dentin sialoprotein during amelogenesis hardens bulk enamel. 2007 , 282, 5340-5	39
1087	Mechanical Properties of Ceramics. 261-324	
1086	Unlubricated Sliding Wear of TiN Particle Reinforced Si3N4 Matrix Composites Against AISI-52100 Steel Ball. 2007 , 280-283, 1327-1330	
1085	Piezoelectric Composite and its Multilayer Actuator. 2007, 539-543, 3237-3242	
1084	Synthesis of WC-W2C Composite Ceramics by Reactive Resistance-Heated Hot Pressing and their Mechanical Properties. 2007 , 54, 281-286	8
1083	MECHANICAL TOUGHNESS AND PIEZOELECTRIC PROPERTIES IN A PIEZOELECTRIC COMPOSITE. 2007 , 90, 12-19	3
1082	On a ferroelastic mechanism governing the toughness of metastable tetragonal-prime (t?) yttria-stabilized zirconia. 2007 , 463, 1393-1408	162

1081	. 2007,	33
1080	Wear behaviour of Al2O3™o and Al2O3™b composites. 2007 , 262, 1346-1352	38
1079	Adhesive and cohesive properties by indentation method of plasma-sprayed hydroxyapatite coatings. 2007 , 253, 4960-4965	56
1078	Encapsulated gadolinium zirconate pyrochlore particles in soda borosilicate glass as novel radioactive waste form. 2007 , 33, 1231-1235	14
1077	On internal cone cracks induced by conical indentation in brittle materials. 2007 , 74, 2535-2546	14
1076	Effect of the addition of YAG (Y3Al5O12) nanopowder on the mechanical properties of lanthanum zirconate. 2007 , 460-461, 504-508	26
1075	Anisotropy in room temperature microhardness and indentation fracture of xenotime. 2007 , 454-455, 227-238	6
1074	Application of indentation fracture mechanics approach for determination of fracture toughness of brittle polymer systems. 2007 , 26, 51-59	22
1073	Highly dense Si3N4 crucibles used for Al casting: An investigation of the aluminumDeramic interface at high temperatures. 2007 , 184, 108-114	8
1072	Handbook of SiC properties for fuel performance modeling. 2007 , 371, 329-377	876
1071	Pressureless sintered self-reinforced Y-BiAlON ceramics. 2007 , 27, 437-443	24
1070	Comparison of fracture resistance as measured by the indentation fracture method and fracture toughness determined by the single-edge-precracked beam technique using silicon nitrides with different microstructures. 2007 , 27, 2347-2354	31
1069	Microstructural dependence of the thermal and mechanical properties of monazite LnPO4 (Ln=La to Gd). 2007 , 27, 3207-3213	35
1068	BAS, CMAS and CZAS glass coatings deposited by plasma spraying. 2007 , 27, 4575-4588	18
1067	On the Vickers Indentation Fracture Toughness Test. <i>Journal of the American Ceramic Society</i> , 2007 , 90, 673-680	483
1066	Lower-Temperature Hot-Pressed Dy-Bialon Ceramics with an LiF Additive. <i>Journal of the American Ceramic Society</i> , 2007 , 90, 1623-1625	15
1065	Development of BiAlON-SiC ceramic composites by liquid phase sintering. 2007 , 25, 77-81	21
1064	Nanoindentation study of single-crystal NaTh2(PO4)3. 2007 , 61, 4797-4799	

1063	Mechanical properties and anisotropy in hydroxyapatite single crystals. 2007, 57, 361-364	122
1062	On the nature of fracture of SrB4O7 and PbB4O7 single crystals. 2007 , 52, 889-893	3
1061	A crack extension force correlation for hard materials. 2007 , 148, 109-114	18
1060	Effect of grain width and aspect ratio on mechanical properties of Si3N4 ceramics. 2007, 42, 5431-5436	21
1059	Nickel and zirconia toughened alumina prepared by hydrothermal processing. 2007, 42, 4707-4711	3
1058	Effect of Feedstock Size and its Distribution on the Properties of Detonation Sprayed Coatings. 2007 , 16, 281-290	29
1057	Phenomena and mechanisms of crack propagation in glass-ceramics. 2008 , 1, 313-25	97
1056	The effects of processing on the ⅓->₲iAlON transformation during cycling heat treatments. 2008 , 487, 278-288	5
1055	Mechanical properties of tricalcium phosphate single crystals grown by molten salt synthesis. 2008 , 4, 1448-54	41
1054	Multifractal properties of Pyrex and silicon surfaces blasted with sharp particles. 2008 , 387, 2083-2090	19
1053	Biological materials: Structure and mechanical properties. 2008 , 53, 1-206	1675
1052	Characterization and determination of FexB layers[mechanical properties. 2008, 206, 231-240	27
1051	Residual stresses in YAG phase of melt growth Al2O3/YAG eutectic composite estimated by indentation fracture test and finite element analysis. 2008 , 28, 2309-2317	15
1050	Determination of the effective zero-point and the extraction of spherical nanoindentation stressEtrain curves. 2008 , 56, 3523-3532	178
1049	The homogeneous dispersion of surfactantless, slightly disordered, crystalline, multiwalled carbon nanotubes in ե lumina ceramics for structural reinforcement. 2008 , 56, 4070-4079	96
1048	Influence of indenter angle on cracking in Si and Ge during nanoindentation. 2008 , 56, 4458-4469	99
1047	Processing Structure Broperty correlation and decarburization phenomenon in detonation sprayed WC 112Co coatings. 2008 , 56, 5012-5026	92
1046	New microstructures in ceramic materials from the melt for high temperature applications. 2008 , 12, 499-505	40

(2009-2008)

1045	dissolution. 2008 , 75, 4898-4908	15
1044	Structure and properties of ultrafine-grained MoSi2+Si3N4 composites synthesized by mechanical alloying. 2008 , 479, 23-30	37
1043	Microstructure and properties of translucent MgBialon ceramics prepared by spark plasma sintering. 2008 , 488, 475-481	17
1042	Study of the effect of the injection molding parameters on physico-mechanical properties of aluminum nitride-based ceramics. 2008 , 30, 255-260	1
1041	In vitro evaluation of a glassderamic restorative material. 2008 , 24, 636-645	2
1040	Mechanical properties of hot-pressed ZrO2NbC ceramic composites. 2008 , 26, 14-18	23
1039	Synthesis and high-pressure sintering of lanthanum magnesium hexaaluminate. 2008 , 62, 923-925	14
1038	Lanthanum zirconate ceramic toughened by BaTiO3 secondary phase. 2008 , 452, 406-409	42
1037	Plasticity characteristic obtained by indentation. 2008, 41, 074013	56
1036	Hot erosion wear and carburization in petrochemical furnaces. 2008, 445-473	
1035	On radial crack and half-penny crack induced by Vickers indentation. 2008 , 464, 2967-2984	30
1034	Effect of Ductile and Brittle Phases on Deformation and Fracture Behaviour of Molybdenum and Niobium Silicide Based Composites. 2008 , 395, 179-192	5
1033	Gelcasting of carbide ceramics. 2008, 116, 694-699	13
1032	Effect of Cerium and Lanthanum Addition on Mechanical Properties of Bismuth Titanate Ceramics. 2009 , 409, 330-333	
1031	Influence of Thermal Effects Produced by Laser Treatment on the Tribological Behavior of Porcelain Ceramic Tiles. 2009 , 423, 41-46	5
1030	Laser gas assisted nitriding of alumina surfaces. 2009 , 25, 235-240	21
1029	Highly textured ZrB2-based ultrahigh temperature ceramics via strong magnetic field alignment. 2009 , 60, 615-618	74
1028	Residual stress in glass: indentation crack and fractography approaches. 2009 , 25, 1453-8	33

1027	Study on the mechanical properties, microstructure and oxidation resistance of Si3N4/Si3N4W/Ti(C7N3) nanocomposites ceramic tool materials. 2009 , 27, 52-60	12
1026	Properties of sintered alumina reinforced with niobium carbide. 2009 , 27, 427-430	27
1025	Fracture toughness of an 🖽 l2O3 ceramic for joint prostheses under sinter and sinter-HIP conditions. 2009 , 27, 722-728	19
1024	Microstructures and Mechanical Properties of Hot-Pressed ZrB2-Based Ceramics from Synthesized ZrB2 and ZrB2-ZrC Powders. 2009 , 11, 206-210	12
1023	Nanocrystalline hydroxyapatite with simultaneous enhancements in hardness and toughness. 2009 , 30, 6565-72	126
1022	Processing of dense nanostructured HAP ceramics by sintering and hot pressing. 2009 , 35, 1407-1413	86
1021	Characteristics of silicate glasses derived from vitrification of manganese crust tailings. 2009 , 35, 1961-1967	14
1020	Production and characteristics of glass-ceramics derived from manganese crust tailings. 2009 , 44, 3508-3513	3
1019	Effects of Tb addition on the microstructure and properties of a Ni-Mn-Ga ferromagnetic shape memory alloy. 2009 , 15, 459-463	4
1018	Hot-Pressed ZrB2BiC Ceramics with VC Addition: Chemical Reactions, Microstructures, and Mechanical Properties. <i>Journal of the American Ceramic Society</i> , 2009 , 92, 2838-2846	39
1017	Effect of artificial saliva storage on microhardness and fracture toughness of a hydrothermal glass-ceramic. 2009 , 18, 324-31	10
1016	Intrinsic stress fracture energy measurements for PECVD thin films in the SiOxCyNz:H system. 2009 , 49, 721-726	44
1015	Indentation induced lateral crack in ceramics with surface hardening. 2009, 507, 226-235	24
1014	NiAlTi coatings obtained by microwave assisted SHS: Effect of annealing on microstructural and mechanical properties. 2009 , 203, 1429-1437	36
1013	Micromechanical properties and erosive wear performance of chromium carbide based cermets. 2009 , 267, 152-159	41
1012	Correlation between phase evolution, mechanical properties and instrumented indentation response of TiB2-based ceramics. 2009 , 29, 505-516	83
1011	Microstructure and mechanical properties of an alumina@lass low temperature co-fired ceramic. 2009 , 29, 1077-1082	28
1010	Effects of Re2O3 (Re=La, Nd, Y and Yb) addition in hot-pressed ZrB2BiC ceramics. 2009 , 29, 3063-3068	37

(2010-2009)

1009	Static and dynamic mechanical properties of boron carbide processed by spark plasma sintering. 2009 , 29, 3395-3400	83
1008	Microhardness and fracture toughness of Ce0.9Gd0.1O1.95 for manufacturing solid oxide electrolytes. 2009 , 517, 91-96	20
1007	Influence of mechanical properties on impact fracture: Prediction of the milling behaviour of pharmaceutical powders by nanoindentation. 2009 , 188, 301-313	93
1006	An effort to fabricate and characterize in-situ formed graded structure in a ceramic-metal system. 2009 , 209, 2681-2692	6
1005	Effect of WC on the residual stress in the laser treated HVOF coating. 2009 , 209, 3172-3181	23
1004	Preparation and characterization of Si3N4/TiN nanocomposites ceramic tool materials. 2009 , 209, 4595-4600	11
1003	Cutting forces in turning of gray cast iron using silicon nitride based cutting tool. 2009 , 30, 2715-2720	37
1002	Effect of Y-TZP addition on the microstructure and properties of titania-based composites. 2009 , 35, 281-288	6
1001	Sintering and mechanical properties of magnesium-containing fluorapatite. 2009 , 10, 242-248	9
1000	Toughness of as-cast and partially crystallized composites of a bulk metallic glass. 2009 , 17, 835-839	27
999	ISE and fracture toughness evaluation by Vickers hardness testing of an Al3NbNb2AlAlNbNi in situ composite. 2009 , 472, 65-70	28
998	Thermophysical properties of lanthanum zirconate coating prepared by plasma spraying and the influence of post-annealing. 2009 , 486, 391-399	67
997	Influence of Chemical Mechanical Treatment on the Quality of Sapphire Article Working Surfaces and on the Evolution of Surfaces under the Action of Forces. 2009 , 363-398	
996	Thermal shock resistance and fracture toughness of liquid-phase-sintered SiC-based ceramics. 2009 , 29, 2387-2394	64
995	Effects of Homogeneous Irradiation of Electron Beam with Low Potential on Microscopic Fracture Resistance of Borosilicate Glass Surface. 2009 , 50, 1519-1525	2
994	Sintering, microstructural and mechanical characterization of combustion synthesized Y2O3 and Yb3+-Y2O3. 2009 , 117, 1258-1262	4
993	References. 439-471	
992	Microwave sintering of fine grained HAP and HAP/TCP bioceramics. 2010 , 36, 595-603	69

991	The effect of the wet-milling process on sintering temperature and the amount of additive of SiAlON ceramics. 2010 , 36, 1283-1288	22
990	Synthesis and mechanical properties of low temperature sintered, Sm3+ doped nanoceria electrolyte membranes for IT-SOFC applications. 2010 , 527, 3645-3650	23
989	Microstructure of (W,Ti)Clo system containing platelet WC. 2010, 527, 7163-7167	29
988	Microwave sintering improves the mechanical properties of biphasic calcium phosphates from hydroxyapatite microspheres produced from hydrothermal processing. 2010 , 45, 3175-3183	37
987	Sintering of self-reinforced ceramics in the ZrO2M2O3MeO2Ml2O3 system. 2010 , 49, 42-49	6
986	Sinter and hot isostatic pressing (HIP) of multi-wall carbon nanotubes (MWCNTs) reinforced ZTA nanocomposite: Microstructure and fracture toughness. 2010 , 28, 399-406	40
985	Hot-Pressed ZrB2 Ceramics With Composite Additives of Zr and B4C. 2010 , 12, 893-898	18
984	WC-reinforced (Ti,W)(CN). 2010 , 30, 793-798	36
983	The production of EsiAlON ceramics with low amounts of additive, at low sintering temperature. 2010 , 30, 2985-2990	16
982	Mechanical properties of hot-pressed ZrO2 reinforced with (W,Ti)C and Al2O3 additions. 2010 , 527, 480-484	18
981	Hardness, toughness and cracking systems of primary (Cr,Fe)23C6 and (Cr,Fe)7C3 carbides in high-carbon Cr-based alloys by indentation. 2010 , 527, 5038-5043	39
980	Intrinsic stress effect on fracture toughness of plasma enhanced chemical vapor deposited SiNx:H films. 2010 , 518, 4898-4907	53
979	Al(2)O(3(w))-Al(2)O(3(n))-ZrO(2) (TZ-3Y)(n) multi-scale nanocomposite: an alternative for different dental applications?. 2010 , 6, 563-70	24
978	Hot Pressed HfB2 and HfB2🛭0 vol%SiC Ceramics Based on HfB2 Powder Synthesized by Borothermal Reduction of HfO2*. 2010 , 7, 830-836	35
977	Elastic and Mechanical Properties of Polycrystalline Transparent Yttria as Determined by Indentation Techniques. <i>Journal of the American Ceramic Society</i> , 2010 , 93, no-no	4
976	Prestressed Ceramics Lateral Confined by Aluminum Alloy. 2010 , 177, 669-672	
975	Alumina-Copper Composites with High Fracture Toughness and Low Electrical Resistance. 2010 , 644, 43-46	3
974	Microstructure and properties of Al2O3-TiC-Ti3SiC2 composites fabricated by spark plasma sintering. 2010 , 109, 394-398	6

973	Feasibility of Using Multilayer Platelets as Toughening Agents. 2010 , 3, 1-8	2
972	Mechanical properties of silicate glasses as a function of composition. 2010 , 356, 2417-2423	61
971	Toughening alumina with layered Ti3SiC2 inclusions. 2010 , 491, 477-482	12
970	Thermal cycling behavior of La2Zr2O7 coating with the addition of Y2O3 by EB-PVD. 2010 , 508, 85-93	12
969	Microstructure and mechanical properties of TiN/Si3N4 nanocomposites by spark plasma sintering (SPS). 2010 , 508, 540-545	30
968	Barium Gallogermanate Glass Ceramics for Infrared Applications. 2010 , 26, 558-563	21
967	Bulk Crystal Growth and Wafering for PV. 2011 , 218-264	7
966	Determination of fracture toughness of bulk materials and thin films by nanoindentation: comparison of different models. 2011 , 91, 1163-1178	45
965	Fracture Toughness Determinations by Means of Indentation Fracture. 2011,	10
964	Si3N4 ceramic cutting tool sintered with CeO2 and Al2O3 additives with AlCrN coating. 2011 , 14, 514-518	5
963	Fabrication and Characterization of Tricalcium Silicate Bioceramics with High Mechanical Properties by Spark Plasma Sintering. 2011 , 8, 501-510	6
962	Effect of Heating Rate on Spark Plasma Sintering of a Nanosized Esi3N4-Based Powder. <i>Journal of the American Ceramic Society</i> , 2011 , 94, 1182-1190	22
961	Effect of Carbon Impurities on Hot-Pressed ZrB2BiC Ceramics. <i>Journal of the American Ceramic Society</i> , 2011 , 94, 3241-3244	19
960	Effect of grain size on the strength of Y3Al5O12 optical ceramics. 2011 , 47, 1160-1167	1
959	Structure and mechanical properties of Saxidomus purpuratus biological shells. 2011 , 4, 1514-30	48
958	Mechanical properties of Y2Ti2O7. 2011 , 64, 548-551	34
957	Compressive strength, hardness and fracture toughness of Al2O3 whiskers reinforced ZTA and ATZ nanocomposites: Weibull analysis. 2011 , 29, 333-340	44
956	Effect of carbon content on the microstructure and properties of (Ti0.7W0.3)C-Ni cermet. 2011 , 29, 424-428	15

955	The effect of the shape and size of the pores on the mechanical properties of porous HAP-based bioceramics. 2011 , 37, 471-479	40
954	Microstructure and fracture behavior of Ebi3N4 based nanoceramics. 2011 , 37, 641-645	14
953	Mechanical properties and bioactivity of ECa2SiO4 ceramics synthesized by spark plasma sintering. 2011 , 37, 2459-2465	36
952	A comparison of the effects of multi-wall and single-wall carbon nanotube additions on the properties of zirconia toughened alumina composites. 2011 , 49, 1599-1607	62
951	Laser controlled melting of pre-treated zirconia surface. 2011 , 257, 6912-6918	10
950	Microstructure evolution and mechanical properties of (Ti0.93W0.07)CWWC00Ni cermets. 2011 , 528, 3090-3095	27
949	Microstructure and mechanical properties of Ti-based solid-solution cermets. 2011 , 528, 2517-2521	35
948	Contribution of plastic deformation of Ti3SiC2 to the crack deflection in the Al2O3/Ti3SiC2 composites. 2011 , 528, 3270-3274	4
947	Dense fine-grained biphasic calcium phosphate (BCP) bioceramics designed by two-step sintering. 2011 , 31, 19-27	48
946	Influence of Esi3N4 particle size and heat treatment on microstructural evolution of EsiAlON ceramics. 2011 , 31, 629-635	27
945	Micro- and macro-indentation behaviour of Ba0.5Sr0.5Co0.8Fe0.2O3d perovskite. 2011 , 31, 401-408	24
944	Microstructure and properties of HfC and TaC-based ceramics obtained by ultrafine powder. 2011 , 31, 619-627	74
943	Novel electrically conductive E iAlON/TiCN composites. 2011 , 31, 903-911	14
942	Densification behavior and properties of hot-pressed ZrC ceramics with Zr and graphite additives. 2011 , 31, 1103-1111	78
941	Crack propagation and residual stress in laminated Si3N4/BN composite structures. 2011 , 31, 1841-1847	11
940	Mechanical and elastic properties of fine-grained polycrystalline scandia and erbia as determined by indentation techniques. 2011 , 31, 1703-1712	10
939	HVOF Coating of Inconel 625 Blended with WC: Fracture Toughness Measurement. 2011 , 264-265, 1972-1981	
938	The Research of SiC and Si3N4 Whiskers Reinforced Si3N4 Composites to Improve its Wear and Mechanical Properties. 2011 , 474-476, 1881-1886	1

937	Surface Cracking and Degradation of Dense Hydroxyapatite through Vickers Microindentation Testing. 2011 , 66-68, 614-619	1
936	Relationship between the Ratio of Young Modulus to Hardness and the Elastic Recovery of Nanoindentation. 2011 , 492, 5-8	2
935	Titanium Effect on Microstructure and Fracture toughness of Al2O3-BASED Composites. 2011 , 691, 32-36	
934	Statistical analysis of fracture toughness of SiC ceramics determined by Vickers indentation method. 2011 , 6, 359	
933	Evaluation of subsurface crack depth during scratch test for optical glass BK7. 2011, 225, 2767-2774	32
932	Effect of nano-TiN particles on microstructure and mechanical properties of Si3N4-based nanoceramics. 2011 , 110, 205-210	7
931	The effect of uncut chip thickness on edge chipping and wheel performance in groove grinding of single crystal silicon. 2011 , 225, 1255-1262	4
930	Effect of Sintering Temperature on Microstructure and Mechanical Properties of Al2O3-TiC-ZrO2 Ceramic Composites. 2012 , 476-478, 1031-1035	1
929	Lithium aluminosilicate reinforced with carbon nanofiber and alumina for controlled-thermal-expansion materials. 2012 , 13, 015007	9
928	Microstructural and Mechanical Properties Changes of Silicon Nitride Based Ceramic Using Post-Sintering Heat Treatment. 2012 , 727-728, 1085-1091	
927	Zirconia Blocks Properties Used for CAD/CAM Dentistry Restorations. 2012, 727-728, 804-808	1
926	Improvement in the Oxidation Resistance of EbiAlON Ceramics Produced from Mechanically Milled Powders. 2012 , 18-19, 281-290	
925	Densification and Microstructure Development in Zirconia Toughened Hardmetals. 2012, 527, 50-55	5
924	The Role of Strength in Determining Composite Material Toughness Using the Interface Indentation Fracture Test. 2012 ,	
923	Fracture Toughness Evaluation of Thin Fe-Al Intermetallic Compound Layer at Reactive Interface between Dissimilar Metals. 2012 , 76, 272-277	8
922	Methods and Investigation Techniques. 2012 , 35-93	
921	Probing material properties with sharp indenters: a retrospective. 2012 , 47, 1-22	63
920	Mechanical properties and microstructure of TiB2IIiC composite ceramic cutting tool material. 2012 , 35, 1-9	48

919	A comparative study of SiAlON ceramics. 2012, 38, 5757-5767	27
918	Use of MAX particles to improve the toughness of brittle ceramics. 2012 , 133-158	1
917	Carbon nanotube reinforced hydroxyapatite composite for orthopedic application: A review. 2012 , 32, 1727-1758	151
916	The Role of Foaming Agent and Processing Route in the Mechanical Performance of Fabricated Aluminum Foams. 2012 , 2, 95-112	23
915	Cohesive interface simulations of indentation cracking as a fracture toughness measurement method for brittle materials. 2012 , 60, 5448-5467	86
914	Polymer toughness transfer in a transparent interpenetrating glasspolymer composite. 2012 , 73, 57-63	16
913	Evaluation of mechanical hardness and fracture toughness of Co and Al co-doped ZnO. 2012 , 558, 456-461	29
912	Stress tensor dependence of the polarized Raman spectrum of tetragonal barium titanate. 2012 , 111, 013504	12
911	Determination of fracture toughness of human permanent and primary enamel using an indentation microfracture method. 2012 , 23, 2047-54	17
910	Alumina-Based Composites Reinforced with Titanium Nanoparticles. 2012 , 165-173	
909	Fabrication of High-Strength & -Fracture Toughness ZrO2/25mol%Al2O3 Composite Ceramics Using High-Pressure (1GPa) Sintering. 2012 , 61, 419-425	1
908	Laser surface treatment of high-speed steel: presence of TiC particles at the surface. 2012 , 44, 150-155	1
907	The effect of grain size on the biocompatibility, cell-materials interface, and mechanical properties of microwave-sintered bioceramics. 2012 , 100, 3059-70	15
906	Mechanical properties of the solid Li-ion conducting electrolyte: Li0.33La0.57TiO3. 2012 , 47, 5970-5977	82
905	Slow growth of microcracks in hydroxyapatite during aging. 2012 , 47, 6542-6552	2
904	Hard and tough carbon nanotube-reinforced zirconia-toughened alumina composites prepared by spark plasma sintering. 2012 , 50, 706-717	53
903	Crystallization behavior and sintering of cordierite synthesized by an aqueous solgel route. 2012 , 38, 1835-1841	16
902	The use of a controlled multiple quasi-static indentation test to characterise through-thickness penetration of composite panels. 2012 , 43, 655-662	10

(2013-2012)

901	Microstructure and mechanical properties of WCI10Co cemented carbide containing VC or (Ta, Nb)C and fracture toughness evaluation using different models. 2012 , 31, 141-146	32
900	Effects of sintering processes on mechanical properties and microstructure of TiB2IIiC+8wt% nano-Ni composite ceramic cutting tool material. 2012 , 540, 235-244	50
899	Microstructure and mechanical properties of three porous Si3N4 ceramics fabricated by different techniques. 2012 , 549, 43-49	33
898	Toughness evaluation of hard coatings and thin films. 2012 , 520, 2375-2389	182
897	A correlation between Vickers Hardness indentation values and the Bond Work Index for the grinding of brittle minerals. 2012 , 224, 217-222	22
896	Valorization of MSWI bottom ash through ceramic glazing process: a new technology. 2012 , 23, 147-157	27
895	Mechanical behaviour of the constituents inside carbon-fibre/carbon-silicon carbide composites characterised by nano-indentation. 2012 , 32, 579-588	16
894	Effect of sintering conditions and heat treatment on the properties, microstructure and machining performance of #BiAlON ceramics. 2012 , 32, 1321-1327	27
893	Microstructure refinement and mechanical properties improvement of HfB2BiC composites with the incorporation of HfC. 2012 , 32, 2557-2563	21
892	Towards physical properties tailoring of carbon nanotubes-reinforced ceramic matrix composites. 2012 , 32, 3001-3020	173
891	Pressureless sintering of HfB2BiC ceramics doped with WC. 2012 , 32, 3627-3635	37
890	Mechanical properties of materials based on MAX phases of the Ti-Al-C system. 2012 , 34, 102-109	20
889	Colorless and high strength MgO/Al2 O3 /SiO2 glass-ceramic dental material using zirconia as nucleating agent. 2012 , 100, 463-70	53
888	Alumina Toughened Zirconia Nanocomposite Incorporating Al2O3 Whiskers. 2013 , 10, 215-223	3
887	High strength glassDeramics in the system MgO/Y2O3/Al2O3/SiO2/ZrO2 without quartz as crystalline phase. 2013 , 48, 3461-3468	22
886	Properties of zirconium carbide for nuclear fuel applications. 2013 , 441, 718-742	156
885	A preliminary investigation of fracture toughness of Li7La3Zr2O12 and its comparison to other solid Li-ionconductors. 2013 , 96, 117-120	61
884	Determination of fracture toughness using the area of micro-crack tracks left in brittle materials by Vickers indentation test. 2013 , 2, 87-102	69

883	Effect of Powder Injection on the Interfacial Fracture Toughness of Plasma-Sprayed Zirconia. 2013 , 22, 166-174		11
882	Injection molding of ceramic cutting tools for wood-based materials. 2013 , 33, 3115-3122		9
881	Effects of whisker-like		22
880	Laser gas assisted treatment of tungsten carbide tile surface. 2013 , 236, 315-319		3
879	Structural characterization and mechanical properties of plasma sprayed nanostructured Cr2O3-Ag composite coatings. 2013 , 236, 91-101		13
878	Solid Particle Erosion Behavior of WC-CoCr Nanostructured Coating. 2013, 56, 781-788		14
877	Structure formation and properties of NbC-Hadfield steel cermets. 2013, 35, 292-297		7
876	Two-step microwave sintering promising technique for the processing of nanostructured bioceramics. 2013 , 93, 251-253		21
875	Formation of MAX solid solutions (Ti,V)2AlC and (Cr,V)2AlC with Al2O3 addition by SHS involving aluminothermic reduction. 2013 , 39, 7537-7544		30
874	The effect of cation type, intergranular phase amount and cation mole ratios on z value and intergranular phase crystallization of SiAlON ceramics. 2013 , 39, 3249-3259		25
873	Vickers indentation crack analysis of solid-phase-sintered silicon carbide ceramics. 2013 , 39, 841-845		14
872	Thermoelectric and mechanical properties of a hot pressed nanostructured n-type Si80Ge20 alloy. 2013 , 564, 65-70		29
871	Multifunctional Properties of Multistage Spark Plasma Sintered HA B aTiO3-Based Piezobiocomposites for Bone Replacement Applications. <i>Journal of the American Ceramic Society</i> , 2013 , 96, 3753-3759	3.8	28
870	Some studies on nucleation, crystallization, microstructure and mechanical properties of mica glass-ceramics in the system 0.2BaO[0.8K2O[4MgO[Al2O3[6SiO2[2MgF2. 2013, 39, 2551-2559]]]		9
869	In situ synthesis of ZrB2ØrCx ceramic tool materials toughened by elongated ZrB2 grains. 2013 , 49, 226-233		34
868	Microstructure and mechanical properties of hot-pressed WCMgO composites with Cr3C2 or VC addition. 2013 , 41, 41-47		7
867	Effect of heat-treatment of in-situ synthesized composite powder on properties of sintered cemented carbides. 2013 , 566, 96-101		14
866	Cavitation-erosion of 3Y-TZPs obtained at different sintering temperatures. 2013 , 300, 163-168		15

865	Preparation and characterization of Al2O3/TiC microflano-composite ceramic tool materials. 2013 , 39, 4253-4262		24	
864	Densification and mechanical properties of hot-pressed ZrN ceramics doped with Zr or Ti. 2013 , 33, 13	363-137	1 16	
863	Microstructure and mechanical properties of BAS/SiC composites sintered by spark plasma sintering. 2013 , 84, 100-104		2	
862	Liquid polycarbosilane derived SiC coating on silicon (1 1 1) wafer for enhanced mechanical properties. 2013 , 270, 219-224		11	
861	Conventional and spark-plasma sintering of cordierite powders synthesized by solgel methods. 2013 , 39, 5845-5854		5	
860	Reactive Hot Pressing of ZrCBiC Ceramics at Low Temperature. <i>Journal of the American Ceramic Society</i> , 2013 , 96, 32-36	3.8	46	
859	Effect of nitrogen and fluorine on mechanical properties and bioactivity in two series of bioactive glasses. 2013 , 23, 133-48		19	
858	Improving high temperature properties of hot pressed ZrB2🛭 0vol% SiC ceramic using high purity powders. 2013 , 39, 871-876		40	
857	Tribology of Thermal-Sprayed Coatings. 2013 , 1-43		4	
856	Study of the mechanical properties, strengthening and toughening mechanisms of Al2O3/TiC micro-nano-composite ceramic tool material. 2013 , 577, 9-15		39	
855	Combustion synthesis of CrAl and CrBi intermetallics with Al2O3 additions from Cr2O3Al and Cr2O3AlBi reaction systems. 2013 , 33, 126-133		58	
854	Synthesis, consolidation and characterization of monolithic and SiC whiskers reinforced HfB2 ceramics. 2013 , 33, 603-614		59	
853	LaNbO4 toughened NiO¥2O3 stabilized ZrO2 composite for the anode support of planar solid oxide fuel cells. 2013 , 38, 4776-4781		9	
852	Effects of the Content of ZrO2 Nanoparticles on the Microstructure and Properties of Al2O3-TiC-ZrO2 Micro-Nano-Composites. 2013 , 652-654, 304-307		O	
851	Microstructure and Mechanical Properties of FeAl Coating Deposited by Low Pressure Plasma Spray. 2013 , 333-335, 1916-1920		6	
850	Correlation between properties and microstructure of laser sintered porous -tricalcium phosphate bone scaffolds. 2013 , 14, 055002		25	
849	Pressureless Sintering of Hafnium CarbideBilicon Carbide Ceramics. <i>Journal of the American Ceramic Society</i> , 2013 , 96, 1751-1756	3.8	34	
848	Reaction Sintering of HfC/W Cermets with High Strength and Toughness. <i>Journal of the American Ceramic Society</i> , 2013 , 96, 867-872	3.8	9	

847	Fracture Toughness Evaluation of Thin Fe–Al Intermetallic Compound Layer at Reactive Interface between Dissimilar Metals. 2013 , 54, 994-1000		10
846	Mechanical Behaviour and Fracture Mechanics of Praseodymium Modified Lead Titanate Ceramics Prepared by Solid-State Reaction Route. 2013 , 2013, 1-9		2
845	Study Anisotropy of a ductile iron class 80-60-03 hardening. 2013, 45, 012010		
844	Carbon Nanotube-Reinforced Ceramic Matrix Composites: Processing and Properties. 2014 , 131-157		5
843	Superhard Materials Based on Fullerenes and Nanotubes. 2014 , 515-538		13
842	Synthesis and Properties of Single Crystalline cBN and Its Sintered Body. 2014 , 587-605		5
841	Liquid phase sintered ceramic bone scaffolds by combined laser and furnace. 2014 , 15, 14574-90		12
840	Laser Duplex Treatment of Surfaces for Improved Properties. 2014 , 279-305		O
839	Effect of Composite Sintering Aids on the Thermal and Mechanical Properties of Hot-Pressed Aluminum Nitride. 2014 , 602-603, 561-564		0
838	Fabrication of novel ZrO2(Y2O3)Al2O3 ceramics having high strength and toughness utilising pulsed electric current pressure sintering (PECPS). 2014 , 113, 73-79		4
837	Mullite Whisker Reinforced Zirconia Toughened Alumina for High Temperature Applications. 2014,		
836	Effect of Copper Oxide and Manganese Oxide on Properties and Low Temperature Degradation of Sintered Y-TZP Ceramic. 2014 , 23, 4328-4335		5
835	Tribological Properties of SiC-Reinforced Basalt-Based Coatings. 2014 , 56, 337-354		О
834	In vitro study of CaTiO3-hydroxyapatite composites for bone tissue engineering. 2014 , 60, 722-9		8
833	Microstructural Characteristic and its Relation to Mechanical Properties of Clinocardium californiense Shell. <i>Journal of the American Ceramic Society</i> , 2014 , 97, 3991-3998	3.8	20
832	High-Strength ZrC Ceramics Doped with Aluminum. <i>Journal of the American Ceramic Society</i> , 2014 , 97, 3367-3370	3.8	14
831	Effects of particulate metallic phase on microstructure and mechanical properties of carbide reinforced alumina ceramic tool materials. 2014 , 40, 2809-2817		13
830	Fracture toughness of glass sealants for solid oxide fuel cell application. 2014 , 115, 75-78		12

829	Comparison of CVD-deposited Ni and dry-blended Ni powder as sintering aids for TiN powder. 2014 , 34, 1955-1961	13
828	Effects of dispersion surfactants on the properties of ceramicBarbon nanotube (CNT) nanocomposites. 2014 , 40, 511-516	61
827	Single- and Two-Layer Coatings of Metal Blends onto Carbon Steel: Mechanical, Wear, and Friction Characterizations. 2014 , 66, 37-45	2
826	Hardness and fracture toughness of thermoelectric La3⊠ Te4. 2014 , 49, 1150-1156	21
825	Strength Characteristics of Resorbable Osteoconductive Ceramics Based on Diphosphates of Calcium and Alkali Metals. 2014 , 56, 1183-1189	4
824	An extended hardness limit in bulk nanoceramics. 2014 , 69, 9-16	121
823	Fracture behaviour of EAl2O3 ceramics reinforced with a mixture of single-wall and multi-wall carbon nanotubes. 2014 , 60, 463-470	39
822	Thermal shock behaviour of ESiAlONIIIN composites. 2014 , 40, 3611-3618	23
821	Laser Treatment of Sintered Silicon Carbide Surface for Enhanced Hydrophobicity. 2014, 66, 87-94	6
820	Fabrication of Zn4Sb3 Bulk Thermoelectric Materials Reinforced with SiC Whiskers. 2014 , 43, 2047-2052	16
819	Study on microstructure and its formation mechanism, and mechanical properties of TiB2IIiC laminated Ti(C5N5) composite ceramic cutting tool material. 2014 , 42, 169-179	8
818	Mechanical alloying, sintering and characterization of Al2O300wt%Cu nanocomposite. 2014, 40, 31-38	47
817	Development of Ce-PSZ-/Y-PSZ-Toughened Alumina Inserts for High-Speed Machining Steel. 2014 , 11, 228-239	6
816	The influence of Sr and Mn incorporated ions on the properties of microwave single- and two-step sintered biphasic HAP/TCP bioceramics. 2014 , 49, 6793-6802	15
815	Laser texturing of zirconia surface with presence of TiC and B 4 C: Surface hydrophobicity, metallurgical, and mechanical characteristics. 2014 , 40, 16159-16167	20
814	Effects of metal phases and carbides on the microstructure and mechanical properties of Ti(C,N)-based cermets cutting tool materials. 2014 , 618, 462-470	23
813	Calcium silicate ceramic scaffolds toughened with hydroxyapatite whiskers for bone tissue engineering. 2014 , 97, 47-56	33
812	Mechanical properties and deformation mechanisms of B4CIiB2 eutectic composites. 2014 , 34, 2043-2050	23

811	Simultaneous strengthening and toughening of reduced graphene oxide/alumina composites fabricated by molecular-level mixing process. 2014 , 78, 212-219	90
810	Material, Mechanical, and Tribological Characterization of Laser-Treated Surfaces. 2014 , 23, 1210-1224	
809	Tribology and Superhydrophobicity of Laser-Controlled-Melted Alumina Surfaces with Hard Particles. 2014 , 66, 1068-1079	7
808	Optical and mechanical properties of calcium phosphate glasses. 2014 , 40, 303-309	23
807	Effects of non-stoichiometry on the mechanical properties of Nd 2 Zr $2+x$ O $7+x/2$ ($x=0$, 0.1, 0.2, 0.3, 0.4, 0.5) ceramics. 2014 , 136, 157-159	30
806	Microstructure and mechanical properties of B4C based ceramics with Fe3Al as sintering aid by spark plasma sintering. 2014 , 34, 2169-2175	36
805	Laser treatment of alumina surface with chemically distinct carbide particles. 2014 , 64, 1-6	8
804	Use of Al4C3 for fabrication of aluminaliobium carbide composites by combustion synthesis. 2014 , 589, 132-136	4
803	Laser treatment of boron carbide surfaces: Metallurgical and morphological examinations. 2014 , 603, 125-131	2
802	Preparation and characterization of Si3N4/(W, Ti)C nano-composite ceramic tool materials. 2014 , 596, 255-263	11
801	Effects of superfine refractory carbide additives on microstructure and mechanical properties of TiB2IIiC+Al2O3 composite ceramic cutting tool materials. 2014 , 585, 192-202	23
800	Correlation between microstructure and properties of fine grained MoMo3SiMo5SiB2 alloys. 2014 , 48, 10-18	63
799	SPS sintering of silicon nitride with fluoride additive. 2014 , 40, 1399-1404	27
798	Microstructure and mechanical properties of La2Zr2O7(Zr0.92Y0.08)O1.96 composite ceramics prepared by spark plasma sintering. 2014 , 40, 13979-13985	12
797	Study of a hot-pressed sintering preparation of Ti(C7N3)-based composite cermets materials and their performance as cutting tools. 2014 , 611, 363-371	25
796	Fracture toughness determination and microstructure investigation of a B4CNanoTiB2 composite with various volume percent of Fe and Ni additives. 2014 , 62, 392-400	19
795	Effects of Al2O3 and NbC additives on the microstructure and mechanical properties of TiB2TiC composite ceramic cutting tool materials. 2014 , 40, 3667-3677	12
794	Fabrication of Novel ZrO2(Y2O3)-Al2O3 Ceramics Having High Strength and Toughness by Pulsed Electric-Current Pressure Sintering (PECPS) of Sol-Gel Derived Solid Solution Powders. 2014 , 1-13	

793 Alumina-Titanium Composites with Improved Fracture Toughness and Electrical Conductivity. **2014**, 37-43

792	Dopant effects on high temperature mechanical properties of zirconium carbide ceramics. 2015 , 114, 338-343		9
791	Prediction of residual stress and deformation of enameled steel. 2015, 16, 1647-1653		9
790	Thermal Stress Cleaving of Si-Wafer: Investigation of Fracture Initiation during Laser Beam Irradiation. 2015 , 1101, 412-418		1
789	Evaluation of Mechanical Properties Variations for Kr Ion-Irradiated 6H-SiC by Nanoindentation Methods. 2015 , 12, 390-398		3
788	The Compelling Case for Indentation as a Functional Exploratory and Characterization Tool. <i>Journal of the American Ceramic Society</i> , 2015 , 98, 2671-2680	3.8	58
787	Toughness Evaluation of Thin Hard Coatings and Films. 2015 , 47-122		4
786	Synthesis of (xMgO-yAl2O3-5SiO2) Ceramic via the Sol-Gel Technique in Air and under Nitrogen Gas Flow. 2015 , 64, 343-345		
7 ⁸ 5	In-situ fabricated TiB2 particle-whisker synergistically toughened Ti(C, N)-based ceramic cutting tool material. 2015 , 28, 338-342		4
784	Microscale resolution fracture toughness profiling at the zirconia-porcelain interface in dental prostheses. 2015 ,		2
783	Laser surface treatment of aluminum based composite mixed with B4C particles. 2015, 66, 129-137		11
782	Fabrication and mechanical properties of Si3N4/(W, Ti)C/Co graded nano-composite ceramic tool materials. 2015 , 41, 3381-3389		24
781	Mechanical properties and microstructure of Ti(C5N5)-TiB2-(W7Ti3)C composite cutting tool materials. 2015 , 79, 949-957		11
780	Spark plasma sintering behavior of AlON ceramics doped with different concentrations of Y2O3. 2015 , 35, 2027-2032		31
779	Densification, microstructure evolution and mechanical properties of WC doped HfB2BiC ceramics. 2015 , 35, 2707-2714		25
778	Toughening and strengthening mechanisms of porous akermanite scaffolds reinforced with nano-titania. 2015 , 5, 3498-3507		27
777	Fracture toughness testing of nanocrystalline alumina and fused quartz using chevron-notched microbeams. 2015 , 86, 385-395		80
776	Fabrication and microstructural stability of spark plasma sintered Al2O3/Er3Al5O12 eutectic. 2015 , 41, 12869-12877		14

775	Fracture Toughness of VVER and PWR Uranium-Dioxide Fuel Pellets with Different Grain Size. 2015 , 118, 117-123	3
774	Geometry of nanoindentation cube-corner cracks observed by FIB tomography: Implication for fracture resistance estimation. 2015 , 35, 2949-2955	23
773	Wear on SiAlON ceramic tools in drilling of aerospace grade CFRP composites. 2015 , 338-339, 11-21	36
772	Effect of sequential turning and burnishing on the surface integrity of CrNi-based stainless steel formed by laser cladding process. 2015 , 276, 327-335	30
771	Determination of fracture toughness of brittle materials by indentation. 2015 , 28, 221-234	17
770	Instrumented and Vickers Indentation for the Characterization of Stiffness, Hardness and Toughness of Zirconia Toughened Al2O3 and SiC Armor. 2015 , 31, 773-783	68
769	Fabrication of transparent mullite ceramic by spark plasma sintering from powders synthesized via solgel process combined with pulse current heating. 2015 , 83, 753-759	15
768	Composition and cooling-rate dependence of plastic deformation, densification, and cracking in sodium borosilicate glasses during pyramidal indentation. 2015 , 419, 97-109	29
767	Enhanced thermal expansion and fracture toughness of Sc2O3-doped Gd2Zr2O7 ceramics. 2015 , 41, 10730-10735	55
766	Microstructural development and mechanical properties of hot pressed SiC reinforced TiB2 based composite. 2015 , 51, 169-179	109
765	Measurement of fracture toughness by nanoindentation methods: Recent advances and future challenges. 2015 , 19, 324-333	129
764	In vitro bioactivity evaluation, mechanical properties and microstructural characterization of NaD-CaO-BDPDIglasses. 2015 , 144, 88-98	27
763	Submicron cubic boron nitride as hard as diamond. 2015 , 106, 121901	26
762	Evaluation of indentation fracture toughness for brittle materials based on the cohesive zone finite element method. 2015 , 134, 304-316	20
761	Evaluation of the fracture toughness of brittle hardening materials by Vickers indentation. 2015 , 148, 134-144	8
760	Effect of short milling time and microwave heating on phase evolution, microstructure and mechanical properties of alumina mullite irconia composites. 2015 , 106, 1269-1279	4
759	Effect of High-Temperature Aging on the Fracture Toughness of 40 mol% Ceria-Stabilized Zirconia. <i>Journal of the American Ceramic Society</i> , 2015 , 98, 331-337	8
758	Fabrication and characterization of Si3N4 reinforced Al2O3-based ceramic tool materials. 2015 , 41, 12798-128	3043

757	Toughening effect of Yb2O3 stabilized ZrO2 doped in Gd2Zr2O7 ceramic for thermal barrier coatings. 2015 , 648, 385-391	56
756	Demonstration of an iron-pnictide bulk superconducting magnet capable of trapping over 1 T. 2015 , 28, 112001	40
755	Nanopowder processing of ultrafine Si3N4 with improved wear resistancePeer review under responsibility of The Ceramic Society of Japan and the Korean Ceramic Society. View all notes. 2015 , 3, 6-12	3
754	Mechanical properties and microstructure of Ti(C, N) based cermet cutting tool materials fabricated by microwave sintering. 2015 , 41, 15017-15023	15
753	Mechanical properties of Mg2Si with metallic binders. 2015 , 54, 07JC03	8
75 ²	The influence of crack forms on indentation hardness test results for ceramic materials. 2015 , 50, 6096-6102	11
751	Circular channel cracks during indentation in thin films on ductile substrates. 2015 , 98, 263-270	5
750	Laser treatment of zirconia surface for improved surface hydrophobicity. 2015 , 625, 208-215	45
749	Spark Plasma Sintering and Characterization of Graphene Platelet/Ceramic Composites. 2015, 17, 716-722	12
748	Wafer Processing. 2015 , 715-755	2
74 ⁸	Wafer Processing. 2015, 715-755 Spark plasma sintering of SiC powders produced by different combustion synthesis routes. 2015, 35, 477-486	28
	Spark plasma sintering of SiC powders produced by different combustion synthesis routes. 2015 ,	
747	Spark plasma sintering of SiC powders produced by different combustion synthesis routes. 2015 , 35, 477-486 Preparation and Mechanical Properties of Graphene Nanosheet Reinforced Alumina Composites.	28
747 746	Spark plasma sintering of SiC powders produced by different combustion synthesis routes. 2015 , 35, 477-486 Preparation and Mechanical Properties of Graphene Nanosheet Reinforced Alumina Composites. 2015 , 17, 28-35	28
747 746 745	Spark plasma sintering of SiC powders produced by different combustion synthesis routes. 2015 , 35, 477-486 Preparation and Mechanical Properties of Graphene Nanosheet Reinforced Alumina Composites. 2015 , 17, 28-35 On the Fracture Toughness Measurement of Thin Film Coated Silicon Wafers. 2015 , 7, 27-30	28 50 4
747 746 745 744	Spark plasma sintering of SiC powders produced by different combustion synthesis routes. 2015, 35, 477-486 Preparation and Mechanical Properties of Graphene Nanosheet Reinforced Alumina Composites. 2015, 17, 28-35 On the Fracture Toughness Measurement of Thin Film Coated Silicon Wafers. 2015, 7, 27-30 A novel two-step sintering for nano-hydroxyapatite scaffolds for bone tissue engineering. 2014, 4, 5599	28 50 4 95
747 746 745 744 743	Spark plasma sintering of SiC powders produced by different combustion synthesis routes. 2015, 35, 477-486 Preparation and Mechanical Properties of Graphene Nanosheet Reinforced Alumina Composites. 2015, 17, 28-35 On the Fracture Toughness Measurement of Thin Film Coated Silicon Wafers. 2015, 7, 27-30 A novel two-step sintering for nano-hydroxyapatite scaffolds for bone tissue engineering. 2014, 4, 5599 Properties of silicon carbide ceramics from gelcasting and pressureless sintering. 2015, 65, 12-16 Processing, Mechanical and Optical Properties of Additive-Free ZrC Ceramics Prepared by Spark	28 50 4 95 46

739	Preparation and characterization of reduced graphene oxide/fluorhydroxyapatite composites for medical implants. 2016 , 688, 657-667		31
738	Superlattice effect for enhanced fracture toughness of hard coatings. 2016 , 124, 67-70		98
737	Directionally Solidified Boride and Carbide Eutectic Ceramics. <i>Journal of the American Ceramic Society</i> , 2016 , 99, 1837-1851	3.8	32
736	Multi-phase quasicrystalline alloys for superior wear resistance. 2016 , 108, 440-447		20
735	Effect of Nanosized TiC0.37N0.63 on Unlubricated Wear Responses of Si3N-Based Nanocomposites Under Low Hertzian Stress. <i>Journal of the American Ceramic Society</i> , 2016 , 99, 971-978	3.8	
734	Simplified method for determining fracture toughness of two dental ceramics. 2016 , 35, 76-81		4
733	Microstructural and geometric influences in the protective scales of Atractosteus spatula. 2016 , 13,		7
732	Effect of Graphite Addition on Structure and Properties of Ti(CN) Coatings Deposited by Reactive Plasma Spraying. 2016 , 25, 1588-1595		4
731	Fracture toughness measurement in fused quartz using triangular chevron-notched micro-cantilevers. 2016 , 112, 132-135		33
730	Effect of Particle Size and Titanium Content on the Fracture Toughness of Particle-Ceramic Composites. 2016 , 3, 249-257		8
729	Enhancing the sinterability and fracture toughness of Al2O3IIIN0.3 composites. 2016 , 42, 3965-3971		8
728	Reducing the erosive wear rate of Cr2AlC MAX phase ceramic by oxidative healing of local impact damage. 2016 , 358-359, 1-6		19
727	LaPO4 as a toughening agent for rare earth zirconate ceramics. 2016 , 111, 389-393		13
726	Pressureless sintering and mechanical properties of 3Y-TZP-reinforced LZAS glass-ceramic composites. 2016 , 42, 18053-18057		4
725	Characteristics of plasma sprayed coatings produced from carbon nanotube doped ceramic powder feedstock. 2016 , 112, 392-401		41
724	Fabrication of fine-grained alumina ceramics by a novel process integrating stereolithography and liquid precursor infiltration processing. 2016 , 42, 17736-17741		25
723	The effects of microstructure on Vickers indentation damage in TiC-316L stainless steel cermets. 2016 , 61, 151-161		17
722	Demonstrating the self-healing behaviour of some selected ceramics under combustion chamber conditions. 2016 , 25, 084019		27

Mechanical Properties of Plasma-Sprayed Mullite-Reinforced TitaniaBioglass Composite. 2016, 13, 1074-1083 1 721 Development of a single-phase Ca-BiAlON ceramic from nanosized precursors using spark plasma 18 720 sintering. 2016, 673, 243-249 Precision superabrasive grinding of plasma sprayed ceramic coatings. 2016, 42, 19302-19319 719 7 Phase structure and thermal conductivities of Er2O3 stabilized ZrO2 toughened Gd2Zr2O7 718 36 ceramics for thermal barrier coatings. 2016, 42, 16584-16588 Effect of microstructure on mechanical, electrical and thermal properties of B4C-HfB2 composites 717 17 prepared by arc melting. 2016, 36, 3929-3937 Processing and characterisation of plasma sprayed oxides: Microstructure, phases and residual 716 30 stress. 2016, 304, 364-374 Suspension High Velocity Oxy-Fuel (SHVOF)-Sprayed Alumina Coatings: Microstructure, 18 715 Nanoindentation and Wear. 2016, 25, 1700-1710 Structure-Properties Relationships. 2016, 75-103 714 Design and fabrication of Si3N4/(W, Ti)C graded nano-composite ceramic tool materials. 2016, 42, 13497-135065 713 Repetitive nano-impact tests as a new tool to measure fracture toughness in brittle materials. 2016 712 10 , 36, 3235-3243 Fracture Toughness of Hard and Superhard Materials: Testing Methods and Limitations. 2016, 135-165 711 Microstructure-Property Correlations for Hard, Superhard, and Ultrahard Materials. 2016, 710 10 Effect of HfC and SiC on microstructure and mechanical properties of HfB2-based ceramics. 2016, 709 19 42, 7861-7867 Effects of heat treatment on the properties of 99.5Ge23Se67Sb10-0.5CsCl glass. 2016, 127, 8379-8385 708 4 Evaluation of Fracture Toughness of Tantalum Carbide Ceramic Layer: A Vickers Indentation 18 707 Method. 2016, 25, 3057-3064 Improved Toughness and Thermal Expansion of Non-stoichiometry Gd2 IkZr2 + xO7 + x/2 Ceramics 706 47 for Thermal Barrier Coating Application. 2016, 32, 28-33 Three-step reactive hot pressing of B4C\(\mathbb{I}\)rB2 ceramics. **2016**, 36, 951-957 18 705 Application of ASTM C1421 to WC-Co fracture toughness measurement. 2016, 58, 8-13 704 7

703	A study on the relationship between microstructure and mechanical properties of acicular ferrite and upper bainite. 2016 , 663, 193-203	38
702	Anisotropic mechanical and functional properties of graphene-based alumina matrix nanocomposites. 2016 , 36, 2075-2086	49
701	Evaluating mechanical properties and crack resistance of CrN, CrTiN, CrAlN and CrTiAlN coatings by nanoindentation and scratch tests. 2016 , 285, 203-213	103
700	The mechanical and thermophysical properties of La2(Zr1⊠Cex)2O7 ceramics. 2016 , 660, 85-92	22
699	Bulk monolithic zirconium and tantalum diborides by reactive and non-reactive spark plasma sintering. 2016 , 663, 351-359	43
698	High-toughness Lu2O3-doped Si3N4 ceramics by seeding. 2016 , 42, 6495-6499	14
697	Simulation-based evaluation of surface micro-cracks and fracture toughness in high-speed grinding of silicon carbide ceramics. 2016 , 86, 799-808	34
696	Bioactive oxynitride glasses: Synthesis, structure and properties. 2016 , 36, 2869-2881	19
695	Vickers microhardness and indentation fracture toughness of tantalum sesquinitride, ∃Ta2N3. 2016 , 42, 982-985	3
694	Thermal expansion and fracture toughness of (RE0.9Sc0.1)2Zr2O7 (RE=La, Sm, Dy, Er) ceramics. 2016 , 42, 583-588	24
693	[INVITED] Laser gas assisted treatment of Ti-alloy: Analysis of surface characteristics. 2016 , 78, 159-166	8
692	Cutting performance of solid ceramic end milling tools in machining hardened AISI H13 steel. 2016 , 55, 24-32	42
691	Preparation and properties of an Al2O3/Ti(C,N) micro-nano-composite ceramic tool material by microwave sintering. 2016 , 42, 4099-4106	27
690	Cutting performance and wear mechanisms of Sialon ceramic cutting tools at high speed dry turning of gray cast iron. 2016 , 54, 330-334	16
689	Machinability evaluation and desirability function optimization of turning parameters for Cr 2 O 3 doped zirconia toughened alumina (Cr-ZTA) cutting insert in high speed machining of steel. 2016 , 42, 3338-3350	40
688	Microstructure and wear behavior of spark plasma sintering sintered Al2O3/WC-based composite. 2016 , 54, 279-283	11
687	On the Development of Experimental Methods for the Determination of Fracture Mechanical Parameters of Ceramics. 2016 , 197-214	2
686	Effect of rare earth dopants on structural and mechanical properties of nanoceria synthesized by combustion method. 2016 , 649, 168-173	9

685	Graphene nanosheet/titanium carbide composites of a fine-grained structure and improved mechanical properties. 2016 , 42, 165-172	28
684	Influence of the vol% SiC on properties of pressureless Al2O3/SiC nanocomposites. 2016 , 50, 1367-1375	23
683	Gradually varying mechanical properties of in situ synthesized NbCEe-graded composite coating. 2017 , 33, 220-226	4
682	Mechanical properties of WC-based hardmetals bonded with iron alloys 🖪 review. 2017 , 33, 507-517	20
681	Effect of Phase Structure Evolution on Thermal Expansion and Toughness of (Nd1-xScx)2Zr2O7 ($x = 0, 0.025, 0.05, 0.075, 0.1$) Ceramics. 2017 , 33, 192-197	9
68o	Fracture mechanisms of zirconium diboride ultra-high temperature ceramics under pulse loading. 2017 ,	1
679	Effect of Al metal precursor on the phase formation and mechanical properties of fine-grained SiAlON ceramics prepared by spark plasma sintering. 2017 , 37, 1975-1983	19
678	Vickers indentation fracture toughness of Y-TZP dental ceramics. 2017 , 64, 14-19	34
677	Mechanical characterization of brittle materials using instrumented indentation with Knoop indenter. 2017 , 108, 58-67	11
676	Microwave-assisted sintering of Al 2 O 3 -MWCNT nanocomposites. 2017 , 43, 6105-6109	11
675	High-strength, translucent glass-ceramics in the system MgO-ZnO-Al 2 O 3 -SiO 2 -ZrO 2. 2017 , 37, 2685-2694	25
674	Plasma sprayed carbon nanotube reinforced splats and coatings. 2017 , 37, 2235-2244	36
673	New method for extracting fracture toughness of ceramic materials by instrumented indentation test with Berkovich indenter. 2017 , 37, 2537-2545	9
672	Wear behavior of solid SiAlON milling tools during high speed milling of Inconel 718. 2017 , 378-379, 58-67	43
671	Graphene oxide/fluorhydroxyapatite composites with enhanced chemical stability, mechanical, and biological properties for dental applications. 2017 , 14, 1088-1100	4
670	Mechanical and biological properties of Al2O3 and TiO2 co-doped zirconia ceramics. 2017 , 43, 10434-10441	12
669	Fabrication of osteoconductive Ca3 \overline{M} M2x (PO4)2 (M = Na, K) calcium phosphate bioceramics by stereolithographic 3D printing. 2017 , 53, 529-535	20
668	Performance of ceramic tools in high-speed cutting iron-based superalloys. 2017 , 21, 279-290	11

667	Identification of residual stress layers at glass surfaces via crack terminating angles. <i>Journal of the American Ceramic Society</i> , 2017 , 100, 4173-4179	1
666	Reinforcement of Al2O3/TiC ceramic tool material by multi-layer graphene. 2017 , 43, 11421-11427	18
665	Methodology for measuring fracture toughness of ceramic materials by instrumented indentation test with vickers indenter. <i>Journal of the American Ceramic Society</i> , 2017 , 100, 2296-2308	7
664	Densification behaviour and physico-mechanical properties of porcelains prepared using spark plasma sintering. 2017 , 116, 307-315	9
663	Effect of two-step sintering on the hydrothermal ageing resistance of tetragonal zirconia polycrystals. 2017 , 43, 7594-7599	14
662	Graded Si3N4 ceramics with hard surface and tough core by two-step hot pressing. 2017 , 43, 7948-7950	6
661	Indentation fracture toughness behavior of FeCo-based bulk metallic glass intrinsic composites. 2017 , 457, 86-92	14
660	Dy 2 O 3 stabilized ZrO 2 as a toughening agent for Gd 2 Zr 2 O 7 ceramic. 2017 , 188, 142-144	16
659	The effect of z value on intergranular phase crystallization of ÆsiAlON-TiN composites. 2017 , 37, 923-930	13
658	Crystallization processes, compressibility, sinterability and mechanical properties of La-monazite-type ceramics. 2017 , 37, 1681-1688	9
657	Processing effects on fracture toughness of metallic glasses. 2017 , 130, 152-156	33
656	Effects of sintering additives on mechanical properties and microstructure of Si 3 N 4 ceramics by microwave sintering. 2017 , 684, 127-134	41
655	Influence of annealing on crucible-free float zone melted LaB6-TiB2 composites. 2017, 729, 749-757	9
654	Critical evaluation of indentation fracture toughness measurements with Vickers indenter on yttria-stabilized zirconia dental ceramics. 2017 , 48, 767-772	4
653	Determination of polysilicon Weibull parameters from indentation fracture. 2017 , 642, 76-81	5
652	Effect of precursor size on the structure and mechanical properties of calcium-stabilized sialon/cubic boron nitride nanocomposites. 2017 , 728, 836-843	18
651	Determining the fracture resistance of B4C-NanoSiB6 nanocomposite by Vickers indentation method and exploring its mechanical properties. 2017 , 68, 159-165	9
650	Dry sliding wear behavior of Esialon ceramics at wide range temperature from 25 to 800 °C. 2017 , 37, 4505-4513	17

649	Wire-electrical discharge machinable alumina zirconia niobium carbide composites Influence of NbC content. 2017 , 37, 4861-4867	5
648	Fabrication techniques and cutting performance of micro-textured self-lubricating ceramic cutting tools by in-situ forming of Al2O3-TiC. 2017 , 68, 121-129	32
647	The preparation and oxidation behavior of Ca-doped Bialon ceramic with elongated grains. 2017 , 722, 400-405	5
646	A reinvestigation of the validity of the indentation fracture (IF) method as applied to ceramics. 2017 , 37, 4437-4441	16
645	Effect of Arc-Current and Particle Morphology on Fracture Toughness of Plasma Sprayed Aluminium Oxide Coating. 2017 ,	
644	IM (Indentation Method) Based Impact Fracture Characteristics of cBN Crystal and Their Influence on High Speed Wheel Performance. 2017 , 41, 535-546	
643	Influences of the compositions and mechanical properties of HVOF sprayed bimodal WC-Co coating on its high temperature wear performance. 2017 , 69, 158-163	34
642	The fracture toughness of inorganic glasses. <i>Journal of the American Ceramic Society</i> , 2017 , 100, 4374-43 <u>9</u> . 6	70
641	Recent progress to understand stress corrosion cracking in sodium borosilicate glasses: linking the chemical composition to structural, physical and fracture properties. 2017 , 50, 343002	18
640	Effect of low-content of carbon nanotubes on the fracture toughness and hardness of carbon nanotube reinforced alumina prepared by sinter, HIP and sinter + HIP routes. 2017 , 4, 085004	12
639	Coherently aligned nanoparticles within a biogenic single crystal: A biological prestressing strategy. 2017 , 358, 1294-1298	67
638	Technological Peculiarities of Chromium Carbide-Based Iron Alloy Bonded Cermet. 2017 , 267, 82-86	1
637	The application of instrumented indentation test for thin coatings mechanical properties evaluation. 2017 , 857, 012030	
636	Tribological study on a novel wear-resistant AlMgB14-Si composite. 2017 , 43, 12362-12371	12
635	Effect of silver nanoparticles on the microstructure and mechanical properties of alumina ceramics. 2017 , 56, 332-339	1
634	Effects of metal binder on the microstructure and mechanical properties of Al2O3-based micro-nanocomposite ceramic tool material. 2017 , 24, 826-832	8
633	The effect of APS parameter on the microstructural, mechanical and corrosion properties of plasma sprayed Ni-Ti-Al intermetallic coatings. 2017 , 309, 959-968	23
632	Effect of the ZrO2 concentration on the crystallization behavior and the mechanical properties of high-strength MgOAl2O3BiO2 glassBeramics. 2017 , 52, 1955-1968	26

631	Reciprocating wear behaviour of TiC-stainless steel cermets. 2017, 105, 250-263	35
630	Monolithic Ceramics for Aerospace Applications. 2017 , 415-437	
629	Structural and mechanical properties of La0.6Sr0.4M0.1Fe0.9O3-I[M: Co, Ni and Cu) perovskites. 2017 , 43, 2089-2094	2
628	Mechanical properties and toughening mechanisms of graphene platelets reinforced Al2O3/TiC composite ceramic tool materials by microwave sintering. 2017 , 680, 190-196	49
627	Fluoride promoted crystallization and mechanical properties of Sr-fluorphlogopite glass. 2017 , 37, 255-260	2
626	In-situ synthesis and densification of HfB2 ceramics by the spark plasma sintering technique. 2017 , 43, 3547-3555	14
625	Fracture toughness in some hetero-modulus composite carbides: carbon inclusions and voids. 2017 , 116, 61-70	8
624	Fabrication of B4C/TiB2 Composite Ceramics Using Pulsed Electric Current Pressure Sintering. 2017 , 64, 538-546	1
623	Comparative Study of Adhesive Wear for CoCr, TiC-NiMo, WC-Co as Potential FSW Tool Materials. 2017 , 267, 224-228	
622	Evaluation of the Fracture Toughness of Titanium Nitride Hardening Coatings According to Kinetic Indentation and Acoustic Emission Parameters. 2017 , 60, 706-710	2
621	Statistical Analysis of Vickers Indentation Fracture Toughness of Y-TZP Ceramics. 2017, 41, 1-16	11
620	2.5 Laser Beam Processing for Surface Modifications. 2017 , 137-153	1
619	3.7 HVOF Coating of Nickel Based Alloys: Surface and Mechanical Characteristics. 2017, 96-110	3
618	Study on Indentation Experiments and Mechanical Behavior of RB-SiC. 2017 , 128, 03010	1
617	High toughness integrated with self-lubricity of Cu-doped Sialon ceramics at elevated temperature. 2018 , 38, 2708-2715	18
616	In situ formation of TiB 2 /TiC and TiB 2 /TiN reinforced NiAl by self-propagating combustion synthesis. 2018 , 151, 185-188	24
615	Electrochemical and biological characterization HA/Al O -YSZ nano-composite coatings using electrophoretic process. 2018 , 106, 1916-1922	8
614	Effect of cooling rate on residual stress and mechanical properties of laser remelted ceramic coating. 2018 , 38, 3932-3944	18

613	Microstructure evolution of TiC cermets with ferritic AISI 430L steel binder. 2018, 61, 197-209	6
612	Fabrication and wear behaviors of graded Si3N4 ceramics by the combination of two-step sintering and Esi3N4 seeds. 2018 , 38, 3457-3462	19
611	Structural, Mechanical, Imaging and in Vitro Evaluation of the Combined Effect of Gd and Dy in the ZrO-SiO Binary System. 2018 , 57, 4602-4612	6
610	Fracture toughness and sliding properties of magnetron sputtered CrBC and CrBCN coatings. 2018 , 443, 635-643	11
609	Graphene nanosheets toughened TiB2-based ceramic tool material by spark plasma sintering. 2018 , 44, 8977-8982	23
608	Online monitoring of laser remelting of plasma sprayed coatings to study the effect of cooling rate on residual stress and mechanical properties. 2018 , 44, 7524-7534	14
607	Tribological behavior of ÆSiAlON-TiN composites. 2018 , 38, 2279-2288	11
606	Fabrication of high-performance Al2O3-ZrO2 composite by a novel approach that integrates stereolithography-based 3D printing and liquid precursor infiltration. 2018 , 209, 31-37	15
605	Scratch-tip-size effect and change of friction coefficient in nano / micro scratch tests using XFEM. 2018 , 120, 398-410	33
604	Microstructure and wear behaviour of powder and suspension hybrid Al2O3№SZ coatings. 2018 , 44, 8498-8504	29
603	Mechanical Characteristics of Sapphire Ribbons Grown Simultaneously by EFG Method. 2018 , 53, 1700258	1
602	Fabrication and Mechanical Characterization of Nanoporous Ceramic Composites for Potential Toughening. 2018 ,	
601	Superstrong micro-grained polycrystalline diamond compact through work hardening under high pressure. 2018 , 112, 061901	16
600	Sintering mechanisms of Al 2 O 3 -based composite ceramic tools having 25% Si 3 N 4 additions. 2018 , 73, 132-138	6
599	Synthesis and characterization of ferrimagnetic glass-ceramic frit from waste. 2018 , 15, 775-782	5
598	Inert atmosphere processing of hydroxyapatite in the presence of lithium iron phosphate. 2018 , 38, 2120-213	330
597	Effects of additive amount, testing method, fabrication process and sintering temperature on the mechanical properties of Al2O3/3Y-TZP composites. 2018 , 191, 446-460	22
596	Fracture toughness, fracture energy and slow crack growth of glass as investigated by the Single-Edge Precracked Beam (SEPB) and Chevron-Notched Beam (CNB) methods. 2018 , 146, 1-11	27

595	Indentation for fracture toughness estimation of high-strength rail steels based on a stress triaxiality-dependent ductile damage model. 2018 , 94, 10-25	15
594	Determination of mode I and II adhesion toughness of monolayer thin films by circular blister tests. 2018 , 94, 34-39	5
593	SrCeO3 as a novel thermal barrier coating candidate for highEemperature applications. 2018 , 740, 519-528	27
592	Sintered TiO2 powder containing metallic Co binder prepared via mechanical carbonization, and its mechanical properties. 2018 , 44, 14044-14052	5
591	A novel method to prepare self-lubricity of Si3N4/Ag composite: Microstructure, mechanical and tribological properties. <i>Journal of the American Ceramic Society</i> , 2018 , 101, 3745-3748	11
590	Microstructure and toughening mechanisms of Al2O3/(W, Ti)C/graphene composite ceramic tool material. 2018 , 44, 13538-13543	18
589	Enhanced mechanical properties of yttrium doped ZnO nanoparticles as determined by instrumented indentation technique. 2018 , 44, 10306-10314	14
588	Microstructure Characteristics and Mechanical Properties of Nb-17Si-23Ti Ternary Alloys Fabricated by In Situ Reaction Laser Melting Deposition. 2018 , 31, 362-370	16
587	Microwave sintering of Ti(C, N)-based cermet cutting tool material. 2018, 44, 1034-1040	24
586	In situ nanostructured (TiCr)CN coating by reactive plasma spraying. 2018, 44, 712-717	5
585	Alumina-graphene nanocomposite coatings fabricated by suspension high velocity oxy-fuel thermal spraying for ultra-low-wear. 2018 , 38, 1819-1828	34
5 ⁸ 4	Influence of microstructure on the wear and corrosion behavior of detonation sprayed Cr2O3-Al2O3 and plasma sprayed Cr2O3 coatings. 2018 , 44, 2351-2357	45
583	Effect of W addition on the glass forming ability and mechanical properties of Fe-based metallic glass. 2018 , 731, 1146-1150	37
582	Evaluation of adhesion and mechanical properties of plasma sprayed NiCrAl/Al2O3-13wt.%TiO2 coatings. 2018 , 32, 801-815	3
581	Sliding wear behavior of HVOF sprayed WC-(nano-WC-Co) coating at elevated temperatures. 2018 , 206, 1-6	31
580	Analyzing the microstructures of W-ZrC composites fabricated through reaction sintering and determining their fracture toughness values by using the SENB and VIF methods. 2018 , 189, 501-513	4
579	Tuning the structural and mechanical properties in ZrO-SiO binary system through Y inclusions. 2018 , 84, 230-235	8
578	The deformation behavior and fracture toughness of single crystal YSZ(111) by indentation. 2018 , 735, 2423-2427	10

(2018-2018)

577	Effect of arcflurrent and spray distance on elastic modulus and fracture toughness of plasma-sprayed chromium oxide coatings. 2018 , 6, 387-394	8
576	A New Formula for Evaluating Indentation Toughness in Ceramics. 2018 , 58, 177-182	3
575	On the fracture toughness of bulk metallic glasses under Berkovich nanoindentation. 2018 , 481, 321-328	17
574	High-pressure sintering of bulk MoSi2: Microstructural, physical properties and mechanical behavior. 2018 , 711, 389-396	17
573	In Situ Formation of TiB2/Al2O3-Reinforced Fe3Al by Combustion Synthesis with Thermite Reduction. 2018 , 8, 288	3
572	Specific Energy of Elastoplastic Deformation Required for Crack Formation at Indentation of Hardening Coatings. 2018 , 54, 1566-1569	
571	Use of Silver Nanoparticles as Tougheners of Alumina Ceramics. 2018,	
57°	Indentation Fracture Behavior of Low Carbon Steel Thermal Spray Coatings: Role of Dry Sliding-Induced Tribolayer. 2018 , 27, 1602-1614	6
569	Fracture toughness estimation for high-strength rail steels using indentation test. 2018, 204, 469-481	3
568	Phase Composition, Thermal Conductivity, and Toughness of TiO2-Doped, Er2O3-Stabilized ZrO2 for Thermal Barrier Coating Applications. 2018 , 8, 253	8
567	Mechanical Properties of Thermoelectric Materials for Practical Applications. 2018,	8
566	Microstructure and properties of a graphene platelets toughened boron carbide composite ceramic by spark plasma sintering. 2018 , 44, 15370-15377	10
565	Enhancing toughness and strength of SiC ceramics with reduced graphene oxide by HP sintering. 2018 , 38, 4329-4337	37
564	Development and machinability evaluation of MgO doped Y-ZTA ceramic inserts for high-speed machining of steel. 2018 , 22, 899-913	20
563	Effect of Ni content and Al2O3 particle size on the thermal and mechanical properties of Al2O3/Ni composites prepared by spark plasma sintering. 2018 , 76, 25-32	18
562	Performance of Si3N4/(W, Ti)C graded ceramic tool in high-speed turning iron-based superalloys. 2018 , 44, 15579-15587	16
561	Analytical estimation of fracture toughness for circumferential cracks in thin hard films on ductile substrates. 2018 , 15, 1407-1414	
560	Microstructure and properties of submicron grained alumina ceramic tool material prepared by two-step microwave sintering. 2018 , 44, 17479-17485	13

559	Properties of 3Y-TZP zirconia ceramics with graphene addition obtained by spark plasma sintering. 2018 , 44, 16931-16936	20
558	Mechanical properties, structure, bioactivity and cytotoxicity of bioactive Na-Ca-Si-P-O-(N) glasses. 2018 , 86, 284-293	7
557	Toughening of MgAl2O4 spinel/ Si3N4 nanocomposite fabricated by spark plasma sintering. 2018 , 44, 18235-18242	14
556	Effect of Ni and graphene on microstructure and toughness of titanium boride ceramic tool material prepared by spark plasma sintering. 2018 , 44, 20299-20305	10
555	High-performance TiN reinforced Sialon matrix composites: A good combination of excellent toughness and tribological properties at a wide temperature range. 2018 , 44, 17258-17265	19
554	Enhanced anti-scratch performance of nanopatterned anti-reflective polymer films. 2018 , 458, 503-511	9
553	Self-Lubricating Si3N4-based composites toughened by in situ formation of silver. 2018 , 44, 14327-14334	18
552	Zrc ceramics incorporated with different-sized SiC particles. 2018 , 117, 383-388	10
551	Ferrimagnetic wollastonite ceramics based on waste valorization. 2018, 15, 1484-1489	2
550	Fracture toughness of Mo2BC thin films: Intrinsic toughness versus system toughening. 2018 , 154, 20-27	25
549	Effect of Co content on microstructure and mechanical properties of ultrafine grained WC-Co cemented carbide sintered by spark plasma sintering. 2018 , 44, 18711-18718	62
548	Sintering of carbon nanotube-reinforced zirconia-toughened alumina composites prepared by uniaxial pressing and cold isostatic pressing. 2018 , 5, 105602	13
547	Microstructure and improved mechanical properties of Al2O3/Ba-EAl2O3/ZrO2 composites with YSZ addition. 2018 , 38, 5113-5121	13
546	Composite nanostructured hydroxyapatite/yttrium stabilized zirconia dental inserts T he processing and application as dentin substitutes. 2018 , 44, 18200-18208	16
545	Influence of oxygen on the glass formation of MoD binary alloys. 2018 , 500, 210-216	5
544	Hydrogen in optical germanium and reduction of its negative impact on the crystal properties by ultrasonic processing. 2018 , 124, 1	1
543	Harmonized toughening and strengthening in pressurelessly reactive-sintered Ta0.8Hf0.2C-SiC composite. 2018 , 38, 5610-5614	7
542	GdPO4 as a novel candidate for thermal barrier coating applications at elevated temperatures. 2018 , 349, 400-406	17

541	Hardness and mechanical anisotropy of hexagonal SiC single crystal polytypes. 2019, 770, 158-165	23
540	Suspension high velocity oxy-fuel (SHVOF) spray of delta-theta alumina suspension: Phase transformation and tribology. 2019 , 371, 97-106	6
539	Phase equilibria in CaNaPO4-CaKPO4 system and their influence on formation of bioceramics based on mixed Ca-K-Na phosphates. 2019 , 39, 5410-5422	9
538	Dense and pure high-entropy metal diboride ceramics sintered from self-synthesized powders via boro/carbothermal reduction approach. 2019 , 62, 1898-1909	43
537	Fabrication of two-dimensional graded Al2O3-(W, Ti)CliNNiMo nano-composites by two-stage sintering. 2019 , 45, 21564-21571	7
536	Characterization of the thermo-mechanical properties of p-type (MnSi1.77) and n-type (Mg2Si0.6Sn0.4) thermoelectric materials. 2019 , 172, 28-32	9
535	Mechanical properties and epitaxial growth of TiN/AlN superlattices. 2019, 375, 1-7	12
534	Micromechanical assessment of Al/Y-substituted NASICON solid electrolytes. 2019 , 45, 21308-21314	9
533	Continuous and symmetric graded Si3N4 ceramics designed by spark plasma sintering at 15 MPa. 2019 , 45, 16703-16706	4
532	Biomimetic micro-textures, mechanical behaviors and intermittent turning performance of textured Al2O3/TiC micro-composite and micro-nano-composite ceramics. 2019 , 45, 19934-19947	10
531	Reactive sintering of TiB2-SiC-CNT ceramics. 2019, 45, 22769-22774	14
530	Determination of microstructure and mechanical properties of graphene reinforced Al2O3-Ti(C, N) ceramic composites. 2019 , 45, 20593-20599	14
529	Microstructures and mechanical properties of graphene platelets-reinforced spark plasma sintered tantalum diboride-silicon carbide composites. 2019 , 6, 115215	2
528	Self-toughening behavior of nano yttria partially stabilized hafnia ceramics. 2019 , 45, 21467-21474	7
527	Influence of carbon incorporation on microstructure and properties of titanium diboride coatings deposited by combining ion beam with magnetron sputtering. 2019 , 45, 22498-22505	2
526	Enhanced Mechanical Properties of NaPbTe/MoTe Thermoelectric Composites Through in-Situ-Formed MoTe. 2019 , 11, 41472-41481	5
525	Nanoscale deformation mechanics reveal resilience in nacre of Pinna nobilis shell. 2019 , 10, 4822	35
524	. 2019,	

523	Mechanical properties and microstructure of spark plasma sintered WC-8 wt.%Co-VC-cBN ultrafine grained cemented carbide. 2019 , 45, 23658-23665	11
522	Raman spectroscopy assisted residual stress measurement of plasma sprayed and laser remelted zirconia splats and coatings. 2019 , 378, 124920	9
521	Mechanical property and ballistic resistance of graphene platelets/B4C ceramic armor prepared by spark plasma sintering. 2019 , 45, 23781-23787	15
520	Biomimetic fabrication, mechanical behavior and interrupted turning performance of the microscopic surface structures of Al2O3/TiC micro-nano-composite ceramic. 2019 , 811, 152012	1
519	Novel HfB2-SiC-MoSi2 composites by reactive spark plasma sintering. 2019 , 809, 151705	20
518	Structure, residual stresses and mechanical properties of LaB6IIiB2 ceramic composites. 2019 , 45, 8677-8683	8
517	Magic high-pressure strengthening in tungsten carbide system. 2019 , 45, 8721-8726	13
516	Diglyceryl acrylate as alternative additive dedicated to colloidal shaping of oxide materials ☐ Synthesis, characterization and application in manufacturing of ZTA composites by gelcasting. 2019 , 39, 3421-3432	10
515	Nanoindentation of Fused Quartz at Loads Near the Cracking Threshold. 2019 , 59, 369-380	9
5 ¹ 4	Field Assisted Sintering of Nanoporous Boron Carbide with Hierarchical Microstructure. 2019,	О
513	Effect of Zr Addition on Microstructure, Hardness and Oxidation Behavior of Arc-Melted and Spark Plasma Sintered Multiphase Mo-Si-B Alloys. 2019 , 50, 2041-2060	9
512	Effect of vanadium oxide addition on thermomechanical behaviors of borosilicate glasses: Toward development of high crack resistant glasses for nuclear waste disposal. 2019 , 515, 88-97	9
511	Preparation and mechanical properties of Si3N4 nanocomposites reinforced by Si3N4@rGO particles. <i>Journal of the American Ceramic Society</i> , 2019 , 102, 6991-7002	13
510	Physical, mechanical properties and antimicrobial analysis of a novel CaOlAlO compound reinforced with Al or Ag particles. 2019 , 97, 385-395	4
509	Composite Bioceramics Engineering Based on Analysis of Phase Equilibria in the Ca3(PO4)2[aNaPO4[aKPO4 System. 2019 , 55, 516-523	4
508	Effect of Co on thermal and mechanical properties of Si3N4 based ceramic tool material. 2019 , 45, 19435-194	41 0
507	Selection principle of the synthetic route for fabrication of HfB2 and HfB2-SiC ceramics. <i>Journal of the American Ceramic Society</i> , 2019 , 102, 6427-6432	7
506	Tribological investigation of MgO/Al2O3 ceramic composite with the inclusion of nano CuO in dry abrasive wear test. 2019 , 6, 085086	11

505	The influence of mechanical activation process on the microstructure and mechanical properties of bulk Ti2AlN MAX phase obtained by reactive hot pressing. 2019 , 45, 17793-17799	12
504	Effect of YSZ with different Y2O3 contents on toughening behavior of Al2O3/Ba-FAl2O3/ZrO2 composites. 2019 , 45, 18037-18043	4
503	Microstructure and mechanical properties of 5.8 GHz microwave-sintered ZrO2/Al2O3 ceramics. 2019 , 45, 18059-18064	11
502	Microstructure and Mechanical Properties of Spark Plasma Sintered SiN/WC Ceramic Tools. 2019 , 12,	9
501	Thermophysical properties of Er3Ce7Ta2O23.5 and Dy3Ce7Ta2O23.5 oxides. 2019 , 45, 11087-11091	1
500	Analysis and characterisation of WC-10Co and AISI 4340 steel bimetal composite produced by powderBolid diffusion bonding. 2019 , 103, 3247-3263	14
499	Microstructure and mechanical properties of high-entropy borides derived from boro/carbothermal reduction. 2019 , 39, 3920-3924	53
498	A comparative study of the mechanical properties of a dinosaur and crocodile fossil teeth. 2019 , 97, 365-374	1
497	Microwave Sintering of SiAlON Ceramics with TiN Addition. 2019 , 12,	3
496	Synthesis and effect of CaTiO3 formation in CaOlAl2O3 by solid-state reaction from CaCO3lAl2O3 and Ti. 2019 , 232, 57-64	3
495	High-temperature stability of nanozirconate-toughed IMF material lanthanum synthesized by an reaction 2019 , 9, 7645-7651	1
494	Effect of molding pressure on structural and densification behavior of microwave-sintered ceramic tool material. 2019 , 16, 2085-2093	4
493	Low temperature synthesis of high-purity Ti3SiC2 via additional Si through spark plasma sintering. 2019 , 789, 313-322	10
492	OXYNITRIDE GLASSES FOR POTENTIAL BIOMEDICAL USAGE. 2019 , 33-46	
491	Mechanical strength enhancement of low temperature co-fired multilayer ceramic substrates by introducing residual stress. 2019 , 45, 10982-10990	2
490	Insights into intragranular precipitation and strengthening effect in Al2O3/SmAlO3 ceramic with eutectic composition. 2019 , 754, 382-389	3
489	Reactive sintering of bulk multi-phase ceramics based on LaB6-TiB2 eutectic granules. 2019 , 118, 217-221	1
488	Small onion-like BN leads to ultrafine-twinned cubic BN. 2019 , 62, 1169-1176	9

487	Fine grained Al2O3/SiC composite ceramic tool material prepared by two-step microwave sintering. 2019 , 45, 11826-11832	18
486	Mechanical properties of boron arsenide single crystal. 2019 , 114, 131903	15
485	Tribological property enhancement of 3Y-TZP ceramic by the combined effect of CaF2 and MgO phases. 2019 , 45, 13447-13455	19
484	Enhanced physical properties of TiSi2 doped Gd2Zr2O7 ceramic for thermal barrier coatings. 2019 , 6, 056547	
483	A review of experimental approaches to fracture toughness evaluation at the micro-scale. 2019 , 173, 107762	99
482	Al2O3/WB2 composite ceramic tool material reinforced with graphene oxide self-assembly coated silicon nitride. 2019 , 81, 173-182	4
481	Effects of SPS parameters on the densification and mechanical properties of TiB2-SiC composite. 2019 , 45, 10550-10557	27
480	Localized plasticity in silicon carbide ceramics induced by laser shock processing. 2019 , 6, 100265	9
479	Nanoscale fracture mechanics of Gondwana coal. 2019 , 204, 102-112	12
478	Effect of Addition of Multimodal YSZ and SiC Powders on the Mechanical Properties of Nanostructured Cr2O3 Plasma-Sprayed Coatings. 2019 , 28, 544-562	3
477	Bio-inspired fabrication, mechanical characterization and cutting performance evaluation of Al2O3/TiC micro-nano-composite ceramic with varying microscopic surfaces. 2019 , 45, 8286-8299	14
476	Preparation of alumina-toughened zirconia via 3D printing and liquid precursor infiltration: manipulation of the microstructure, the mechanical properties and the low temperature aging behavior. 2019 , 54, 7447-7459	10
475	Physical and mechanical properties of Si3N4/Mo laminated composite. 2019 , 544, 012017	
474	Effect of nanosized titanium and silicon carbides on synthesis and consolidation of titanium silicon carbide during spark plasma sintering. 2019 , 558, 012019	
473	Abrasive wear behavior of nano-ceria modified NiCoCrAlY coatings deposited by the high-velocity oxy-fuel process. 2019 , 6, 1250d6	17
472	Evaluation of mechanical and frictional properties of CuO added MgO/ZTA ceramics. 2019 , 6, 125208	5
47 ¹	Microstructures, thermophysical properties and thermal cycling behavior of LaZnAl11O19 thermal barrier coatings deposited by atmospheric plasma spraying. 2019 , 6, 3302-3314	8
470	Preparation of Ti-Al-N-O Ceramics by Mechanical Alloying and Spark Plasma Sintering. 2019 , 83, 136-142	

469	Additive Manufacturing Methods. 2019 , 12,	17
468	Effects of Microwave Sintering Temperature and Holding Time on Mechanical Properties and Microstructure of SiN/n-SiC ceramics. 2019 , 12,	2
467	Synthesis of the ZrN᠒rB2 Composite by Spark Plasma Sintering. 2019 , 58, 416-430	O
466	Rock-welding materials development for deep borehole nuclear waste disposal. 2019 , 221, 178-187	1
465	Thermal Behavior, Sintering and Mechanical Characterization of Multiple Ion-Substituted Hydroxyapatite Bioceramics. 2019 , 29, 87-100	25
464	Micromechanical evaluation of DP1000-GI dual-phase high-strength steel resistance spot weld. 2019 , 54, 1703-1715	5
463	Crystallization, microstructure and mechanical behavior of titanium doped barium fluormica glass-ceramics. 2019 , 16, 1471-1480	1
462	Using blister test to predict the failure pressure in bonded composite repaired pipes. 2019 , 211, 125-133	7
461	Enhanced performance of thermoelectric nanocomposites based on Cu12Sb4S13 tetrahedrite. 2019 , 57, 835-841	26
460	Temperature-driven wear behavior of Si3N4-based ceramic reinforced by in situ formed TiC0.3N0.7 particles. <i>Journal of the American Ceramic Society</i> , 2019 , 102, 4333-4343	7
459	Tribological Influences of CuO Into 3Y-TZP Ceramic Composite in Conformal Contact. 2019 , 141,	12
458	Effect of nano-size oxy-nitride starting precursors on spark plasma sintering of calcium sialons along the alpha/(alpha + beta) phase boundary. 2019 , 45, 9638-9645	11
457	Sintering behaviour and interfacial toughness of HAp/TCP coatings on HAp/Ti nanocomposite substrates. 2019 , 42, 1	1
456	Composition-microstructure-mechanical property relationships and toughening mechanisms of GdPO4-doped Gd2Zr2O7 composites. 2019 , 161, 473-482	12
455	An investigation on strength distribution, subcritical crack growth and lifetime of the lithium-ion conductor Li7La3Zr2O12. 2019 , 54, 5671-5681	18
454	Strontium doped hydroxyapatite from Mercenaria clam shells: Synthesis, mechanical and bioactivity study. 2019 , 90, 328-336	24
453	Microstructure and mechanical behaviour of SrO doped Al2O3 ceramics. 2019 , 739, 186-192	9
452	Densification and mechanical properties of spark plasma sintered Si3N4/ZrO2 nano-composites. 2019 , 776, 798-806	30

451	Effects of Yb3+ doping on phase structure, thermal conductivity and fracture toughness of (Nd1-xYbx)2Zr2O7. 2019 , 45, 3133-3139	11
450	Mechanical properties and microstructure of Ti5Si3 based composites prepared by combination of MASHS and SPS in Ti-Si-Ni and Ti-Si-Ni-C systems. 2019 , 222, 286-293	10
449	THE EFFECT OF FIBER REINFORCEMENT ON FRACTURE TOUGHNESS ASSESSMENT OF NANOCLAY FILLED POLYMER COMPOSITES. 2019 , 26, 1950050	4
448	Improvement in microstructure and mechanical properties of Ti(C, N) cermet prepared by two-step spark plasma sintering. 2019 , 45, 752-758	11
447	Mechanical and tribological evaluation of CrSiCN, CrBCN and CrSiBCN coatings. 2019, 130, 146-154	11
446	Optimum selection of tool materials for machining of high-strength steels based on fuzzy comprehensive evaluation method. 2019 , 233, 145-153	11
445	Microstructure and mechanical properties of (TiZrNbTaMo)C high-entropy ceramic. 2020, 39, 99-105	56
444	Effects of metal phases on microstructure and mechanical properties of microwave-sintered Ti(C, N)-based cermet tool. 2020 , 17, 761-770	3
443	Characterization and strengthening of porous alumina-20 wt% zirconia ceramic composites. 2020 , 46, 893-902	10
442	Tribological and wear behaviour of alumina toughened zirconia nanocomposites obtained by pressureless rapid microwave sintering. 2020 , 101, 103415	16
441	Fracture Toughness of Cold Sprayed Pure Metals. 2020 , 29, 147-157	14
440	Measurement of the mechanical properties of silver and enamel thick films using nanoindentation. 2020 , 11, 195-206	4
439	Effect of sintering temperature and TiB2 content on the grain size of B4C-TiB2 composites. 2020 , 23, 100875	8
438	Dynamic ball indentation for powder flow characterization. 2020 , 360, 1047-1054	4
437	Statistical analysis of propagation rates of indentation-induced radial cracks in soda-lime-silica glass. 2020 , 527, 119739	3
436	Performances and aging stability of new Al2O3-ZrO2-TiO2 ternary ceramic composites. 2020 , 243, 122586	3
435	Fracture behaviour of nc-TiAlN/a-Si3N4 nanocomposite coatings under cyclic nano impact testing. 2020 , 36, 671-679	3
434	Mechanical properties and machinability of GYGAG:Ce ceramic scintillators. 2020, 46, 4550-4555	5

433	Grinding of hard and brittle ceramic coatings: Force analysis. 2020, 40, 1453-1461	4
432	Wear behavior and mechanism of TiB2-based ceramic inserts in high-speed cutting of Ti6Al4V alloy. 2020 , 46, 8135-8144	8
431	Mechanical properties and microstructure of Al2O3-SiCw ceramic tool material toughened by Si3N4 particles. 2020 , 46, 8845-8852	6
430	Micro-sized polycrystalline cubic boron nitride with properties comparable to nanocrystalline counterparts. 2020 , 46, 8806-8810	4
429	Formation of MoSi/MoSi-MgAlO Composites via Self-Propagating High-Temperature Synthesis. 2019 , 25,	7
428	Cutting mechanics of wood by beetle larval mandibles. 2020 , 112, 104027	5
427	Assessing fracture toughness in sintered Al2O3@rO2(3Y)BiC ceramic composites through indentation technique. 2020 , 46, 27143-27149	4
426	Sliding of a diamond sphere on fused silica under ramping load. 2020 , 25, 101684	4
425	Applications of Micro-Indentation Technology to Estimate Fracture Toughness of Shale. 2020, 13,	1
424	Effect of SiC on Microstructure, Phase Evolution, and Mechanical Properties of Spark-Plasma-Sintered High-Entropy Ceramic Composite. 2020 , 3, 359-371	3
423	Effect of in situ VSi and SiC phases on the sintering behavior and the mechanical properties of HfB-based composites. 2020 , 10, 16540	12
422	Strong and tough HfC-HfB2 solid-solution composites obtained by reactive sintering with a SiB6 additive. 2020 , 46, 16257-16265	3
421	Reactive hot pressing route for dense ZrB2-SiC and ZrB2-SiC-CNT ultra-high temperature ceramics. 2020 , 40, 5012-5019	19
420	Improving electrical properties and toughening of PZT-based piezoelectric ceramics for high-power applications via doping rare-earth oxides. 2020 , 9, 14254-14266	10
419	Slurry erosion resistance of thermally sprayed Nb2O5 and Nb2O5+WC12Co composite coatings deposited on AISI 1020 carbon steel. 2020 , 46, 27670-27678	3
418	Performance improvement of Si3N4 ceramic cutting tools by tailoring of phase composition and microstructure. 2020 , 46, 26182-26189	8
417	Intermetallic/Ceramic Composites Synthesized from AlNiTi Combustion with B4C Addition. 2020 , 10, 873	4
416	Evolution mechanism of the microstructure and mechanical properties of plasma-sprayed yttria-stabilized hafnia thermal barrier coating at 1400 °C. 2020 , 46, 23417-23426	6

415	Preparation of complex-shaped Al2O3/SiCp/SiCw ceramic tool by two-step microwave sintering. 2020 , 46, 27362-27372	8
414	Laser treatment of SiAlON and surface characteristics. 2020 , 56, 1230-1241	2
413	High-pressure sintering of ultrafine-grained high-entropy diboride ceramics. <i>Journal of the American Ceramic Society</i> , 2020 , 103, 6655-6658	6
412	Study of the structure and mechanical properties of engineering products made of austenitic-martensitic steel, using the metal magnetic memory technique. 2020 , 64, 1887-1895	
411	Sintering behavior, mechanical properties, and biocompatibility of TiO2to-calcium phosphates composites prepared by AROS process. 2020 , 252, 123255	
410	Combustion synthesis of FeAlAl2O3 composites with TiB2 and TiC additions via metallothermic reduction of Fe2O3 and TiO2. 2020 , 30, 2510-2517	1
409	Corrosion Resistance of Ceramics Based on SiC under Hydrothermal Conditions. 2020 , 55, 672-682	2
408	Experimental and Theoretical Estimation of Fracture Toughness in Salt Rocks in Testing of Samples with Wedge-Shaped Cut. 2020 , 56, 167-173	
407	Effect of annealing temperature on the microstructure evolution, mechanical and wear behavior of NiCrWCI o HVOF-sprayed coatings. 2020 , 35, 2798-2807	3
406	High Velocity Oxygen Liquid-Fuel (HVOLF) Spraying of WC-Based Coatings for Transport Industrial Applications. 2020 , 10, 1675	5
405	Characterization and evaluation of copper-doped akermanite ceramic. 2020, 943, 012008	1
404	Reinforcing effect of laminate structure on the fracture toughness of Al3Ti intermetallic. 2020 , 27, 678-686	4
403	Lubrication degradation mechanism of Mo-S-Ti composite films irradiated by heavy ions. 2020 , 517, 146131	1
402	Performance of Ceramic-Metal Composites as Potential Tool Materials for Friction Stir Welding of Aluminium, Copper and Stainless Steel. 2020 , 13,	7
401	Physico-mechanical behaviour of alkali and alkaline earth metal-containing mica glassderamics: a comparative evaluation. 2020 , 57, 520-529	1
400	Performance of different coating materials against slurry erosion failure in hydrodynamic turbines: A review. 2020 , 115, 104622	22
399	Effect of ZrC and ZrO2 Additions on the Microstructure and Properties of ZrB2BiC Ceramics. 2020 , 56, 522-527	О
398	Phase evolution, mechanical properties and MRI contrast behavior of GdPO doped hydroxyapatite for dental applications. 2020 , 111, 110858	3

(2020-2020)

397	Neural network implementation for the prediction of load curves of a flat head indenter on hot aluminum alloy. 2020 , 88, 543-548	3
396	Thermal cycling effect on the phase stability and fracture resistance of synthetic barium/magnesium aluminosilicate systems. 2020 , 46, 24129-24136	1
395	Addition of h-BN for enhanced machinability and high mechanical strength of AlN/Mo composites. 2020 , 46, 20097-20104	4
394	Effect of high-temperature oxidation on Si3N4 containing Ti3AlC2. 2020 , 46, 14697-14705	4
393	Novel process for the production of 3Y-TZP ceramics: comparison between ageing in artificial saliva and accelerated ageing. 2020 , 7, 065402	
392	Stress-localization induced toughening in CNTBilica nanocomposites. 2020 , 127, 154306	1
391	Characterization and in vitro bioactivity study of a new glass ceramic from mica/apatite glass mixtures. 2020 , 9, 7558-7569	5
390	Fabrication and characterization of FAST sintered micro/nano boron carbide composites with enhanced fracture toughness. 2020 , 40, 5272-5285	8
389	Influence of doping Mg2+ or Ti4+ captions on the microstructures, thermal radiation and thermal cycling behavior of plasma-sprayed Gd2Zr2O7 coatings. 2020 , 46, 13054-13065	4
388	Preparation and characterization of SrZrO3IIa2Ce2O7 composite ceramics as a thermal barrier coating material. 2020 , 247, 122904	9
387	Performance analysis of laser-induced biomimetic ceramic tools in interrupted cutting. 2020 , 177, 105589	3
386	Microstructure and mechanical properties of B4C-TiB2 composite ceramic fabricated by reactive spark plasma sintering. 2020 , 92, 105307	7
385	Multifunctional Response of Piezoelectric Sodium Potassium Niobate (NKN)-Toughened Hydroxyapatite-Based Biocomposites 2020 , 3, 5287-5299	6
384	Low temperature synthesis of highly pure cordierite materials by spark plasma sintering nano-oxide powders. 2020 , 46, 23910-23921	3
383	The effects of adding CNTs and GNPs on the microstructure and mechanical properties of hexagonal-boron nitride. 2020 , 46, 22005-22014	1
382	Dissimilar sintered calcium phosphate dental inserts as dentine substitutes: Shear bond strength to restorative materials. 2020 , 108, 2461-2470	1
381	The novel Sialon-Sn composite with high toughness and wear resistance prepared at a lower-temperature. 2020 , 147, 106239	3
380	On the relation between fracture toughness and crack resistance in oxide glasses. 2020 , 534, 119946	14

379	Surface Reflectance: an Optical Method for Multiscale Curvature Characterization of Wear on Ceramic-Metal Composites. 2020 , 13,	3
378	Silicon nitride composites with magnesia and alumina additives: Toughening mechanisms and mechanical properties. 2020 , 779, 139140	8
377	Effects of density on the mechanical properties of spark plasma sintered EiC. 2020, 46, 13244-13254	8
376	Thermal radiation and cycling properties of (Ca, Fe) or (Sr, Mn) co-doped La2Ce2O7 coatings. 2020 , 40, 2020-2029	14
375	High fracture toughness of 3Y-TZP ceramic over a wide sintering range. 2020 , 244, 122693	8
374	Grindability of plasma sprayed thermal barrier coating using super abrasive wheel. 2020 , 98, 30-36	5
373	Strain rate and shear-transformation zone response of nanoindentation and nanoscratching on Ni50Zr50 metallic glasses using molecular dynamics. 2020 , 583, 412021	4
372	Toughening of Boron Carbide Composites with Hierarchical Microstructuring. 2020,	O
371	Vickers indentation tests on olivine: size effects. 2020 , 47, 1	4
370	Adaptation and self-healing effect of tribo-oxidizing in high-speed sliding friction on ZrB2-Si⊞-ceramic composite. 2020 , 446-447, 203204	9
369	Preparation and vacuum tribological properties of composite coatings fabricated by effective introduction of soft metal Ag into spray-formed YSZ templates. 2020 , 518, 146176	9
368	Mechanical Properties and Electrical Discharge Machinability of Alumina-10 vol% Zirconia-28 vol% Titanium Nitride Composites. 2020 , 3, 199-209	3
367	Microstructure and thermoelectric properties of higher manganese silicides fabricated via gas atomization and spark plasma sintering. 2020 , 249, 122990	2
366	Yb2O3-Gd2O3 codoped strontium zirconate composite ceramics for potential thermal barrier coating applications. 2020 , 17, 1608-1618	8
365	High-entropy M2AlC-MC (M=Ti, Zr, Hf, Nb, Ta) composite: Synthesis and microstructures. 2020 , 183, 33-38	19
364	Electro-mechanical and Polarization-Induced Antibacterial Response of 45S5 Bioglass-Sodium Potassium Niobate Piezoelectric Ceramic Composites. 2020 , 6, 3055-3069	3
363	Fabrication of electrically conductive barium aluminum silicate/silicon nitride composites with enhanced strength and toughness. 2021 , 56, 1221-1230	4
362	Hydroxyapatite Darium/strontium titanate composite coatings for better mechanical, corrosion and biological performance. 2021 , 44, 3618-3621	3

(2021-2021)

361	Effect of volume ratio on optical and mechanical properties of Y2O3-MgO composites fabricated by spark-plasma-sintering process. 2021 , 41, 2096-2105	6
360	On the governing fragmentation mechanism of primary intermetallics by induced cavitation. 2021 , 70, 105260	19
359	Ultra-low thermal conductivity and enhanced mechanical properties of high-entropy rare earth niobates (RE3NbO7, RE = Dy, Y, Ho, Er, Yb). 2021 , 41, 1052-1057	21
358	High entropy alloy borides prepared by powder metallurgy process and the enhanced fracture toughness by addition of yttrium. 2021 , 257, 123715	8
357	Fabrication of textured (Hf0.2Zr0.2Ta0.2Cr0.2Ti0.2)B2 high-entropy ceramics. 2021 , 41, 1015-1019	7
356	Densification, microstructure and mechanical properties of multicomponent (TiZrHfNbTaMo)C ceramic prepared by pressureless sintering. 2021 , 72, 23-28	14
355	A NillowB composite developed by devitrification of NillowB bulk metallic glass. 2021, 803, 140479	3
354	Susceptor-assisted fast microwave sintering of TiN reinforced SiAlON composites in a single mode cavity. 2021 , 47, 828-835	2
353	Thermal conductivity and thermal shock resistance of TiB2-basedUHTCs enhanced by graphite platelets. 2021 , 26, 101756	2
352	Enhancement of mechanical properties of hydroxyapatite coating prepared by electrophoretic deposition method. 2021 , 18, 147-153	2
351	Microstructure and wear performance of alumina/graphene coating on textured Al2O3/TiC substrate composites. 2021 , 41, 1438-1451	5
350	Optimal preparation of high-entropy boride-silicon carbide ceramics. 2021 , 10, 173-180	8
349	Effect of nano CuO addition on the tribo-mechanical behavior of alumina ceramics in non-conformal contact. 2021 , 18, 110-118	2
348	Measurement of Mechanical Properties for NiFe2O4 Nano-cermet. 2021 , 147-175	
347	Thermal shock and thermal fatigue resistance of Al2O3/(W, Ti)C/TiN/Mo/Ni multidimensional graded ceramics. 2021 , 18, 972-980	
346	Effect of atomic layer deposited Al2O3 and subsequent annealing on the nanomechanical properties on various substrates. 2021 , 56, 7879-7888	2
345	Indentation of Ceramics. 2021, 718-732	
344	Nanoindentation and Mechanical Properties of Materials at Submicro- and Nanoscale Levels: Recent Results and Achievements. 2021 , 63, 1-41	4

343	Influence of Elemental Carbon (EC) Coating Covering nc-(Ti,Mo)C Particles on the Microstructure and Properties of Titanium Matrix Composites Prepared by Reactive Spark Plasma Sintering. 2021 , 14,	2
342	Effect of the Heating Rate on the Spark-Plasma-Sintering (SPS) of Transparent Y2O3 Ceramics: Microstructural Evolution, Mechanical and Optical Properties. 2021 , 4, 56-69	3
341	Dense and core-rim structured B4C-TiB2 ceramics with Mo-Co-WC additive. <i>Journal of the American Ceramic Society</i> , 2021 , 104, 2860-2867	2
340	Semi-solid alkali metal electrodes enabling high critical current densities in solid electrolyte batteries. 2021 , 6, 314-322	22
339	Critical Raw Materials Saving by Protective Coatings under Extreme Conditions: A Review of Last Trends in Alloys and Coatings for Aerospace Engine Applications. 2021 , 14,	8
338	Hexagonal (CoCrCuTi)100-Fe multi-principal element alloys. 2021 , 261, 124190	1
337	Recent Developments in Carbon Nanotubes-Reinforced Ceramic Matrix Composites: A Review on Dispersion and Densification Techniques. 2021 , 11, 457	3
336	Phase composition, microstructure and thermophysical properties of the Srx(Zr0.9Y0.05Yb0.05)O1.95+x ceramics. 2021 , 41, 2734-2745	1
335	Improved machinability of TiB2IiC ceramic composites via laser-induced oxidation assisted micro-milling. 2021 , 47, 11514-11525	1
334	The MoNITaN system: Role of vacancies in phase stability and mechanical properties. 2021, 202, 109568	2
333	Dual-phase rare-earth-zirconate high-entropy ceramics with glass-like thermal conductivity. 2021 , 41, 2861-2869	19
332	Ta2O5 in-situ composite Ta-based nanocrystalline coating with wonderful wear resistance and related wear mechanisms. 2021 , 130000	2
331	Alloying of TiC-FeCr cermet in manganese vapor. 2021 , 1140, 012043	
330	The influence of yttria-stabilised zirconia and cerium oxide on the microstructural morphology and properties of a mica glass-ceramic for restorative dental materials. 1-8	
329	Improvement of mechanical properties of HfB-based composites by incorporating in situ SiC reinforcement through pressureless sintering. 2021 , 11, 9835	5
328	Quantitative relationship between microstructure and mechanical properties in Nd: YAG transparent ceramics. 2021 , 47, 12144-12152	1
327	Single-phase (Hf-Mo-Nb-Ta-Ti)C high-entropy ceramic: A potential high temperature anti-wear material. 2021 , 157, 106883	13
326	Textured and toughened high-entropy (Ti0.2Zr0.2Hf0.2Nb0.2Ta0.2)C-SiCw ceramics. 2021 ,	3

325	Fine-grained dual-phase high-entropy ceramics derived from boro/carbothermal reduction. 2021 , 41, 3189-3195	9
324	Densification, solid solution formation, and microstructural investigation of reactive pressureless sintered HfB2-TiB2-SiC-MoSi2 quadruplet composite. 2021 , 47, 16794-16800	4
323	Powder synthesis, densification, microstructure and mechanical properties of Hf-based ternary boride ceramics. 2021 , 41, 3922-3928	3
322	Columnar Thermal Barrier Coatings Produced by Different Thermal Spray Processes. 2021 , 30, 1437-1452	6
321	Thermo-mechanical study of a novel rotating disk volumetric receiver. 2021 , 223, 302-317	1
320	Interplay of microstructure and mechanical properties of WC-6Co cemented carbides by hot oscillating pressing method. 2021 , 47, 20731-20735	5
319	Influences of B4C content and particle size on the mechanical properties of hot pressed TiB2 B 4C composites. 1-9	1
318	Sintering of Potassium Doped Hydroxy-Fluorapatite Bioceramics. 2021 , 11, 858	1
317	Indentation-induced cracking behavior of a Cu(In,Ga)Se2 films on Mo substrate. 2021, 13, 1132-1138	
316	Liquid media effect on the abrasion response of WC/Co hardmetal with different cobalt percent. 2021 , 477, 203815	1
315	Microstructural evolution and mechanical properties of ZrO2 (3Y)私2O3BiC(w) ceramics under oscillatory pressure sintering. 2021 , 819, 141445	4
314	Stress intensity factors for micro- and macroscale bimaterial cantilevers and bend specimens. 2021 , 732, 138750	2
313	Mechanical properties of hydrated cesium-lithium aluminoborate glasses. 2021 , 5,	1
312	Metallothermic Reduction of MoO on Combustion Synthesis of Molybdenum Silicides/MgAlO Composites. 2021 , 14,	1
311	Pressureless densification of HfB2-based ceramics using HfB2 powders by borothermal reduction. 2021 , 47, 33922-33922	1
310	Effect of erbium doping on phase composition, mechanical and thermal properties of ZrO2-based ceramics. 2021 ,	O
309	Interlaminar Fracture Toughness Measurement of Multilayered 2D Thermoelectric Materials Bi2Te3 by a Tapered Cantilever Bending Experiment. 2021 , 1	1
308	New class of high-entropy defect fluorite oxides RE2(Ce0.2Zr0.2Hf0.2Sn0.2Ti0.2)2O7 (RE = Y, Ho, Er, or Yb) as promising thermal barrier coatings. 2021 , 41, 6080-6086	10

307	Micromechanical and microstructure characterization of BaO-Sm2O3BTiO2 ceramic with addition of Al2O3. 2021 , 48, 992-992	1
306	Determination of the Fracture Toughness of Glasses via Scratch Tests with a Vickers Indenter. 1	O
305	Effect of ternary particles size distribution on rheology of slurry and microstructure of DLP printed ZTA ceramic. 2021 , 269, 124656	2
304	Effect of Si content on the microstructure and properties of TiBill composite coatings prepared by reactive plasma spraying. 2021 , 47, 24438-24452	1
303	Influences of ZrSiO4 doping on microstructure and mechanical properties of Y2SiO5@rSiO4 ceramics. 2021 , 48, 1277-1277	
302	High-hard and high-tough WC-TiC-Co cemented carbide reinforced with graphene. 2021 , 102841	2
301	Fabrication and mechanical properties of homogeneous and gradient nanocomposites by two-step sintering. 2021 , 47, 25645-25654	O
300	Phase relations and thermomechanical properties of (Gd2Zr2O7)1図(YbSZ)x based thermal barrier coatings (0.版心.98). 2021 , 36, 3226	O
299	Effect of nano- and micro-sized Si3N4 powder on phase formation, microstructure and properties of &SiAlON prepared by spark plasma sintering. 2021 , 48, 1916-1916	0
298	Microstructural optimization and anti-wear performance of supersonic atmospheric plasma sprayed nickel based self-lubricating coatings under heavy load. 2021 , 421, 127383	2
297	Sea snail shells for synthesis of ceramic compounds reinforced with metallic oxide: Microstructural, mechanical and electrical behavior. 2021 , 28, 102656	
296	Influence of calcined halloysite on technological & mechanical properties of wall tile body. 1-14	O
295	Development of pressureless sintered and hot-pressed CNT/alumina composites including mechanical characterization. 2021 , 3, 237-248	0
294	Influence of nucleating agents on crystallization and electrical properties of SiO2MgOMgF2K2O mica glass-ceramics. 2021 , 47, 25997-26009	1
293	A novel strategy for c-axis textured silicon nitride ceramics by hot extrusion. 2021 , 41, 6059-6063	1
292	Pressureless sintering of HfB2-based ceramics as control rod materials: Synergistic effects of the sintering additive and solid solution. 2021 ,	1
291	Fracture toughness of Si3N4 ceramic composites: Effect of texture. 2021 , 41, 6346-6355	2
2 90	Development of WIrC composite coating on graphite by a TIG-aided surface cladding process. 2021 , 47, 27958-27971	1

289	Subsurface multilayer evolution of ZrB2BiC ceramics in high-speed sliding and adhesion transfer conditions. 2021 , 482-483, 203956	1
288	Tailoring microstructure of double-layered thermal barrier coatings deposited by suspension plasma spray for enhanced durability. 2021 , 425, 127704	1
287	Influence of powder mixing processes on phase composition, microstructure, and mechanical properties of ÆSiAlON ceramic tool materials. 2021 , 47, 30256-30265	4
286	Preparation of (Ti,Zr,Hf,Nb,Ta)C high-entropy carbide ceramics through carbosilicothermic reduction of oxides. 2021 , 41, 6934-6942	1
285	Recent advances in the mechanical characterization of shales at nano-to micro-scales: A review. 2021 , 162, 104043	0
284	Incorporation of graphene nano platelets in suspension plasma sprayed alumina coatings for improved tribological properties. 2021 , 570, 151227	3
283	EFFECT OF TITANIUM PARTICLES ON THE MICROSTRUCTURE AND MECHANICAL PROPERTIES OF ALUMINA MATRIX COMPOSITES. 2021 , 1-9	
282	Erosion Performance of Atmospheric Plasma Sprayed Thermal Barrier Coatings with Diverse Porosity Levels. 2021 , 11, 86	10
281	An Effective Approach of Nanoscale CaF2 Addition into ZTA Composite to Enhance Tribological Characteristics in Dry Sliding. 2021 , 80, 19-27	1
280	Experimental and FEM based investigation of the influence of the deposition temperature on the mechanical properties of SiC coatings. 2021 , 10, 139-151	3
279	Preparation and Thermal Properties of Rare Earth Tantalates (RETaO4) High-Entropy Ceramics. 2021 , 36, 411	2
278	Standard Reference Material 2100: Fracture Toughness of Ceramics. 2005 , 499-529	4
277	Piezoelectric Response in the Contact Deformation of Piezoelectric Materials. 2008, 151-173	1
276	Piezoelectric and Related Materials for Actuator Applications. 1997 , 71-120	2
275	The Indentation Crack as a Model Surface Flaw. 1983 , 1-25	22
274	Indentation Fracture Toughness of Brittle Materials for Palmqvist Cracks. 1983 , 97-105	67
273	Fracture Toughness Measurement by Indentation Fracture Method at Elevated Temperature. 1992 , 509-521	5
272	The Indentation Fracture Resistance of SelfReinforced Mullites. 1992 , 119-133	4

271	Fracture Mechanics and Microstructural Design. 1978 , 799-819	4
270	Role of Stress-Induced Phase Transformation in Enhancing Strength and Toughness of Zirconia Ceramics. 1978 , 877-889	3
269	Subcritical Crack Growth in PZT. 1978 , 687-709	8
268	High-Temperature Mechanical Properties of Al2O3-SiC Composites. 1986, 103-116	27
267	Precipitation and Toughness in Alumina-Rich Spinel Single Crystals. 1986 , 61-67	1
266	Effect of Static Loading on the Fracture Toughness of Indentation-Precracked Alumina. 1986 , 101-112	1
265	Influence of Grain Boundary Silica Impurity on Alumina Toughness. 1981 , 317-322	4
264	A Simple Method for Adhesion Measurements. 1981 , 603-617	38
263	Explosive Consolidation of Aluminum Nitride Ceramic Powder: A Case History. 1984 , 657-671	2
262	Cracked Indents E riend or Foe?. 1990 , 145-208	4
261	Superplastic Deformation of a Monolithic Silicon Nitride. 1995 , 351-358	4
260	Fracture Toughness Modifications By Means of CO2 Laser Beam Surface Processing of a Silicon Nitride Engineering Ceramic. 2010 , 519-522	1
259	Application of SPM and Related Techniques to the Mechanical Properties of Biotool Materials. 2009 , 71-103	1
258	Fracture Mechanics. 1999 , 19-51	1
258 257	Fracture Mechanics. 1999, 19-51 Indentation Testing of Sic-Whisker Reinforced Al2O3 Composites. 1989, 84-97	3
257	Indentation Testing of Sic-Whisker Reinforced Al2O3 Composites. 1989 , 84-97	3

253	邳iAlON Transformation. 1994 , 125-136	8
252	New Post-Sintering Treatments for Improved High-Temperature Performance Si3N4-Based Ceramics. 1997 , 311-326	1
251	Mechanical and Optical Properties of ZrO2 Doped Silicate Glass Ceramics. 2021 , 13, 877-883	2
250	Sprak plasma sintering behavior of hydroxyapatite t itanium nano-composite. 2017 , 53, 449-455	4
249	Bulk Semiconductors for Infrared Applications. 2001 , 239-305	1
248	Properties of Zirconium Carbide for Nuclear Fuel Applications. 2020 , 419-456	1
247	Preparation and characterization of Si3N4-based composite ceramic tool materials by microwave sintering. 2017 , 43, 16248-16257	11
246	Thermo-physical and mechanical properties of Yb2O3 and Sc2O3 co-doped Gd2Zr2O7 ceramics. 2020 , 46, 18888-18894	6
245	Indentation deformation and cracking in oxide glass B oward understanding of crack nucleation. 2019 , 1, 100009	17
244	Fracture Toughness and Strength of SiC-Whisker-Reinforced Si3N4Composites. 1988 , 3, 357-360	33
243	Tough, strong, hard, and chemically durable enstatite-zirconia glass-ceramic. <i>Journal of the American Ceramic Society</i> , 2020 , 103, 5036-5049	3 5
242	Enhancement of Dry Sliding Tribological Characteristics of Perforated Zirconia Toughened Alumina Ceramic Composite Filled With Nano MoS2 in High Vacuum. 2021 , 143,	1
241	Microstructure and mechanical properties of hot pressed Al2O3IIrO2 ceramics prepared from ultrafine powders. 1991 , 7, 490-494	16
240	Effect of whisker orientation on toughening behaviour and cutting performance of SiCwAl2O3 composite. 1993 , 9, 21-25	3
239	Topics in indentation hardness. 1982 , 16, 127-138	32
238	Modeling the Compression Behavior of ParticleAssemblies from the Mechanical Properties of Individual Particles. 1995 , 375-417	1
237	REFRACTORY CERAMICS SYNTHESIS BY SOLID-STATE REACTION BETWEEN CaCO[[MOLLUSK SHELL] AND All [DIPOWDERS. 2018, 355-363]	4
236	MICROSTRUCTURE, MECHANICAL PROPERTIES AND FRICTION/WEAR BEHAVIOR OF HOT-PRESSED SiN月BN CERAMIC COMPOSITES. 2018 , 1-10	2

235	Optimisation of properties of silicon carbide ceramics with the use of different additives. 2018 , 25, 496-504	3
234	Mechanical properties of microwave sintered Si3N4-based ceramics. 2002 , 34, 223-229	10
233	Indentation Hardness Testing of Ceramics. 2000 , 244-251	1
232	Microstructure and Properties of TiSi2based Composites in situ Prepared by SPS. 2008 , 23, 209-211	3
231	Fabrication of a Complex-Shaped Silicon Nitride Part with Aligned Whisker Seeds Using LOM Technique. 2003 , 40, 931-935	1
230	Fracture Toughness of 3Y-TZP Dental Ceramics by Using Vickers Indentation Fracture and SELNB Methods. 2019 , 56, 37-48	8
229	Strengthening of Alumina-Based Ceramics with Titanium Nanoparticles. 2014 , 05, 467-474	4
228	A new EiAlON ceramic tool prepared by microwave sintering and its cutting performance in high-speed dry machining Inconel718. 1	1
227	Nanosecond laser-induced controllable oxidation of TiB2IIiC ceramic composites for subsequent micro milling. 2021 , 48, 2470-2470	0
226	Effect of carbon content on the microstructure and mechanical properties of high-entropy (Ti0.2Zr0.2Nb0.2Ta0.2Mo0.2)Cx ceramics. 2021 , 42, 336-336	2
225	Effect of the Amount of the Sintering Additives on the Microstructural Development and the Mechanical Properties of Silicon Nitride with Aligned Whisker Seeds. 2002 , 39, 715-720	
224	Strengthening of Substrate Glass for LCD by Single ton Exchange Process. 2002 , 39, 675-679	
223	Mechanical properties. 2002,	
222	Wear Mapping and Wear Characterization Methodology. 2004,	
221	Variation of Microstructure Upon Residual Stress, as Obrained by the Vickers Indentation Method in Al2O3 Ceramics with Differing Aspect Ratios. 2005 , 54, 965-970	
220	Fabrication of Fibrous A12O3-(m-ZrO2)/t-ZrO2Composites Having 2, 3-Dimensional Array. 2005 , 15, 608-612	
219	Growth of GaN Thin-Film from Spin Coated GaOOH Precursor. 2007 , 17, 1-5	1
218	Synthesis of PSZ-seeding Mullite Composite from Metal Alkoxides and Its Characteristics of Sintered Body. 2007 , 17, 18-24	

(2013-2007)

Sodium borosilicate glass produced from coal fly ash upon vitrification in an induction-melting 217 furnace. 2007, 32, 619-622 Application of SPM and Related Techniques to the Mechanical Properties of Biotool Materials. 2010 216 . 81-113 Design of LED Driving Circuit using Voltage Controlled Ring Oscillator and Lighting Controller. 2010 215 , 24, 1-9 Fabrication and Physical Properties of ZrO2(m)-Al2O3ZrO2(t)-Al2O3Structural Ceramics. 2010, 24, 140-148 214 The Fundamentals of Hard and Superhard Nanocomposites and Heterostructures. 2010, 13-46 213 Toughness and Toughening of Hard Nanocomposite Coatings. 2010, 99-145 212 Synthesis Process and Microstructure for Al2O3/TiC/Ti Functionally Gradient Materials. 207-211 211 1 Preparation and Their Mechanical Properties of Al2O3/Ti Composite Materials. 111-116 210 Biomechanical Function of the Dentino-Enamel Junction Reflects Genetic Control, 133-145 209 208 Influence of Geometrical Irregularities on the Creep Behaviour of Ceramic Fibres. 163-174 Fabrication of Mullite-Zirconia Composites by Reaction Sintering of Zircon, Alumina, and Zirconia 207 Dopant Mixtures. 83-94 Open Forum: Vickers Indentation Technique-Problems and Solutions. 153-159 206 Accuracy of Empirical Formulae to Measure the Toughness of Transformation-Toughened Ceramics 205 Thow Accurate do You Need Your KIC?, 1-12 Production of Al2O3-Ti3Al Cermets by the Pressureless Reaction Sintering Process. 81-87 204 Effects of Vickers Cracks on the Mechanical Properties of Solid-phase-sintered Silicon Carbide 203 Ceramics. 2012, 27, 965-969 Synthesis, Shaped and Mechanical Properties of HydroxyapatiteAnatase Biomaterials. 45-54 Various Physical and Chemical Properties of Lotus Metals. 2013, 183-209 201 Mechanical Properties of Si3N4Ceramic Composites with Aligned Whisker Seeds. 2013, 27, 8-12 200

199	Kyanite-Al2O3-ZrO2-t Mixtures. 111-117
198	Evaluation of Indentation Fracture Toughens in Brittle Materials Based on FEA Solutions. 2013 , 37, 1503-1512
197	Fabrication of Si3N4 Ceramics with Additives Of Metal Nitrides by High Pressure Hot-Pressing and Hiping. 1984 , 583-589
196	Effects of Miorostructure Control on Ferroelectric Ceramics. 1987 , 707-718
195	EVALUATING MECHANICAL PROPERTIES OF Si3N4 WITH MICRO-STRENGTH METHOD. 1988 , 1305-1309
194	FRACTURE TOUGHNESS ANALYSIS AND ESTIMATION OF SURFACE ENERGY OF SEVERAL GLASSES. 1988, 1341-1346
193	Bruchmechanik. 1989, 21-68
192	Failure Analysis. 1991 , 137-142
191	Deformation, Structure and Properties of High-Tc Superconducting Ceramics and Single Crystals. 1993 , 45-88
190	Mechanical Properties of Fiber-Reinforced YBa2Cu3Ox and Bi2Sr2CaCu2Ox Bars. 1994 , 63-70
189	Design and Engineering Properties of Glasses. 1995 , 1171-1187
188	The Variation of Indentation Fracture with Temperature in Silicon Carbide, Silicon Nitride and Zirconia. 1996 , 539-550
187	Effect of processing on the characteristics of a 20 vol.% Al2O3 platelet-reinforced hydroxyapatite composite. 1997 , 549-552
186	SiAlON/SiC Micro-Nano-Composites. 1997 , 179-187
185	Superplastic Forming of an Phase Rich Silicon Nitride. 1997 , 363-369
184	Nanomechanical Properties of Solid Surfaces and Thin Films. 1998,
183	Literature. 1999 , 159-173
182	Subcritical growth of microstructurally small cracks in silicon nitride ceramics. 1999 , 271-282

181	Fabrication and Characterization of MgO-Al2O3-SiO2-ZrO2Based Glass Ceramic. 2014, 27, 712-717	
180	Evaluation of the Effect of Spray Distance on Fracture Toughness of Thermally Sprayed Coatings. 2015 , 15, 709-714	
179	Pseudo-icosahedral Cr55Al232las a high-temperature protective material. 2018 , 2,	
178	DEPENDENCE OF SIAION-TIN COMPOSITE PROPERTIES ON TIN REINFORCEMENT PARTICLE SIZES. 1-1	1
177	ENDBTREYEL SEALON-TEN KESECE UERETEMENDE PROSES KOÜLLARININ ETKESE 2018 , 6, 716-724	2
176	Mechanics of wood boring by beetle mandibles.	
175	The Microstructure and the Mechanical Properties of Sintered TiO2-Co Composite Prepared Via Thermal Hydrogenation Method. 2019 , 26, 290-298	
174	Determination of fracture toughness and elastic module in materials based silicon nitride. 2019 , 20, 1-13	1
173	Crack Growth Resistance and Segregation in Amorphous Alloy F \$_ {73.6}\$Si\$_{15.8}\$B\$_{7.2}\$Cu\$_{1.0}\$Nb\$_{2.4}\$ (FINEMET) under Microindentation. 2019 , 41, 1217-1230	
172	Effect of SiC Particle Size on the Microstructural, Mechanical and Oxidation Properties of In-situ Synthesized HfB2-SiC Composites.	
171	Numerical modeling of Vickers indentation on polycrystalline alumina. 2020 , 1633, 012046	
170	Study of colored on the microwave sintering behavior of dental zirconia ceramics. 2021, 9, 188-196	
169	Determination of Strength and Fracture Toughness from Indentation Tests in the Framework of Finite Fracture Mechanics. 2021 , 44-51	Ο
168	Fabrication of mullite nano ceramic through addition of long-chain carbohydrates. 2020 , 25, 101196	Ο
167	An investigation about crystallization properties of vermiculite based machinable glass-ceramics. 2022 , 276, 125369	Ο
166	Fracture toughness assessment of the X80 steel by nanoindentation technique and a modified constitutive model. 2022 , 117, 103195	O
165	Structure and Properties of WCILo Composites with Different CrB2 Concentrations, Sintered by Vacuum Hot Pressing, for Drill Bits. 2021 , 43, 344-354	2
164	Hardness and toughness improvement of SiC-based ceramics with the addition of (Hf 0.2 Mo 0.2 Ta 0.2 Nb 0.2 Ti 0.2)B 2. <i>Journal of the American Ceramic Society</i> ,	Ο

163	Compatible performance of low thermal conductivity and high infrared radiation of Sm2O3-HfO2 series ceramics applied for thermal protection coatings. 2021 , 48, 6372-6372		О
162	Spark Plasma Sintering of SiAlON Ceramics Synthesized via Various Cations Charge Stabilizers and Their Effect on Thermal and Mechanical Characteristics. 2021 , 11, 1378		1
161	Microstructures and mechanical properties of BiC ceramics after high-temperature laser shock peening. <i>Journal of the American Ceramic Society</i> ,	3.8	O
160	Hydraulic fracture propagation and interaction with natural fractures by coupled hydro-mechanical modeling. 2022 , 8, 1		O
159	Optimization of microstructure and mechanical properties of oscillatory pressure sintered ZrO2Al2O3-SiCp ceramics. 2021 , 48, 7512-7512		0
158	Tribological Behaviour of Alumina Ceramics with Nano TiO2 as a sintering aid in Non-Conformal Contact. 1-21		
157	Mechanical and thermal properties of ZrC/ZTA composites prepared by spark plasma sintering. 2021 , 48, 6453-6453		1
156	Enhanced Mechanical Properties and Oxidation Resistance of Zirconium Diboride Ceramics via Grain-Refining and Dislocation Regulation 2022 , 9, e2104532		O
155	Fabrication and mechanical properties of TiN/ZrO2(2Y) composites by hot isostatic pressing. 1996 , 15, 1615-1617		
154	Mechanical properties of SiC/TiC composites by hot isostatic pressing. 1996 , 15, 394-396		5
153	Optimization of the sintering thermal treatment and the ceramic ink used in direct ink writing of #Al2O3: Characterization and catalytic application. 2022 ,		3
152	Mechanical properties of beryllium-titanium intermetallic compounds fabricated by plasma sintering. 2022 , 30, 101117		O
151	Copper reinforced SiAlON matrix composites produced by spark plasma sintering. 2022,		O
150	Reaction Sintering of Biocompatible AlO-hBN Ceramics 2022 , 7, 2205-2209		1
149	B4CIIiB2 composites fabricated by hot pressing TiCB mixtures: The effect of B excess. 2022,		2
148	Cutting performance of a new spark plasma sintered SiAlON ceramic tool for high-speed milling of Inconel 718. 2022 , 119, 7327		1
147	Microstructure and Mechanical Properties of CoWB Based Composites Produced by Crystallization of Ni-Co-Zr-Ta-W-B Bulk Metallic Glass. 2022 , 12, 251		О
146	Fully dense ZrB 2 ceramics by borothermal reduction with ultra-fine ZrO 2 and solid solution. Journal of the American Ceramic Society,	3.8	O

145	Sr,Mg co-doping of calcium hydroxyapatite: Hydrothermal synthesis, processing, characterization and possible application as dentin substitutes. 2022 ,	О
144	Fabrication, transport behaviors and green interrupted cutting performance of bio-inspired microstructure on Al2O3/TiC composite ceramic surface. 2022 , 75, 203-218	Ο
143	Hard and tough ultrafine-grained B4C-cBN composites prepared by high-pressure sintering. 2022 , 42, 2015-2020	Ο
142	Evaluation of mechanical and tribological characteristics of hot-pressed self-lubricating CuO/MgO/ZTA ceramic composites. 2022 , 50, 2522-2527	
141	Mechanical Behavior of Fe- and Co-Based Amorphous Alloys after Thermal Action. 2022 , 12, 297	О
140	High Pressure Synthesis of Al2o3-Cbn-Hbn Self-Lubricating Ceramic.	
139	Phase Formation and Physicomechanical Properties of WCIIoIIrB2 Composites Sintered by Vacuum Hot Pressing for Drill Tools. 2022 , 44, 1-11	0
138	Effect of Y3Al5O12 addition on the microstructural evaluation and mechanical properties of spark plasma sintered ZrB2-SiC composites. 2022 , 54, 1-9	
137	Simultaneous effect of CaF2 and TiC on tribological properties of ZTA ceramics for high temperature application. 2022 ,	1
136	Microstructures and mechanical properties of functionally graded TiCNIIaC ceramics prepared by a novel layer processing strategy. 2022 ,	Ο
135	Microwave synthesis of duplex 哲iAlON ceramic cutting inserts: Modifying m, n, z values, synthesis temperature, and excess Y2O3 synthesis additive. 2022 , 11, 589-602	О
134	An Indentation Method for Determining the Film Thickness, Young's Modulus, and Hardness of Bilayer Materials.	Ο
133	(Hf0.99Ta0.01)B2-based ceramics prepared by pressureless sintering with boron additive. 2022 , 48, 8605-861	1
132	Dense SiC ceramics prepared by using amorphous sintering additives. 2022 ,	O
131	AlO-Cu-Ni Composites Manufactured via Uniaxial Pressing: Microstructure, Magnetic, and Mechanical Properties 2022 , 15,	
130	Long-term tribocorrosion resistance and failure tolerable of multilayer carbon-based coatings. 1	O
129	Ceramic Toughening Strategies for Biomedical Applications 2022 , 10, 840372	1
128	Phase transformation and thermal conductivity of the APS Y2O3 doped HfO2 coating with hybrid structure. 2022 ,	

127	Methods for Accuracy Increasing of Solid Brittle Materials Fracture Toughness Determining. 2022 , 13, 40-49	
126	High-Pressure Synthesis of Al2O3-cBN-hBN Self-lubricating Ceramic. 2022 , 110638	1
125	Erosion performance of suspension plasma spray thermal barrier coatings IA comparison with state of art coatings. 2022 , 437, 128311	О
124	Preparation and application of sustainable nanofluid lubricant from waste soybean oil and waste serpentine for green intermittent machining process. 2022 , 77, 508-524	0
123	The effect of heat treatment at 1200 °C on microstructure and mechanical properties evolution of AlCoCrFeNiSiYHf high entropy alloys. 2022 , 200, 111039	0
122	The microstructural in-sight to the mechanical behavior of alumina after high energy proton irradiation. 2022 , 31, 101173	
121	Orthorhombic to tetragonal polymorphic transformation of YTa3O9 and its inhibition through the design of high-entropy (Y0.2La0.2Ce0.2Nd0.2Gd0.2)Ta3O9. 2022 , 42, 3559-3569	О
120	Effect of TZP nanoparticles synthesized by RCVD on mechanical properties of ZTA composites sintered by SPS. 2022 , 42, 3550-3558	o
119	Bionic multifunctional surface microstructure for efficient improvement of tool performance in green interrupted hard cutting. 2022 , 305, 117587	1
118	Structure Monitoring of the LaB\$_6\$\mathbb{\Pi}iB\$_2\$ Composites. 2021 , 43, 1653-1665	
118	Structure Monitoring of the LaB\$_6\$\subseteq \text{Ii}B\$_2\$ Composites. 2021 , 43, 1653-1665 Tailoring 18 Mol.% Yo1.5 Stabilized Hfo2 with Lamgal11o19 Platelets for Thermal/Environmental Barrier Coatings Applications on Sic-Based Ceramic Matrix Composite.	
	Tailoring 18 Mol.% Yo1.5 Stabilized Hfo2 with Lamgal11o19 Platelets for Thermal/Environmental	O
117	Tailoring 18 Mol.% Yo1.5 Stabilized Hfo2 with Lamgal11o19 Platelets for Thermal/Environmental Barrier Coatings Applications on Sic-Based Ceramic Matrix Composite. Fabrication and modelling of Si3N4 ceramics with radial grain alignment generated through	0
117 116	Tailoring 18 Mol.% Yo1.5 Stabilized Hfo2 with Lamgal11o19 Platelets for Thermal/Environmental Barrier Coatings Applications on Sic-Based Ceramic Matrix Composite. Fabrication and modelling of Si3N4 ceramics with radial grain alignment generated through centripetal sinter-forging. 2022, Low-temperature densification of high-entropy (Ti,Zr,Nb,Ta,Mo)Clo composites with high	
117 116 115	Tailoring 18 Mol.% Yo 1.5 Stabilized Hfo2 with Lamgal 11o 19 Platelets for Thermal/Environmental Barrier Coatings Applications on Sic-Based Ceramic Matrix Composite. Fabrication and modelling of Si3N4 ceramics with radial grain alignment generated through centripetal sinter-forging. 2022, Low-temperature densification of high-entropy (Ti,Zr,Nb,Ta,Mo)Clo composites with high hardness and high toughness. 2022, 11, 805-813 Understanding the role of in-flight particle temperature and velocity on the residual stress depth	1
117 116 115	Tailoring 18 Mol.% Yo1.5 Stabilized Hfo2 with Lamgal11o19 Platelets for Thermal/Environmental Barrier Coatings Applications on Sic-Based Ceramic Matrix Composite. Fabrication and modelling of Si3N4 ceramics with radial grain alignment generated through centripetal sinter-forging. 2022, Low-temperature densification of high-entropy (Ti,Zr,Nb,Ta,Mo)CCo composites with high hardness and high toughness. 2022, 11, 805-813 Understanding the role of in-flight particle temperature and velocity on the residual stress depth profile and other mechanical properties of atmospheric plasma sprayed Al2O3 coating. 2022, Pyrochlore-Fluorite Dual-Phase High-Entropy Re2(Ce0.2zr0.2hf0.2sn0.2ti0.2)2o7 (Re2he2o7, Re =	1
117 116 115 114 113	Tailoring 18 Mol.% Yo1.5 Stabilized Hfo2 with Lamgal11o19 Platelets for Thermal/Environmental Barrier Coatings Applications on Sic-Based Ceramic Matrix Composite. Fabrication and modelling of Si3N4 ceramics with radial grain alignment generated through centripetal sinter-forging. 2022, Low-temperature densification of high-entropy (Ti,Zr,Nb,Ta,Mo)Clo composites with high hardness and high toughness. 2022, 11, 805-813 Understanding the role of in-flight particle temperature and velocity on the residual stress depth profile and other mechanical properties of atmospheric plasma sprayed Al2O3 coating. 2022, Pyrochlore-Fluorite Dual-Phase High-Entropy Re2(Ce0.2zr0.2hf0.2sn0.2ti0.2)2o7 (Re2he2o7, Re = La, Nd, Sm, EU, Gd, Dy) Ceramics with Glass-Like Thermal Conductivity. Development of a high-performance green Fe-Al2O3 composites using Bayan Obo minerals:	1

109	Mechanical Properties and Residual Stress Depth Profiles of Plasma Sprayed Ceramic Coatings Deposited Under Comparable Particle Temperature and Velocity.	О
108	Non-conventional Small-Scale Mechanical Testing of Materials. 1	
107	Mechanical Properties of Oxide Glasses. 2022 , 87, 229-281	1
106	Indentation Fracture Toughness of Semiconducting Gallium Arsenide at Elevated Temperatures. 2022 , 106417	
105	The influence of Si3N4 on the microstructure, mechanical properties and the wear performance of TiB2BiC synthesized via spark plasma sintering. 2022 , 5, 326-338	1
104	Microstructures and mechanical properties of (Nb0.25Mo0.25Ta0.25W0.25)C and (Nb0.2Mo0.2Ta0.2W0.2Hf0.2)C high-entropy carbide ceramics produced by arc melting. 2022 , 107, 105859	Ο
103	TEM exploration of in-situ nanostructured composite coating fabricated by plasma spraying 8YSZ-Al-SiC composite powder. 2022 ,	О
102	High Densification of Tungsten via Hot Pressing at 1300 °C in Carbon Presence. 2022 , 15, 3641	Ο
101	Heterogeneous Diamond-cBN Composites with Superb Toughness and Hardness.	0
100	Microstructure and Mechanical Properties of In-Situ B4C-(TiZrHfNbTa) B2 Composite by Reactive Spark Plasma Sintering.	О
99	High temperature tribological performance of molybdenum reinforced zirconia toughened alumina composites prepared by pressure-less sintering. 2022 ,	0
98	Rattler effect on the properties of multicomponent rare-earth-zirconate ceramics. 2022,	О
97	Novel (Zr, Ti)(C, N)BiC ceramics via reactive hot-pressing at low temperature. 2022 ,	1
96	High-density ceramics obtained by andesite basalt sintering. 2022 , 16, 143-152	О
95	The Mechanics of Fracture in Dental Ceramics. 2022 , 39-67	
94	Effects of ZrB2 powders on microstructure and mechanical properties of ZrB2-SiCw ceramics. 2022 ,	
93	Comparison between different fracture toughness techniques in zirconia dental ceramics.	
92	The mechanical properties of inorganic thermoelectric materials: A review on characterization methods and correlations.	Ο

91	Effects of SiC on the Microstructure, Densification, Hardness and Wear Performance of TiB2 Ceramic Matrix Composite Consolidated Via Spark Plasma Sintering.	O
90	Mechanical properties and calciumthagnesiumtluminotilicate corrosion behaviour of Ce/Gd co-doped SrZrO3 ceramics. 2022 ,	O
89	Cohesive fracture measurement technique for free-hanging thin films using highly stressed superlayer. 2022 , 757, 139379	
88	High toughness Si3N4 ceramic composites synergistically toughened by multilayer graphene/ESi3N4 whisker: Preparation and toughening mechanism investigation. 2022 , 921, 166183	1
87	Influence of order-disorder transition on the mechanical and thermophysical properties of A2B2O7 high-entropy ceramics. 2022 , 11, 1222-1234	3
86	Quantifying the composite microhardness and fracture toughness of iron ore sinter La phase-based approach. 1-13	O
85	Phase Formation and Physical and Mechanical Properties of Fe-CuNi-SnVN Composites Sintered by Vacuum Hot Pressing for the Diamond Stone Processing Tools. 2022 , 44, 160-169	
84	Effect of Carbonate Contents on the Thermal Stability and Mechanical Properties of Carbonated Apatite Artificial Bone Substitute.	O
83	Enhanced bioactivity and low temperature degradation resistance of yttria stabilized zirconia/clay composites for dental applications. 2022 ,	
82	Wear behavior and microstructure of alumina-mullite-zirconia composites prepared by a novel method: Coating of zircon powder by aluminum alkoxide. 2022 ,	O
81	Synthesis of single-phase (ZrTiTaNbMo)C high-entropy carbide powders via magnesiothermic reduction process. 2022 ,	
80	Thermal properties of (Zr0.2Ce0.2Hf0.2Y0.2RE0.2)O1.8 (RE= La, Nd and Sm) high entropy ceramics for thermal barrier materials. 2022 ,	O
79	Evaluations on Ceramic Fracture Toughness Measurement by Edge Chipping. 2022 , 12, 1146	1
78	Spark plasma sintering of multi-cation doped (Yb, Sm) 抵SiAlON ceramic tool materials: Effects of cation type, composition, and sintering temperature. 2022 ,	1
77	Influence of CrB2 additive on the morphology, structure, microhardness and fracture resistance of diamond composites based on WC-Co matrix. 2022 , 25, 101546	1
76	Low temperature synthesis and densification of (Ti,V,Nb,Ta,Mo)(C,N) high-entropy carbonitride ceramics. 2022 , 927, 167095	O
75	Effects of (Ta0.2w0.2nb0.2mo0.2v0.2)C High-Entropy Carbide Content on the Microstructure and Properties of Ti(C0.7n0.3)-Based Cermet.	О
74	Microstructures, thermophysical properties and thermal cyclic behaviors of Nd2O3 and Sc2O3 co-doped LaMgAl11O19 thermal barrier coating deposited by plasma spraying. 2022 ,	O

73	Study of the evolution of nanopores and microstructural degradation of fine-grained YSZNiO(Ni) anode materials in a hydrogen sulfide containing atmosphere.	O
72	Micromechanical properties of Dy3+ ion-doped (Lu Y1-)3Al5O12 ($x = 0, 1/3, 1/2$) single crystals by indentation and scratch tests. 2022 ,	Ο
71	Toughness mechanism and plastic insensitivity of submicron second phase Ta in a novel Ta⊞f6Ta2O17 composite ceramic. 2022 ,	0
70	Microstructure and Tribological Behavior of Supersonic Atmospheric Plasma-Sprayed Mo-/Fe-Based Amorphous Coating.	Ο
69	Analysis of mechanical properties of Al 2 O 3 -cBN-hBN composites and identification of main influencing factors. 2022 , 19, 3255-3266	0
68	Study of the Resistance to Degradation of Al2O3/Al2TiO5 Composites for Possible Use as Bone Tissue. 2022 , 16, 398-403	O
67	Instrumented indentation based methods to assess fracture toughness (KIC) of self-compacting concrete: Influence of water to binder (w/b) ratio and type of concrete. 2022 , 108796	0
66	Pyrochlorefluorite dual-phase high-entropy RE2(Ce0.2Zr0.2Hf0.2Sn0.2Ti0.2)2O7 (RE2HE2O7, RE = La, Nd, Sm, Eu, Gd, Dy) ceramics with glass-like thermal conductivity.	Ο
65	Thermally-enhanced dislocation density improves both hardness and fracture toughness in single-crystal SrTiO 3.	0
64	Integrated simulation, machine learning, and experimental approach to characterizing fracture instability in indentation pillar-splitting of materials. 2022 , 105092	O
63	Synthesis of Mg-stabilized nitrogen rich alpha sialons along Si 3 N 4 $\rm I\!I\!I$ Mg 3 N 2 :3AlN line via field-assisted sintering.	0
62	Low-temperature densification of high entropy diboride based composites with fine grains and excellent mechanical properties. 2022 , 110331	Ο
61	Effect of adding CsI on properties of Ge20Sb10Se65Te5 glass. 2022 , 126, 104370	О
60	Fracture Toughness Characterization of TBCs. 2022 , 447-512	Ο
59	Fracture behavior of ceramic restorative materials in the active environments. 2022, 49, 111-86	Ο
58	In-situ solid solution of Mo or Cr in WB2: Densification, microstructure, and properties. 2022,	Ο
57	Realization of complex-shaped and high-performance alumina ceramic cutting tools via Vat photopolymerization based 3D printing: A novel surface modification strategy through coupling agents aluminic acid ester and silane coupling agent. 2022 ,	1
56	Fabrication of Basalt Matrix Composite Material by Pressureless Aluminum Melt Infiltration in Air Atmosphere. 2022 , 5, 780-788	O

55	Tailoring thermal and mechanical properties of rare earth niobates by coupling entropy and composite engineering. 2022 ,	0
54	Indentation cracking in mono and polycrystalline cubic zirconia: Methodology of an apparent fracture toughness evaluation. 2022 , 144261	О
53	Synergistic effect of graphene and Ei3N4 whisker enables Si3N4 ceramic composites to obtain ultra-low friction coefficient. 2022 , 108045	О
52	Spark plasma sintering of A6B2O17 (A´=ʿHf, Zr; B´=ʿTa, Nb) high entropy ceramics. 2023 , 330, 133381	О
51	Development of yttria-stabilized zirconia and graphene coatings obtained by suspension plasma spraying: Thermal stability and influence on mechanical properties. 2022 ,	0
50	Effect of Two-Step Sintering on Properties of Alumina Ceramics Containing Waste Alumina Powder. 2022 , 15, 7840	O
49	Enhanced Mechanical Properties of Yellow ZrN Ceramic with Addition of Solid Solution of TiN. 2022 , 15, 7866	О
48	Ultrafine-grained B 6 O-diamond composites with superb mechanical properties.	O
47	Effects of (Ta0.2W0.2Nb0.2Mo0.2V0.2)C high-entropy carbide content on the microstructure and properties of Ti(C0.7N0.3)-based cermet. 2022 ,	0
46	Design strategy of phase and microstructure of Si 3N 4 ceramics with simultaneously high hardness and toughness. 2023 , 12, 122-131	0
45	Highly electro-conductive B 4Clib 2 composites with three-dimensional interconnected intergranular TiB 2 network. 2023 , 12, 182-195	0
44	Improvement of cutting performance of high x value ÆSiAlON ceramic cutting inserts via tailoring microstructure and oxidation behavior. 2023 , 111, 106087	O
43	Low-temperature sintered (Ti, Zr, Nb, Ta, Mo)C-based composites toughened with damage-free SiCw. 2023 , 43, 1740-1745	0
42	Microstructure and mechanical properties of WB 2 ${f B}$ 4 C composites fabricated by boro/carbothermal reduction and SPS.	O
41	Cutting performance improvement of Si 3 N 4 ceramic cutting tools by adding boride.	0
40	Evaluation of the Fracture Toughness KIc for Selected Magnetron Sputtering Coatings by Using the Laugier Model. 2022 , 15, 9061	O
39	Structural and Mechanical Characterization of 3D Printed Hydroxyapatite Scaffolds Designed for Biomedical Applications. 339, 109-114	О
38	Synthesis of cBN-hBN-SiCw Nanocomposite with Superior Hardness, Strength, and Toughness. 2023 , 13, 37	О

37	Friction and wear behavior of fluoride added Si3N4-SiC ceramic composites at elevated temperature. 2022 ,	O
36	Yttria-stabilized tetragonal zirconia prepared using gel casting and two-stage sintering. 1-8	O
35	Effect of volume ratio on the performance of mid-wave infrared transparent Gd2O3MgO composite ceramics. 2023 ,	O
34	Study of toughening behavior of SiC whiskers on 8YSZ thermal barrier coatings. 2023 , 455, 129232	O
33	Crystallization kinetics, structural and mechanical properties of transparent lithium aluminosilicate glass-ceramics. 2023 , 603, 122113	О
32	Influence of Cr content on sintering, textured structure, and properties of (Hf, Zr, Ta, Cr, Ti)B2 high-entropy boride ceramics. 2023 ,	O
31	Vat photopolymerization-based 3D printing of complex-shaped and high-performance Al2O3 ceramic tool with chip-breaking grooves: Cutting performance and wear mechanism. 1-11	O
30	Performance of multi-bionic hierarchical texture in green intermittent cutting. 2023, 247, 108203	O
29	Deterioration of Crack Growth Resistance Characteristics of a Fine-Grained YSZNiO(Ni) Anode Material During Its Degradation in a Hydrogen Sulfide Containing Atmosphere. 2023 , 149-165	O
28	Fast-low temperature microwave sintering of ZrSiO4@rO2 composites. 2023 ,	0
27	Characterization of MoAlB ceramics Synthesized via Spark Plasma Sintering with Si addition and SiC Reinforcement. 2023 , 170115	О
27		0
	Reinforcement. 2023, 170115 Effect of substrate bias voltage on structural and tribological properties of W-Ti-C-N thin films	
26	Reinforcement. 2023, 170115 Effect of substrate bias voltage on structural and tribological properties of W-Ti-C-N thin films produced by combinational HiPIMS and DCMS co-sputtering. 2023, 520-521, 204654 Low-temperature and single-step synthesis of fully-dense MgAl2O4 by reaction spark plasma	O
26	Reinforcement. 2023, 170115 Effect of substrate bias voltage on structural and tribological properties of W-Ti-C-N thin films produced by combinational HiPIMS and DCMS co-sputtering. 2023, 520-521, 204654 Low-temperature and single-step synthesis of fully-dense MgAl2O4 by reaction spark plasma sintering Al2O3 and MgO nano-oxides. 2023, 100, 100989 A (Hf0.2Mo0.2Nb0.2Ta0.2Ti0.2)C system high-entropy ceramic with excellent mechanical and	0
26 25 24	Reinforcement. 2023, 170115 Effect of substrate bias voltage on structural and tribological properties of W-Ti-C-N thin films produced by combinational HiPIMS and DCMS co-sputtering. 2023, 520-521, 204654 Low-temperature and single-step synthesis of fully-dense MgAl2O4 by reaction spark plasma sintering Al2O3 and MgO nano-oxides. 2023, 100, 100989 A (Hf0.2Mo0.2Nb0.2Ta0.2Ti0.2)C system high-entropy ceramic with excellent mechanical and tribological properties prepared at low temperature. 2023, 184, 108471 Revisiting lead magnesium niobate-lead titanate piezoceramics for low-frequency mechanical	0 0
26 25 24 23	Effect of substrate bias voltage on structural and tribological properties of W-Ti-C-N thin films produced by combinational HiPIMS and DCMS co-sputtering. 2023, 520-521, 204654 Low-temperature and single-step synthesis of fully-dense MgAl2O4 by reaction spark plasma sintering Al2O3 and MgO nano-oxides. 2023, 100, 100989 A (Hf0.2Mo0.2Nb0.2Ta0.2Ti0.2)C system high-entropy ceramic with excellent mechanical and tribological properties prepared at low temperature. 2023, 184, 108471 Revisiting lead magnesium niobate-lead titanate piezoceramics for low-frequency mechanical vibration-based energy harvesting. 2023, 945, 169298	0 0 1

19	R-curve evaluation of 3YTZP/graphene composites by indirect compliance method. 2023 , 43, 3486-3497	Ο
18	3D Finite Element Simulations of Indentation Fracture Test of ZrO2-Ceramics with Taking into Account its Microstructure. 2022 ,	O
17	Mechanical properties of TiC reinforced MgOZrO2 composites via spark plasma sintering. 2023 , 49, 17255-17260	0
16	Effects of Crystal Orientation in Deterministic Microgrinding of Sapphire. 1994,	О
15	Synthesis of (HfZrTiNbTa)N powders via nitride thermal reduction with soft mechano-chemical assistance. 2023 , 12, 565-577	О
14	Composite vitreous enamel coatings with the addition of 316L stainless steel flakes: Novel insights on their behaviour under mechanical stresses. 2023 , 459, 129393	O
13	B4C-(Hf,Zr,Ta,Nb,Ti)B2 composites prepared by reactive and non-reactive spark plasma sintering. 2023 , 49, 19556-19560	0
12	Microstructures and Enhanced Mechanical Properties of (Zr, Ti)(C, N)-Based Nanocomposites Fabricated by Reactive Hot-Pressing at Low Temperature. 2023 , 16, 2145	O
11	Hydroxyapatite materials-synthesis routes, mechanical behavior, theoretical insights, and artificial intelligence models: a review.	0
10	Preparation of In Situ Growth Multiscale Esialon Grain-Reinforced Al2O3-Based Composite Ceramic Tool Materials. 2023 , 16, 2333	O
9	Effect of zirconia addition amount in glaze on mechanical properties of porcelain slabs. 2023,	0
8	The Effect of Sintering Temperature on Crack Growth Resistance Characteristics of Fine-Grained Partially Stabilized Zirconia Determined by Various Test Methods. 2023 , 331-345	O
7	Estimation of the Role of Nanosized Stabilizing Powders in Gaining High-Level Crack Growth Resistance of Partially Stabilized Zirconia. 2023 , 311-330	0
6	The Effect of Ultra-fine Alloying Elements on High-Temperature Strength and Fracture Toughness of TiBiX and Tiប៊ែស៊េ Composites. 2023 , 195-216	O
5	B 4 C-TiB 2 composite with modified microstructure and enhanced properties from optimal size coupling of raw powders.	0
4	3D Printing of Robust 8YSZ Electrolytes with a Hyperfine Structure for Solid Oxide Fuel Cells.	О
3	Temperature-dependent mechanical and oxidation behavior of in situ formed ZrN/ZrO 2 -containing Si 3 N 4 -based composite.	О
2	Phase, microstructure and property evolutions of reactively synthesized YSZ-ZrC composite coating based on the content regulation of the precursor. 2023 , 170176	O

Effect of yttrium on phase composition and microstructure of FeCoNiAlCrB high entropy alloys. **2023**, 873, 145058

О